PRODUCTION OF MEDIUM-CHAIN-LENGTH POLY(3-HYDROXYALKANOATES) USING *PSEUDOMONAS CITRONELLOLIS* DSM50332 AND *P. PUTIDA* KT2440 IN CONTINUOUS REACTOR SYSTEMS

by

James Edward Gillis

A thesis submitted to the Department of Chemical Engineering

in conformity with the requirements for the

degree of Master of Applied Science

Queen's University

Kingston, Ontario, Canada

December, 2011

Abstract

In vivo production of medium-chain-length poly(3-hydroxyalkanoates) (MCL-PHA) containing a side chain carboxyl group from azelaic acid (AzA), a nine-carbon α,ω-dicarboxylic acid, was investigated using *Pseudomonas citronellolis* DSM 50332 in a phosphate (P)-limited chemostat. Co-feeding with nonanoic acid (NA) and inhibition of β-oxidation with acrylic acid (AA) were strategies that were used to stimulate the incorporation of carboxylated monomers, but both were unsuccessful. *P. citronellolis* DSM50332 was capable of growing on AzA as a sole source of carbon and energy, indicating that enzymes in β-oxidation utilized AzA and its derivatives. However, the MCL-PHA produced from AzA comprised 3-hydroxyoctanoate (C8) and 3-hydroxydecanoate (C10) monomers, which was consistent with precursor supplied via the *de novo* fatty acid biosynthesis pathway. This evidence suggests that one or more of 3-ketoacyl-CoA reductase (FabG), enoyl-CoA hydratase (PhaJ) and PHA synthase (PhaC) of this organism do not have the low specificity required to utilize a carboxylated substrate. Future work involving mutations may broaden the substrate specificity of these key enzymes to overcome this obstacle.

Two-stage high-cell density carbon (C)-limited chemostat cultivation of *P. putida* KT2440 was examined for MCL-PHA production from nonanoic acid (NA) at high intracellular polymer content and volumetric productivity. Growth conditions stimulating good PHA production were first established in single-stage chemostat, which yielded 63.1 wt% PHA containing 90 mol% C9 units and a productivity of 1.52 g $L^{-1}h^{-1}$ at a dilution rate of 0.30 h^{-1}. This productivity was higher than any value reported in literature for continuous MCL-PHA production systems and comparable to the upper range of fed-batch results. Two-stage production yielded promising results, notably the increase in polymer content from the first to second stage. However, complications involving foaming and an unexplained decline in PHA content adversely affected system performance. The best PHA content and overall productivity were 58.5 wt% and 0.76 g $L^{-1}h^{-1}$, respectively. Nonetheless, the results demonstrate the potential to achieve high PHA content without the need for pure oxygen at high dilution rates, warranting further investigation focusing on the optimization of growth conditions.

Co-Authorship

The author was supervised by Drs. Bruce and Juliana Ramsay, who contributed to the preparation of this thesis.

Acknowledgements

There are several people that must be acknowledged for their contributions in helping me complete my thesis over the past two years. Firstly, my supervisors Drs. Bruce and Juliana Ramsay for their guidance, support and constructive criticism that helped shape my research. They challenged me to think critically and persevere through the many challenges I encountered in my work. I am grateful for all I have learned and the skills I have developed while under their supervision.

I would be remiss if I did not acknowledge the special contributions of Dr. Zhiyong Sun and Hang Li throughout my work. From the time I started, they were both incredibly helpful in demonstrating techniques, providing suggestions and answering my countless questions. They helped me hit the ground running, which allowed me to be productive during my time as a graduate student. I would not have been able to succeed without their help. To the rest of my lab mates Eric, Natalie, Siqing and Dr. Xian Jiang, thanks for your help and friendly conversation in the lab. I wish everyone the best of luck with their future endeavours.

I am extremely fortunate to have such a loving and supportive family in my life. I would not be anywhere without my parents, Loretta and Scott, my brother, Matthew, and my large extended family.

To my girlfriend Amanda, thank you for putting up with me the past couple of years. I wasn't always a pleasure to around on account of the long nights in the lab, but your love, patience and encouragement kept me going.

Finally, I need to mention the amazing group of friends. You helped me blow off steam, relax and truly enjoy my six years at Queen's. To my long-term friends and housemates Anthony and Martino, our friendship has been forged through some great experiences and I know we have many more good times ahead. Dan, you have been my chemical engineering buddy since second year. I appreciate all of our

stimulating discussion, especially over the last couple of years.

This work was funded was provided by the Natural Sciences and Engineering Research Council of Canada (NSERC). I was largely supported by scholarships from NSERC (2009-2010), Ontario Graduate Scholarship Program (OGS, 2010-2011) and the Queen's Graduate Award (2009-2011).

Table of Contents

List of Figures

List of Tables

List of Symbols and Abbreviations

5POHV 3-hydroxy-5-phenoxyvalerate

7POHH 3-hydroxy-7-phenoxyheptanoate

9POHN 3-hydroxy-9-phenoxynonanoate

11-POU 11-phenoxyundecanoic acid

AA Acrylic acid

ACP Acyl carrier protein

ATP Adenosine-5'-triphosphate

AMP Adenosine monophosphate

CoA Co-enzyme A

CO_2 Carbon dioxide

C6 3-hydroxyhexanoate

C7 3-hydroxyheptanoate

C8 3-hydroxyoctanoate

C9 3-hydroxynonanoate

C9:1 3-hydroxynonenoate

C10 3-hydroxydecanoate

C11 3-hydroxyundecanoate

C11:1 3-hydroxyundecenoate

C12 3-hydroxydodecanoate

C12:1 3-hydroxydodecenoate

C14:1 3-hydroxytetradecenoate

CPR CO2 production rate

D Dilution rate (h^{-1}, D equals to μ at steady state in chemostat fermentation)

DCW Dry cell weight

DO Dissolved oxygen

Glu Glucose

GC Gas chromatography

MCL Medium-chain-length

MCL-PHA medium chain length poly-3-hydroxyalkanoates

NA Nonanoic acid

NAD^+ Nicotinamide adenine dinucleotide

NADH Nicotinamide adenine dinucleotide (reduced)

$NADP^+$ Nicotinamide adenine dinucleotide phosphate

NADPH Nicotinamide adenine dinucleotide phosphate (reduced)

O_2 Oxygen

OA Octanoic acid

PHA Poly-3-hydroxyalkanoate

PPi Pyrophosphate

rRNA ribosomal ribonucleic acid

rpm Revolutions per minute

SCL Short-chain-length

SCL-PHA Short-chain-length poly-3-hydroxyalkanoates

μ Specific growth rate (h^{-1})

$UDA^{=}$ 10-undecenoic acid

vvm The volumetric air flow rate (ml min^{-1}) divided by the working volume of the fermentor

$Y_{PHA/NA}$ Yield of PHA from nonanoic acid (g/g)

Chapter 1

Introduction

1.1 Overview of the polymer industry

The synthetic polymer industry is a vital contributor to the economy because the manufacture of virtually all goods, from automobile parts to food packaging, depends on plastics as an input. Their good mechanical properties, customizability and low costs have driven the industry's staggering growth over the past 60 years. In 2000, worldwide production of polymers was 120 million tonnes and the consumption per capita reached 20 kg per year (Meyer and Keurentjes, 2005). However, a major concern is that these ubiquitous materials (polyethylene, polypropylene, polyvinyl chloride, etc.) are derived from finite petroleum feedstocks, whose worldwide demand continues to grow. Consequently, there is a need for economically viable polymers derived from renewable resources that have good mechanical properties. A promising option is a class of polyesters known as poly(3-hydroxyalkanoates) (PHAs) that are not only produced from renewable resources but are biodegradable and biocompatible as well.

1.2 MCL-PHA structure and properties

PHAs are classified into two large categories according to the length of the side chain (R group in Figure 1-1): short-chain-length PHA (SCL-PHA) has monomer units with fewer than six carbon atoms, while medium-chain-length (MCL) PHA monomer units typically have six to fourteen carbon atoms. MCL-PHA is of special interest because it has elastomeric properties, contrary to its more brittle SCL counterparts. In general, MCL-PHA has melting points (T_m) in the range of 40°C to 60°C and glass transition temperatures (T_g) between -50°C to -25°C (Witholt and Kessler, 1999). Potential applications for PHA that have been discussed in literature include films and coatings (Dufresne and Samain, 1998, Marchessault *et al*., 1995) and various applications in the medical field due to their biodegradability and biocompatibility, such as drug delivery, tissue engineering, medical devices and implants (Wu *et al*., 2009).

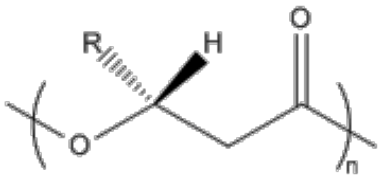

Figure 1-1: General structure of PHA
R is less than three carbon atoms in SCL-PHA; R is equal to or greater than three carbon atoms in MCL-PHA

1.3 Synthesis of MCL-PHA

MCL-PHA is produced by bacteria belonging to the ribosomal ribonucleic acid (rRNA) homology group I, predominantly fluorescent pseudomonads, as a carbon and energy reserve (Huisman *et al.,* 1989; Timm and Steinbüchel, 1990). Bacteria accumulate MCL-PHA intracellularly as granules, which may be extracted and purified from the fermentation broth during downstream processing. It has been well established that the β-oxidation pathway, which catabolizes fatty acids, supplies substrates to enzymes in the MCL-PHA production pathway (Eggink *et al.*, 1992). Consequently, the chemical structure of the fatty acid carbon source provided to the bacteria directly influences the structure, and therefore properties, of the polymer. It has been found that some PHA synthase enzymes, particularly those found in *Pseudomonads*, have relatively low substrate specificity allowing a broad range of MCL-PHA to be produced (Rehm, 2003). Researchers have experimented with many different types of fatty acids, leading to the synthesis of MCL-PHA with features such as double bonds and various functional groups in the side chains (Steinbüchel and Valentin, 1995).

1.3.1 *In vivo* production of MCL-PHA containing a side-chain carboxyl group

Interestingly, the incorporation of side chain carboxyl functionality into MCL-PHA has never been done through the conventional *in vivo* route. Carboxyl groups are desirable because they improve the hydrophilicity of MCL-PHA (Lee and Park, 2000; Kurth *et* al., 2002; Stigers and Tew, 2003), which should facilitate easier blending with other relatively inexpensive biopolymers such as polylactic acid (PLA) and thermoplastic starch. The ultimate goal is to develop cost-competitive blends with the desirable properties of MCL-PHA at a lower cost. Furthermore, carboxyl groups increase reactivity for subsequent chemical reactions. To date, the only reported method for producing carboxylated MCL-PHA involved *ex vivo* chemical modification of MCL-PHA containing a double bond (Lee and Park, 2000; Kurth *et* al., 2002; Stigers and Tew, 2003). Although effective, this process is economically unfavorable due to the added

complexity in manufacturing. In addition, it can result in an undesirable loss of molecular weight. *In vivo* synthesis should be a considerably simpler process that eliminates the additional expense of downstream chemical modification and unwanted molecular weight losses.

1.4 Economic considerations in MCL-PHA production

In addition to blending with inexpensive bioplastics, another way to overcome the economic barrier to market entry is by decreasing the costs associated with MCL-PHA production. Sun *et al*. (2007b) identified that the production costs associated with MCL-PHA production are roughly split evenly between purchasing the carbon source, running the fermentation and performing the separation. Accordingly, reductions to these costs can be realized by achieving specific performance goals. Firstly, increasing MCL-PHA yield from the carbon source minimizes the amount of fatty acid, which is relatively expensive, that is not converted to polymer. A successful strategy developed by Sun and coworkers (2009b), co-feeds an inexpensive carbon source like glucose with the more expensive fatty acid. The rationale is that bacteria use inexpensive carbon source as a source of carbon and energy to yield rest biomass, while the fatty acid can be used almost exclusively for polymer production. Secondly, improving reactor productivity and reducing operating costs help to decrease fermentation costs. Typically, fed-batch processes are used for producing MCL-PHA because they have good productivity and are effective in achieving high product concentrations. Unfortunately, to achieve high product concentrations, fed-batch systems eventually require pure oxygen (O_2) for aeration to meet the increased O_2 demand at higher biomass concentrations, creating additional expense. Finally, since the cost of separation is inversely proportional to the intracellular MCL-PHA content (Sun *et al*., 2007b), improving the average amount of polymer in bacterial cells translates to downstream process cost savings.

1.4.1 High-cell density two-stage carbon-limited chemostat for MCL-PHA production

A high-cell density, carbon-limited (C-limited), two-stage chemostat for MCL-PHA production was identified as a system that had potential to achieve the aforementioned performance goals, thereby reducing costs in all phases of the process. Although fed-batch systems are the standard for larger scale production, Jung *et al*. (2001) illustrated that a two-stage nitrogen-limited (N-limited) chemostat was able to achieve

good productivity and MCL-PHA content from fatty acids. Positive results were also obtained for single-stage chemostats in work done by Hazenberg and Witholt (1997) and Jiang (2010). Although biomass concentrations are considerably lower in continuous processes compared to fed-batch processes, a high-cell density setup helps to partially alleviate this concern. There are also key advantages offered by continuous systems, namely no process downtime and precise control over the specific growth rate. A two-stage chemostat provides additional cell residence time through a second reactor in series, which is believed to have an enhancing effect on intracellular MCL-PHA content. In addition, the additional O_2 transfer capacity provided by a second reactor allowed relatively high biomass concentrations to be reached without the need for costly pure O_2 aeration.

1.5 Objectives

The principal objectives of this thesis encompassed two focused strategies for more economical production of MCL-PHA: the *in vivo* production of hydrophilic MCL-PHA containing a side chain carboxyl group for biopolymer blending and the use of a high-cell density, C-limited, two-stage chemostat system for increased productivity and intracellular MCL-PHA content. In order to accomplish these objectives, a series of tasks were defined and completed. For *in vivo* production of carboxylated MCL-PHA, the following tasks were undertaken:

- Selection of an appropriate fatty acid carbon source, according to the fundamentals of the metabolic pathways involved in MCL-PHA synthesis
- Selection of a suitable bacterial strain through literature review and data obtained from specially designed shake flask screening experiments
- Design and completion of chemostat studies providing the best growth conditions for carboxylated MCL-PHA production

For the high-cell density, C-limited, two-stage chemostat system for MCL-PHA, the following were addressed:

- Determination of two-stage feeding conditions yielding high MCL-PHA content based on single-stage experimentation

- Design and operation of a high-cell density, C-limited, two-stage chemostat system for MCL-PHA production
- Aeration without using pure O_2 (air only) for economical operation

The selection of the MCL-PHA production strain and carbon sources used was based on previous work completed by the Ramsay group using fed-batch and chemostat setups. In these works by Sun *et al*. (fed-batch, 2007a; 2009a; 2009b) and Jiang (chemostat, 2010) *P. putida* KT2440 was proven to be an excellent producer of MCL-PHA from nonanoic acid (NA). As previously described, glucose co-feeding was discovered as a strategy for increasing MCL-PHA yield from NA in a fed-batch setup (Sun *et al*., 2009b), which was used in subsequent single-stage chemostat work (Jiang, 2010). Therefore, investigated as the second principal objective of this thesis, the high-cell density, C-limited, two-stage chemostat system for MCL-PHA production used *P. putida* KT2440 and NA co-fed with glucose.

1.6 Scope

The scope of this thesis project comprises six distinct chapters:

- Background, justification and motivation for the project, including a brief outline of the work completed (Chapter 1)
- A review of relevant literature (Chapter 2)
- A detailed description of the materials and methods used to complete the experimental work (Chapter 3)
- Results, interpretation and discussion of the work pertaining to *in vivo* production of MCL-PHA containing a side chain carboxyl group (Chapter 4)
- Results, interpretation and discussion of the work pertaining to high-cell density, C-limited, two-stage chemostat for MCL-PHA production (Chapter 5)
- Conclusions and recommendations for future work based on the findings discussed herein (Chapter 6)

Chapter 2

Literature Review

2.1 Synthesis of MCL-PHA in pseudomonads

MCL-PHA is produced by pseudomonads belonging to rRNA homology group I, which includes *Pseudomonas putida, P. aeruginosa* and *P. fluorescens* (Madison and Huisman, 1999), as a carbon and energy reserve. Until recently it was believed that nutrient-limited growth conditions (nitrogen (N) or phosphorus (P)) stimulated MCL-PHA production in pseudomonads. However, this was determined to be unnecessary for *P. putida* KT2440, a common production strain, which accumulates MCL-PHA readily under carbon-limited (C-limited) conditions (Sun *et al*., 2007a).

2.1.1 Classification of MCL-PHA by carbon source

There are two categories of MCL-PHA, classified according to the pathways from which they are derived: MCL-PHA from related carbon sources and MCL-PHA from unrelated carbon sources (Lu *et al*., 2009). MCL-PHA from related carbon sources is composed of monomers that are structurally similar to the carbon source provided to the bacteria. Carbon sources in this group include aliphatic alkanes, alkenes and fatty acids (Lenz *et al.*, 1992; Steinbüchel and Valentin, 1995). On the other hand, MCL-PHA from unrelated carbon sources contains monomers that do not bear structural similarities to the carbon source provided for growth. These include compounds such as glucose (Huijberts *et al*., 1992), gluconate (Timm and Steinbüchel, 1990), fructose (Sanchez *et al*., 2003) and other carbohydrates (Haywood *et al*., 1990). The difference between these categories of MCL-PHA derives from the metabolic pathways that supply precursors for MCL-PHA synthesis. As shown by Eggink *et al*. (1992) though ^{1}H-NMR and ^{13}C-NMR studies with *P. putida* KT2442, MCL-PHA precursors are supplied by the β-oxidation and the *de novo* fatty acid biosynthesis pathways.

2.1.2 Metabolic pathways involved in MCL-PHA production

2.1.2.1 β-oxidation

The β-oxidation cycle is used to catabolize fatty acids and comprises five enzyme-catalyzed steps: activation (fatty acid thioester formation), first dehydrogenation ((*S*)-acyl-CoA formation), hydration (*trans*-2-enoyl CoA formation), second dehydrogenation (3-ketoacyl-CoA formation) and thiolysis (Prescott, Harley and Klein, 2002). The final step cleaves an acyl-CoA molecule to generate a molecule of acetyl-CoA, leaving an acyl-CoA fragment that is two carbon atoms shorter than the original initial fatty acid. This remaining acyl-CoA fragment can then undergo subsequent cycles of β-oxidation. In pseudomonads, a series of enzymes oxidizes *n*-alkanes into their analogous carboxylic acids (*n*-alkane → primary alcohol → aldehyde → carboxylic acid), which are then degraded by the β-oxidation pathway (Grund *et al*., 1975).

2.1.2.2 *De novo* fatty acid biosynthesis

The *de novo* fatty acid biosynthesis pathway synthesizes fatty acids through the addition of acetyl-acyl carrier protein (acetyl-ACP) with each turn of the cycle. The process is essentially the reverse of the β-oxidation cycle. There are six enzymatic steps in this pathway: formation of malonyl-CoA, activation of malonyl-CoA (conversion to malonyl-ACP), addition of acetyl-ACP to acyl-ACP (3-ketoacyl-ACP formation), first reduction ((*R*)-3-hydroxyacyl-ACP formation), dehydration (*trans*-2-enoyl-ACP formation) and second reduction (acyl-ACP formation) (Madison and Huisman, 1999).

2.1.2.3 PHA synthase

PHA synthase or PhaC (encoded by *phaC* genes) is the key enzyme involved in the production of PHA; its role is to polymerize a substrate, (*R*)-3-hydroxyacyl-CoA, into polyester (Steinbüchel *et al*., 1992). Synthases have affinities for different substrate lengths depending on the bacterial strains from which they originate, which ultimately determine the kind of PHA produced. MCL-PHA producing pseudomonads have class II synthases that low substrate specificity and a preference for (*R*)-3-hydroxyl-CoA substrates having between six and fourteen carbons in length (Rehm, 2003). The low specificity of class II synthases is reflected in the diversity of MCL-PHA that has been produced (Lu *et al*., 2009).

2.1.2.4 PhaG: a link between *de novo* fatty acid biosynthesis and PHA synthase

In order for MCL-PHA production to occur from products of *de novo* fatty acid biosynthesis, a key enzyme must bridge the gap between the metabolic pathways and PHA synthase by converting pathway intermediates into (*R*)-3-hydroxyacyl-CoA. Rehm and coworkers (1998) established that the enzymatic link between *de novo* fatty acid biosynthesis and MCL-PHA synthesis is (*R*)-3-hydroxyacyl-ACP to (*R*)-3-hydroxyacyl-CoA transferase (PhaG, encoded by *phaG*). Subsequent work by Fiedler *et al*. (2000) conclusively established the role of PhaG in a publication that investigated recombinant strains of *P. fragi*, a non-MCL-PHA producer. In this study, a recombinant strain expressing *phaG* ((*R*)-3-hydroxyacyl-ACP:CoA transferase) from *P. putida* U and *phaC* (PHA synthase) from *P. aeruginosa* PAO1 produced a significant amount of MCL-PHA from gluconate, an unrelated carbon source.

2.1.2.5 PhaJ and FabG: links between β-oxidation and PHA synthase

Identifying the enzymes linking β-oxidation and (*R*)-3-hydroxyacyl-CoA has been a heavily studied area of PHA research. Lageveen *et al*. (1988) first postulated that an epimerase was responsible for converting (*S*)-3-hydroxyacyl-CoA to the *R* enantiomer required by PHA synthase. However, to date there has been no conclusive evidence to support this hypothesis and advances in genome sequencing have directed research in the past decade towards other possibilities. Tsuge and coworkers (2000; 2003) identified four different enoyl-CoA hydratases (PhaJ) in *P. aeruginosa* PAO1, with different substrate specificities that convert *trans*-2-enoyl-CoA into (*R*)-3-hydroxyacyl-CoA. Results from PHA synthesis studies using recombinant *Escherichia coli* strains provided compelling evidence to support the role of PhaJ as a supplier of (*R*)-3-hydroxyacyl-CoA. Recombinants expressing a *phaJ* from *P. aeruginosa* PAO1 and *phaC* from *Pseudomonas* sp. 61-3 produced considerably more MCL-PHA from dodecanoate than the recombinant expressing *phaC* alone. The specific *phaJ* from *P. aeruginosa* PAO1 that was expressed also had a large influence on the monomeric composition of the polymer due to its preference for substrates with a certain chain length (Tsuge *et al*., 2003). More supporting data was provided in recombinant *E. coli* studies by Fiedler *et al*. (2002) expressing *phaJ* genes from two prolific MCL-PHA producers, *P. putida* KT2440 and *P. putida* GPo1 (formerly *P. oleovorans*). A recombinant *E. coli* strain expressing *phaJ* and *phaC* from *P.*

putida GPo1 was able to produce MCL-PHA from decanoate containing C10, C8 and C6 monomers. Furthermore, this recombinant strain produced MCL-PHA containing a significantly higher proportion of longer chain monomers (C10 and C8) than a recombinant *E. coli* expressing only *phaC*. As noted by Tsuge *et* al. (2003) this data suggested that PhaJ was responsible for channeling intermediates from β-oxidation to PHA synthase because the specificity of the PhaJ influenced the composition of (*R*)-3-hydroxyacyl-CoA precursors, and therefore the monomeric composition of the polymer. Similar results were found in a recent publication by Sato *et al*. (2011), in which PhaJs from *P. putida* KT2440 were investigated.

Evidence for a second link between β-oxidation and MCL-PHA synthesis has been provided in recent literature. Using *P. aeruginosa* PAO1 it was shown that 3-ketoacyl-ACP reductase (FabG) in the *de novo* fatty acid biosynthesis pathway also acts as a 3-ketoacyl-CoA reductase, catalyzing the conversion from 3-ketoacyl-CoA to (*R*)-3-hydroxyacyl-CoA (Ren *et al*., 2000). In this study, MCL-PHA production from two recombinant *E. coli* mutants expressing *fabG* and *phaC* from *P. aeruginosa* PAO1 were compared: one deficient in β-ketothiolase (encoded by *fadA*) and another deficient in 3-hydroxyacyl-CoA dehydrogenase (encoded by *fadB*). 3-ketoacyl-CoA is the product of 3-hydroxyacyl-CoA dehydrogenase and the substrate of both β-ketothiolase and 3-ketoacyl-CoA reductase (FabG). When grown on hexadecanoate, the *fadA* mutant produced more MCL-PHA than the *fadB* mutant, providing strong support for FabG as a supplier of precursor for PHA synthase (Ren *et al*., 2000). More recent work with recombinant *E. coli* by Park and coworkers (2002) and Nomura and coworkers (2008) supports the role of FabG as a linking enzyme that converts 3-ketoacyl-CoA, an intermediate in β-oxidation, to (*R*)-3-hydroxyacyl-CoA, substrate for PHA synthase.

2.1.2.6 Implications for MCL-PHA synthesis

Figure 2-1 illustrates the pathways involved in the synthesis of MCL-PHA in pseudomonads based on the current literature findings. Due to the nature of the pathways supplying precursor, MCL-PHA is typically synthesized as a natural copolymer. For a single bacterial strain, MCL-PHA derived from unrelated carbon sources like carbohydrates has roughly the same composition, comprising primarily 3-hydroxydecanoate

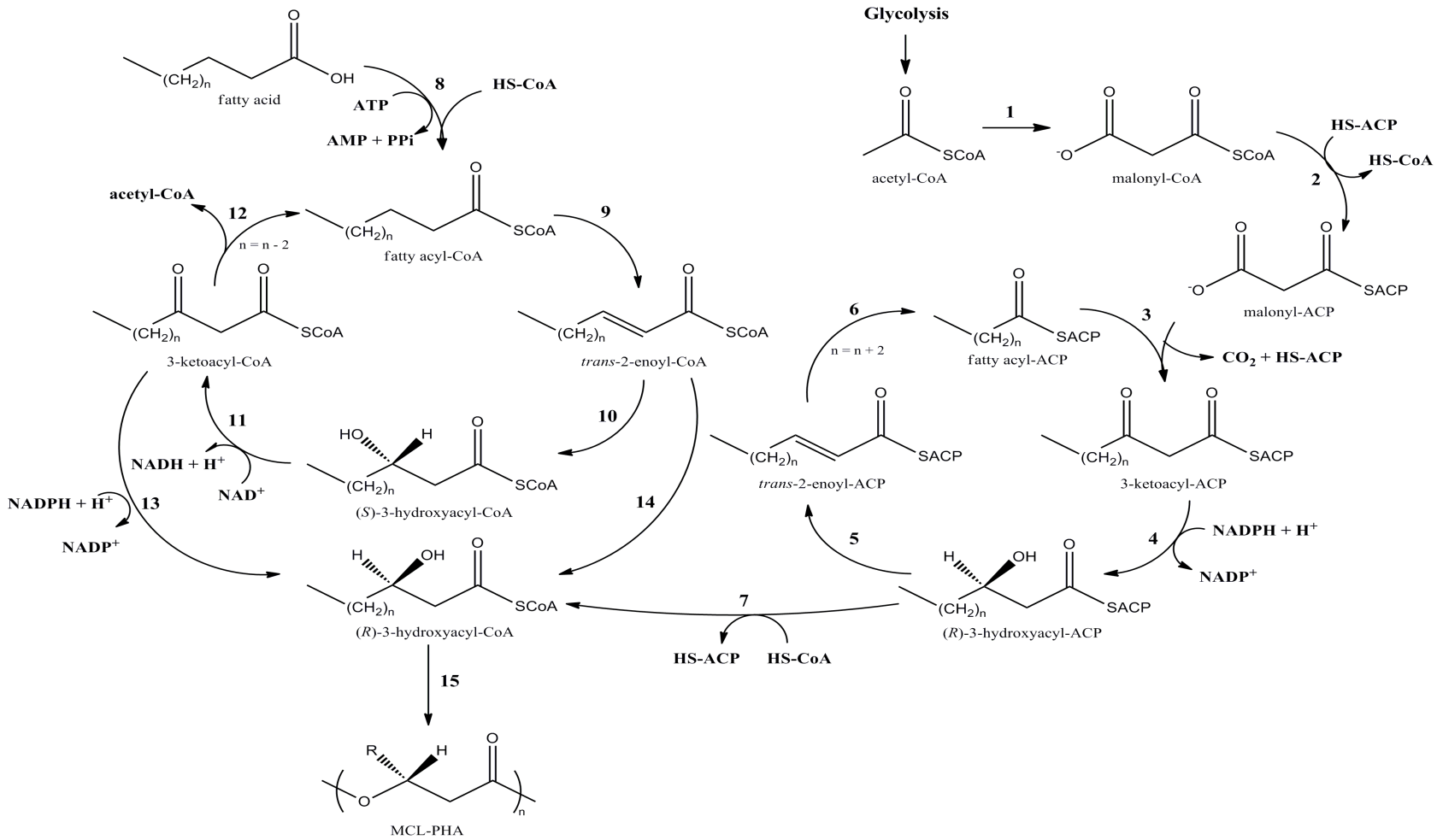

Figure 2-1: MCL-PHA synthesis pathways in pseudomonads (adapted from Lu *et al*., 2009)
Enzyme key: 1) acetyl-CoA carboxylase; 2) malonyl transacylase; 3) 3-ketoacyl-ACP synthase; 4) 3-ketoacyl-ACP reductase (FabG); 5) 3-hydroxyacyl-ACP dehydratase; 6) enoyl-ACP reductase; 7) (*R*)-3-hydroxylacyl-ACP to (*R*)-3-hydroxyacyl-CoA transferase (PhaG); 8) acyl-CoA thiokinase; 9) acyl-CoA dehydrogenase; 10) enoyl-CoA hydratase; 11) 3-hydroxyacyl-CoA dehydrogenase; 12) β-ketothiolase; 13) 3-ketoacyl-CoA reductase (FabG); 14) (*R*)-specific enoyl-CoA hydratase (PhaJ); PHA synthase (PhaC).

(C10) and 3-hydroxyoctanoate (C8) monomers (Haywood *et al*., 1990; Huijberts *et al*., 1992). The structure of MCL-PHA derived from related carbon sources, like fatty acids, is determined by the structure of carbon source fed for growth. Monomer units have length C_{n-2x} where n is the number of carbon atoms in the fatty acid fed to the bacteria and x is the number of cycles of β-oxidation that occur (Eggink *et al*., 1992). For eight to ten carbon fatty acids, the most efficient with respect to MCL-PHA synthesis, monomer units of length C_n and C_{n-2} comprise the vast majority of the polymer composition (Brandl *et* al., 1988, Lageveen *et* al., 1988; Huisman *et al*., 1989; Gross *et al*., 1989). For example, *P. putida* GPo1 produced MCL-PHA containing 91 mol% C8 and 9 mol% C6 when grown on octanoate (Huisman *et al*., 1989). Similarly, *P. putida* KT2440 produced MCL-PHA consisting of approximately 70 mol% 3-hydroxynonanoate (C9) and 30 mol% 3-hydroxyheptanoate (C7) monomers from nonanoic acid (NA) (Sun *et al*., 2007a). Due to the specificity of enzymes in the relevant pathways, monomer units longer than 14 carbons cannot be incorporated into polymer (Huisman *et al*., 1989; Madison and Huisman, 1999). For instance, when *P. putida* KT2442 produced MCL-PHA from oleic acid (18 carbons), five different monomers were represented, the largest of which was 3-hydroxytetradecenoate (C14:1), followed by 3-hydroxydodecanoate (C12), C10, C8 and C6 (Kellerhals *et al*., 2000).

MCL-PHA synthesized from mixtures of carbon sources yields polymer that contains monomer units derived both carbon sources, the distribution of which is related to their ratio in feeding, as illustrated by Sun and coworkers (2009a). In this study, *P. putida* KT2440 produced MCL-PHA consisting of predominantly C9, C7, 3-hydroxyundecenoate (C11:1) and 3-hydroxynonenoate (C9:1) from mixtures of NA and 10-undecenoic acid ($UDA^{=}$) in fed-batch fermentations. When the ratio of $UDA^{=}$:NA was increased in the feed, MCL-PHA contained a greater proportion of C11:1 and C9:1 and C7:1 monomers derived from $UDA^{=}$ (Sun *et al*., 2009a).

2.2 MCL-PHA containing functionalized side chains

The synthesis of MCL-PHA containing unique functional groups is especially pertinent to one of the main objectives of this thesis: the *in vivo* synthesis of MCL-PHA containing a side chain carboxyl group. Comprehensive reviews by Steinbüchel and Valentin (1995) and Lu *et al*. (2009) list the various functional groups that have been reported in MCL-PHA in literature, including unsaturated, branched, phenyl, halogen and ester groups in monomer side chains. Because β-oxidation occurs from the carboxyl terminus of fatty acids (Figure 2-1), functional groups at the opposite end of the molecule can be incorporated into MCL-PHA, the success of which is contingent on the specificity enzymes upstream of the polymer. For example, *P. putida* GPo1 produced MCL-PHA with methyl branched side chains when grown on the methyl branched carbon source, 7-methyl octanoate (Fritzsche *et al*., 1990).

Also using *P. putida* GPo1, Lenz and coworkers (1992) demonstrated that carbon sources that do not support PHA production, like 11-bromoundecanoic acid, can been incorporated into MCL-PHA through co-metabolism with good substrates for PHA production like octanoic acid (OA) and NA. Another example included *P. putida* GPo1 and *P. putida* KT2442 producing MCL-PHA containing fluorinated side chains when fluorinated acids were provided as co-substrates with NA (Kim *et al*., 1996). However, the mechanism for this phenomenon remains unknown.

2.2.1 Incorporation of side chain carboxyl groups *ex vivo*

The synthesis of carboxylated MCL-PHA has been accomplished by three similar methods of chemical carboxylation of unsaturated side chains in purified poly(3-hydroxyoctanoate-*co*-3-hydroxyundecenoate) (PHOU) (Lee and Park, 2000; Kurth *et* al., 2002; Stigers and Tew, 2003). The reactions described by Lee and Park (2000) and Kurth *et* al. (2002) use potassium permanganate ($KMnO_4$) as the oxidizing agent (Figure 2-2), while Stigers and Tew (2003) used osmium tetroxide (OsO_4) and potassium peroxymonosulftate (Oxone® by DuPont).

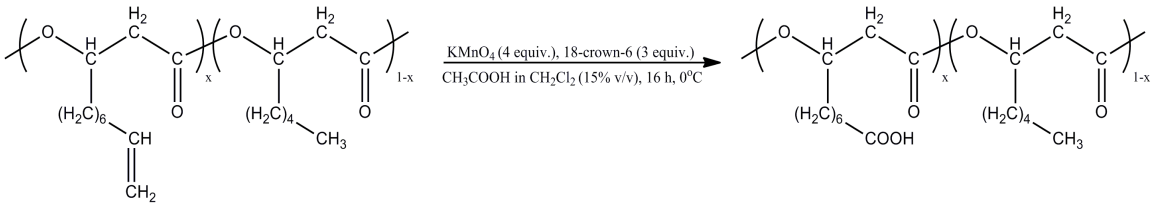

Figure 2-2: Carboxylation of PHOU using the method of Kurth and coworkers (2002)
x refers to the fraction of monomers containing an unsaturated side chain
reagent equivalents calculated based on number of unsaturated units

In all studies, the presence of carboxyl groups was detected using infrared (IR) spectroscopy and proton nuclear resonance imaging (^{1}H-NMR). Characterizing polymer solubility in solvents with a range of polarities, before and after modification, showed improved hydrophilicity. For example, Stiger and Tew (2003) observed that modified PHOU containing 9% carboxyl groups was soluble in more polar solvents including: 10% water in acetone, 10% water in tetrahydrofuran (THF) and 20% water in THF. Prior to modification, PHOU was insoluble in these solvents. All three *ex vivo* synthesis methods reported some loss of molecular weight, which was severe in the case of Lee and Park (2000). *In vivo* production of carboxylated MCL-PHA has not been reported in literature.

2.2.2 Dicarboxylic acids as candidate substrates for *in vivo* production of carboxylated MCL-PHA

According literature findings and the mechanism of β-oxidation, a compound with two terminal carboxyl groups should be a good candidate carbon source for *in vivo* production of MCL-PHA containing a side chain carboxyl group. In order to produce this type of functionalized MCL-PHA, one of the two terminal carboxyl groups must be preserved through β-oxidation so that the resultant (*R*)-3-hydroxyacyl-CoA also contains a carboxyl group. If this occurs, polymerization by PHA synthase will result in monomers that contain side chain carboxyl groups. However, the critical requirement for success is that PHA synthase and all enzymes located upstream of PHA synthase must be able to catalyze substrates containing a carboxyl group. Even if carboxylated intermediates are present, one key enzyme incapable of utilizing its substrate will prevent the desired MCL-PHA from being synthesized. The demonstrated broad specificity of several of these enzymes in literature suggests that this requirement is likely to be met. Due to the efficiency with

which OA and NA are converted to MCL-PHA, azelaic acid (AzA), a nine-carbon α,ω-dicarboxylic acid, was selected as the carbon source for the experimental work completed in chapter 4 of this thesis.

2.2.2.1 Catabolism of dicarboxylic acids

The ability to catabolize AzA and other higher dicarboxylic acids is possessed by some pseudomonads, including: *P. azelaica* (Janota-Bassalik and Wright, 1964), *P. aeruginosa*, some strains of *P. fluorescens, P. stutzeri,* and *P. acidovorans* (Stanier *et al*., 1966) and *P. citronellolis* (Choi and Yoon, 1994). Degradation of dicarboxylic acids was shown to occur via β-oxidation in *P. aeruginosa* 8602 (Chapman and Duggleby, 1967) and *P. fluorescens* St. 18 (Hoet and Stanier, 1970) and is generally accepted as the route by which capable pseudomonads degrade dicarboxylic acids. In this thesis, *P. fluorescens* ATCC 17400 and *P. citronellolis* DSM 50332 were the strains selected for examination with respect to carboxylated MCL-PHA production.

2.2.2.2 Azelaic acid degrader: *P. fluorescens* ATCC 17400

P. fluorescens ATCC 17400 is a psychrophilic bacterium that was isolated from a hen's egg. It is capable of growing on a diverse range of compounds as sole sources of carbon and energy (Stanier *et al*., 1966). Several studies have focused on its ability to produce iron-chelating compounds (siderophores), however there are no publications in the context of PHA production.

2.2.2.3 Azelaic acid degrader: *P. citronellolis* DSM 50332

P. citronellolis DSM 50332 was isolated from soil under pine trees through an enrichment culture that employed citronellol as a sole source of carbon (Seubert, 1960). It has been shown to have the unusual ability to grow on recalcitrant branched hydrocarbons (Fall *et al*., 1979) and terpenes on account of its acyclic terpene utilization pathway (Förster-Fromme and Jendrossek, 2010). However, only one publication has studied *P. citronellolis* DSM 50332 in the context of MCL-PHA production. Choi and Yoon (1994) assessed PHA production from a vast and diverse number of substrates, revealing that that *P.*

citronellolis DSM 50332 produced MCL-PHA from both related and unrelated carbon sources. Moreover, it was able to accumulate MCL-PHA from unusual carbon sources, including a variety of 3-methyl branched compounds and α,ω-dicarboxylic acids. Interestingly, all α,ω-dicarboxylic acids tested, ranging from succinic acid (four carbons) to sebacic acid (ten carbons), yielded MCL-PHA consisting of C10 and C8 monomers in nearly identical proportions. This MCL-PHA was remarkably similar to the MCL-PHA obtained from acetate, propionate, butyrate, glucose and gluconate (Choi and Yoon, 1994).

On the other hand, medium chain length monocarboxylic acids produced MCL-PHA containing monomer units consistent with precursor supply via β-oxidation. For example, NA yielded MCL-PHA composed of C9 and C7 monomers, while its dicarboxylic analogue (AzA) resulted in C8 and C10 MCL-PHA (Choi and Yoon, 1994). Presumably, like other pseudomonads, *P. citronellolis* degrades α,ω-dicarboxylic acids by β-oxidation as discussed in Section 2.2.2.1. Therefore, the most likely explanation for the composition of MCL-PHA derived from these carbon sources is as follows: complete degradation by β-oxidation to acetate followed by production of MCL-PHA precursors via *de novo* fatty acid biosynthesis. By this route, MCL-PHA accumulated from α,ω-dicarboxylic acids is essentially unrelated to the carbon source, explaining the similarities to MCL-PHA derived from other unrelated carbon sources such as glucose. However, techniques such as co-metabolism and β-oxidation inhibition may provide a way to channel carboxylated intermediates derived from AzA to PHA synthase and were therefore investigated as part of this thesis.

2.2.3 Inhibition of key enzymes for enhanced MCL-PHA production

Chemical inhibitors have been used to impair the function of specific enzymes involved in β-oxidation to selectively channel precursors to PHA synthase. Acrylic acid (AA) has been used most commonly because it inhibits β-ketothiolase, the final enzyme in the β-oxidation pathway, responsible for cleaving acetyl-CoA from 3-ketoacyl-CoA (Thijsse, 1964). As a result of β-ketothiolase inhibition with AA, the supply of acetyl-CoA to Krebs cycle diminishes. Therefore, the provision of a second source of carbon energy is essential for bacterial growth.

2.2.3.1 Increased PHA content

In a 1998 publication by Qi *et al*., the use of AA resulted in a drastic increase in PHA content from decanoate in various recombinant strains of *E. coli* expressing a *phaC* gene from *P. aeruginosa*. In shake flask experiments, a concentration of 0.2 g/L AA increased PHA content by as much as 30 times, compared to identical growth medium containing no AA. Similar PHA content was achieved in in a 20-L fed-batch fermentation using decanoate and the same concentration of AA, reaching a maximum of 38 wt%. LB medium provided supplemental carbon in all cases (Qi *et al*., 1998).

2.2.3.2 Compositional shift towards longer chain monomers

Inhibition of β-ketothiolase has also been shown to shift the composition of MCL-PHA toward longer chain monomers. Choi and coworkers (2009) investigated the effect of AA on MCL-PHA production from fructose and 11-phenoxydecanoaic acid (11-POU) using *P. fluorescens* BM07 in shake flask experiments. The presence of AA had a negligible effect on the polymer content derived from 11-POU, however it shifted the monomer distribution towards longer units. An AA concentration of 2 mM resulted in 52 mol% 3-hydroxy-5-phenoxyvalerate (5POHV), 42 mol% 3-hydroxy-7-phenoxyheptanoate (7POHH) and 6 mol% 3-hydroxy-9-phenoxynonanoate (9POHN) compared to 81 mol% 5POHV, 15 mol% 7POHH and 4 mol% 9POHN in the absence of inhibitor. Salicylic acid (SA) produced comparable results in an identical experiment, suggesting that SA inhibited β-ketothiolase in a similar fashion to AA (Choi *et al*., 2009).

2.2.3.3 Enhanced PHA content and compositional control

Jiang (2010) observed significant enhancement in PHA content and the proportion of long chain monomers in *P. putida* KT2440 when AA was used in a C-limited chemostat system ($D=0.25\ h^{-1}$) co-feeding glucose and OA or NA. For inlet carbon concentrations of 3.6 g/L OA and 3.9 g/L glucose, an AA concentration of 0.2 g/L resulted in 48 wt% PHA containing 98 mol% C8 and 2 mol% C6, compared to 15 wt% PHA having 88 mol% C8 and 12 mol% C6 in the absence of inhibitor. Similarly, for 2.9 g/L NA and 3.9 g/L glucose, an AA concentration of 0.15 g/L resulted in 64 wt% PHA containing 95 mol% C9 and 5 mol% C7,

compared to 11 wt%, 69 mol% C9 and 31 mol% C7 without AA. Incorporation of AA into a fed-batch fermentation using glucose and NA produced equally impressive results: 71.4 g/L biomass, 75.5 wt% PHA containing 88.9 mol% C9 (balance C7) and reactor productivity of 1.8 g $L^{-1}h^{-1}$ for a mass feeding ratio of 1.25 NA to 1.00 glucose to 0.05 AA (Jiang, 2010).

2.2.3.4 Implications for *in vivo* production of carboxylated MCL-PHA

The inhibition of β-oxidation may improve the probability of producing carboxylated MCL-PHA *in vivo*. Reducing the extent or rate at which a dicarboxylic acid is degraded via β-oxidation increases the likelihood of that intermediates in the pathway contain a carboxyl group. If carboxylated intermediates are present, inhibition of β-ketothiolase is an effective strategy to channel them towards PHA synthase via PhaJ and FabG. To this end, utilizing AA to stimulate *in vivo* production of MCL-PHA containing a side-chain carboxyl group was a major component of chapter 4 of this thesis project.

2.2.4 Summary

Incorporation of carboxyl groups into MCL-PHA improves hydrophilicity, which is desirable for blending with other biopolymers. However, the only synthesis method reported is *ex vivo* carboxylation using an oxidizing agent, which increases cost and complexity and decreases molecular weight. *In vivo* synthesis is therefore an attractive prospect. Since MCL-PHA precursors are derived from β-oxidation, functional groups on fatty acids can be incorporated into the final polymer. Accordingly, dicarboxylic acids like AzA are good candidate carbon sources for the synthesis of carboxylated MCL-PHA. Inhibition of β-oxidation by AA is a technique that may increase the likelihood of producing carboxylated precursors. PHA synthase and other key enzymes have shown to have broad substrate specificity, but must be able to utilize carboxylated substrates to produce MCL-PHA.

2.3 Production of MCL-PHA in reactor systems

MCL-PHA production has been widely studied in fed-batch and, to a lesser extent, continuous culture systems. *P. putida* strains GPo1, KT2440 and its spontaneous rifampicin-resistant derivative KT2442 (Franklin *et al*., 1981), have been used almost exclusively in studies involving the MCL-PHA production due to their ability to accumulate large amounts of polymer from a variety of carbon sources. This section reviews literature from benchtop and pilot-scale fermentations producing MCL-PHA, with a focus on bioreactor setup, performance and productivity.

2.3.1 Fed-batch systems

2.3.1.1 *P. putida* GPo1 as a production strain

One of the first high-cell density fed-batch studies for MCL-PHA production was conducted Preusting *et al*. (1993a), using a 2.6 L two-phase bioreactor (12.5% v/v *n*-octane, 87.5% v/v aqueous) to study the accumulation of MCL-PHA from *n*-octane by P. *putida* GPo1. Cells were cultivated in batch mode to establish biomass, after which a constant nutrient feeding rate was used to establish N-limited conditions to stimulate MCL-PHA production. After a fermentation time of 38 h, 37 g/L biomass concentration was reached with 33 wt% PHA, having a composition of 87 mol% C8 and 13 mol% C6, for a total productivity of 0.25 g $L^{-1}h^{-1}$. Air had to be pre-saturated with *n*-octane to prevent stripping it from the reactor and, due to the flammability of *n*-octane, pure O_2 or O_2-enriched air could not be used in this fashion.

Kellerhals and coworkers (1999a) built on the work of Preusting *et al*. (1993a), by developing a two-stage N-limited setup that enabled O_2-enriched air, up to 40% pure O_2, to be used. Since O_2-enriched air could not be saturated with *n*-octane, the stripping losses were estimated based on the saturation concentration of *n*-octane in air and added to the reactor during the fermentation. A 3 L two-phase bioreactor was used, with an *n*-octane phase representing 17 % v/v of the working volume (balance aqueous phase), a slight increase over the fraction reported by Preusting *et al*. (1993a). Exponential feeding at $\mu = 0.05\ h^{-1}$ was

accomplished by controlling the feeding rate of concentrated ammonium solution. Although a very high cell concentration was achieved (112 g/L), PHA content decreased sharply after the midpoint of the fermentation, falling from 25 wt% to a final value of approximately 4 wt%, resulting in a low overall productivity of 0.07 g $L^{-1}h^{-1}$. The authors attribute this decrease in PHA content to an unknown effect relating to high-cell density, however, the exact cause was unknown. The concentration of divalent cations (Mg^{2+}) was identified as a critical factor in achieving high cell densities due to its stabilizing effect on cell membranes, especially in the presence of solvents like *n*-octane.

The publications by Preusting *et al*. (1993a) and Kellerhals *et al*. (1999a) clearly illustrate the drawbacks of using volatile *n*-alkanes as carbon sources for MCL-PHA production. They are easily stripped from the reactor and highly flammable, which presents a safety hazard during operation. Consequently, the vast majority of publications used pure fatty acids or salts of fatty acids as carbon sources.

Dufresne and coworkers (1998) used a pH-stat fed-batch feeding strategy to produce MCL-PHA from octanoate using *P. putida* GPo1 in a 10 L fermentor. A slightly basic (pH 8) 1 M solution of ammonium octanoate (pH 8) was used to deliver carbon and nitrogen in a fixed ratio, where nitrogen was the limiting factor for growth. The concentration of octanoate was maintained at a virtually constant and non-inhibitory concentration in the reactor by using pure octanoic acid (OA) to control the pH at 6.85. Feeding of ammonium octanoate was accomplished using a three-staged process designed to limit O_2 demand in order to achieve a higher final biomass concentration. The following feeding protocol was used: exponential feeding from 0.5 to 5.0 mmol $L^{-1}h^{-1}$ (12 h), constant feeding at 5.0 mmol $L^{-1}h^{-1}$ (7 h) and constant feeding at 1.3 mmol $L^{-1}h^{-1}$ (24 h). The authors note that the biomass increased exponentially for the first two stages (μ = 0.192 h^{-1} and 0.067 h^{-1}, respectively) and linearly for the final stage. For a fermentation time of 48 h a final biomass concentration of 47 g/L having a PHA content of 55 wt% (C8 and C6 monomers) was obtained, resulting in reactor productivity of 0.53 g $L^{-1}h^{-1}$.

2.3.1.2 *P. putida* KT2442 as a production strain

P. putida KT2442 was used to produced MCL-PHA from oleic acid in high-cell density fed-batch culture (Weusthuis *et al*., 1996). In order to circumvent the issue of substrate toxicity, DO-stat feeding was employed in which oleic acid was added to the reactor following a rise in DO that indicated depletion of the carbon source. Using only air as the aeration gas, 92 g/L biomass containing 45 wt% PHA was obtained after a fermentation time of 26 h, resulting in an impressive productivity of 1.6 g $L^{-1}h^{-1}$. Polymer contained C14:1, C12, C10, C8 and C6 monomers. Exponential growth occurred for 13 h, after which conditions became O-limited. However, MCL-PHA was accumulated during the exponential growth phase, suggesting that nutrient limitation was not required to stimulate polymer production.

Kellerhals *et al*. (1999b) developed a control system using an automatic sampler and on-line gas chromatograph (GC) to regulate octanoate concentration in a 2 L fermentor. This closed loop control system kept the octanoate concentration at a nearly constant and non-inhibitory level during N-limited fed-batch production of MCL-PHA using *P. putida* KT2442. Exponential feeding of the nitrogen source at μ = 0.10 h^{-1} was used for the duration of the fermentation, however, conditions ceased to be N-limited after 23 h due to overfeeding. A total fermentation time of 43 h resulted in 51.5 g/L biomass containing 34 wt% PHA (C8 and C6), resulting in an overall productivity of 0.40 g $L^{-1}h^{-1}$. Up to 50% pure O_2 was used for aeration to satisfy O_2 demand. Although this novel closed-loop control system effectively controlled substrate concentration, performance was below average with respect to PHA content and reactor productivity for fed-batch systems. Two major drawbacks include high complexity and substantial reductions in reactor volume due to continuous sampling. The latter may have contributed to the overfeeding of nitrogen reported by the authors during operation.

A subsequent paper by Kellerhals *et al*. (2000) focused on lab (2 L) and pilot-scale (30 L) fed-batch production of MCL-PHA from octanoate and oleic acid by *P. putida* KT2442. Lab-scale fermentations using fatty acids derived from the saponification of plant and animal fats were also investigated.

Fermentations were N-limited and used exponential feeding of the nitrogen source to control the specific growth rate. A DO-stat setup was used for carbon feeding at the lab scale, while a manually adjusted profile was used at the pilot scale. For octanoate and oleic acid, results at the pilot scale were comparable to results obtained at the lab scale, but PHA content and productivity values were not especially high, ranging from 20.0 to 35.8 wt% and 0.22 to 0.57 g $L^{-1}h^{-1}$, respectively. A fermentation using vegetable fatty acids produced similar results, while animal fatty acids yielded high PHA content (54.0 wt%) but low cell density (28.5 g/L).

Lee *et al*. (2000) produced also investigated MCL-PHA from oleic acid in a high-cell density fed-batch culture of *P. putida* KT2442. A combination of DO-stat and pH-stat strategies were used to control oleic acid feeding to the 6.6 L bioreactor. Growth conditions became P-limited after the initial amount of phosphorus in the medium was depleted, which resulted in a substantial increase in PHA content. Pure O_2 was used to maintain the DO at 30% of saturation, and later at 10% for higher cell densities. The cell density and reactor productivity for this study are the highest values ever reported for an MCL-PHA production system: 141 g/L and 1.91 g $L^{-1}h^{-1}$, respectively. Cells also contained an average of 51.4 wt% PHA, which was in the range of average values reported for fed-batch fermentations in literature.

Kim (2002) used a N-limited fed-batch setup to produce MCL-PHA from OA using *P. putida* GPo1. A pH-stat feeding method was used to deliver a mixture of OA and ammonium nitrate to a 2.5 L bioreactor. Three different fed-batch fermentations were completed with different carbon to nitrogen (C/N) ratios: 10, 20 and 100 g OA per g ammonium nitrate. The best results were obtained for the lowest C/N ratio, yielding 63 g/L biomass, 62 wt% PHA and 1 g $L^{-1}h^{-1}$ volumetric productivity. A PHA content of 75 wt% was obtained for the second highest C/N ratio, however cell density and productivity values were much lower: 55 g/L and 0.63 g $L^{-1}h^{-1}$, respectively.

2.3.1.3 *P. putida* BM01 as a production strain

Kim *et al*. (1997) used *P. putida* BM01 in a two-stage fed-batch reactor setup (5 L) to produce MCL-PHA from octanoate (sodium salt) using *P. putida* BM01. The first stage consisted of balanced growth on 1) octanoate, 2) glucose, or 3) glucose and octanoate, followed by a second N and O-limited stage where only octanoate was provided. It was found that feeding glucose and octanoate in the first growth stage yielded the best results: 54.8 g/L biomass, 65.5 wt% PHA consisting of C8 and C6 monomers and 0.92 g $L^{-1}h^{-1}$ productivity in 39 h fermentation time. The introduction of a small amount of octanoate in the first stage eliminated the lag that was observed at the beginning of the second stage when cells were first grown on glucose, allowing such high polymer content to be reached. In the first stage, glucose concentration in the reactor was maintained between 10 and 20 g/L, while octanoate was fed at a constant rate initially and later maintained between 0.2 and 2.0 g/L in the second stage. Nonetheless, the use of glucose to support the bulk of cell growth was an effective strategy to maximize the conversion of octanoate to MCL-PHA. As with Weusthuis *et al*. (1996), a small amount of PHA was accumulated before the onset of nutrient limitation.

2.3.1.4 Recombinant strains for production

Prieto *et al*. (1999) completed a fed-batch fermentation (3 L bioreactor) using a recombinant strain of *E. coli* (193MC1) containing a *phaC* from *P. putida* GPo1. Cells were grown on hexadecanoic acid in the presence of an inducer to stimulate the expression of the PHA synthase gene (*phaC*) required for polymer production. As a proof of concept, the experiment was a success as the recombinant *E. coli* 193MC1 was stable in a reactor environment and produced MCL-PHA consisting of C6, C8 and C10 monomers. In comparison to literature values, the results were considerable lower: 3.55 g/L biomass, 12 wt% PHA and 0.011 g $L^{-1}h^{-1}$ overall productivity.

Diniz *et al*. (2004) took a different approach with respect to carbon source selection for MCL-PHA production. The authors used an equimolar mixture of glucose and fructose, to cultivate *P. putida* IPT 046.

Constant rate feeding was used in conjunction with P-limitation was used to achieve 50 g/L biomass containing 63 wt% PHA in a fermentation time of 42 h, resulting in an overall productivity of 0.80 g $L^{-1}h^{-1}$. Air only was used to maintain the DO level 15% of saturation in the 10 L bioreactor. Polymer composition was typical for cells grown on carbohydrates, consisting of C10 and C8 monomers. Interestingly, this was the only high-cell density fed-batch fermentation that looked at producing MCL-PHA from unrelated carbon sources. These results are comparable to average fed-batch systems producing MCL-PHA from related carbon sources like fatty acids.

2.3.1.5 *P. putida* KT2440 as a production strain

A series of three publications by Sun and coworkers investigated fed-batch production of MCL-PHA from NA using *P. putida* KT2440. It was demonstrated in the first publication (Sun *et al*., 2007a) that *P. putida* KT2440 was capable of accumulating large amounts of MCL-PHA without the need for nutrient (N or P) limitation. Two C-limited fed-batch fermentations were completed using exponential NA feeding at specific growth rates (μ) of 0.15 and 0.25 h^{-1} in a 5 L bioreactor. Results for both fermentations were impressive: 70.2 g/L biomass, 75.4 wt% PHA and 1.11 g $L^{-1}h^{-1}$ productivity for μ of 0.15 h^{-1}, and 56.0 g/L, 66.9 wt% and 1.44 g $L^{-1}h^{-1}$ for μ of 0.25 h^{-1}. Despite decreased biomass concentration and PHA content, enhanced productivity was achieved at the higher feeding rate due to a significantly shorter fermentation time. Incorporating an N-limited second stage after the initial exponential growth phase did not result in any further increase in PHA content. This clearly illustrated that high cell density, PHA content and productivity could be achieved under C-limited conditions with *P. putida* KT2440 grown on fatty acids like NA. In subsequent work (Sun *et al*., 2009b) NA and glucose co-feeding was shown to increase the yield of MCL-PHA from NA.

An identical setup was used to produce MCL-PHA from a combination of NA and $UDA^{=}$ from *P. putida* KT2440 (Sun *et al*., 2009a). Three fed-batch fermentations were completed at different μ values and different molar ratios of NA to $UDA^{=}$ in the feed. It was shown that the distribution of monomers derived

from each carbon source was proportional to their ratio in the feed. The best results were obtained at a μ of 0.23 h^{-1} and a molar ratio of NA to $UDA^{=}$ of 5.07:1 in the feed, yielding 48.1 g/L biomass containing 55.8 wt% PHA resulting in an overall productivity of 1.09 g $L^{-1}h^{-1}$.

Jiang (2010) incorporated β-oxidation inhibition into the C-limited fed-batch process using NA and glucose co-feeding described by Sun *et al*. (2009b). Carbon was fed exponentially at 0.15 h^{-1} followed by constant rate feeding to delay O-limitation. A mass ratio of NA to glucose to AA of 1.25:1.00:0.05 yielded some of the best results ever reported for MCL-PHA production: cell density of 71.4 g/L, PHA content of 75.5 wt% and productivity of 1.8 g $L^{-1}h^{-1}$. Most impressive, however, were the improvements in C9 monomer content (65.0 to 88.9 mol%) and PHA yield from NA (0.66 to 0.78 g/g) compared to the results of Sun *et al*. (2009b), in the absence of inhibitor. These results demonstrated that the inhibition of β-oxidation by AA in a fed-batch system is an effective strategy for enhanced performance and compositional control of MCL-PHA.

2.3.2 Continuous production systems

In early MCL-PHA research, chemostat systems were primarily used as a tool to study the effect of specific growth conditions on MCL-PHA accumulation and other physiological phenomena. More recently, however, chemostats have been investigated as true MCL-PHA production systems with high volumetric productivity. The following section reviews continuous reactor systems discussed in literature, with an emphasis on growth conditions and performance.

2.3.2.1 *P. putida* GPo1 as a production strain

N-limited chemostat production of MCL-PHA from octanoate was examined using *P. putida* GPo1 (Ramsay *et al*., 1991) and *P. resinovorans* (Ramsay *et al*., 1992) in a 2 L fermentor. Lower dilution rates were found to have a positive effect on PHA content in *P. putida* GPo1, while N-limitation had little to no effect. By contrast, N-limitation had a strong positive effect on PHA content in *P. resinovorans*.

Interestingly, for both strains, the polymer synthesized from octanoate contained a small proportion of 3-hydroxybutryrate (C4) and C10 monomers in addition to the expected C8 and C6 monomers. The best results for *P. putida* GPo1 occurred at a dilution rate 0.25 h^{-1}: 4.4 g/L biomass containing 13 wt% PHA, resulting in reactor productivity was 0.14 g $L^{-1}h^{-1}$. Similarly, *P. resinovorans* at a dilution rate of 0.24 h^{-1} yielded 4.7 g/L biomass containing 8.5 wt% PHA resulting in a productivity of 0.10 g $L^{-1}h^{-1}$.

Three articles have examined MCL-PHA synthesis from *n*-octane in a continuous system using *P. putida* GPo1. Preusting *et al*. (1993a) and Hazenberg and Witholt (1997) used a single stage N-limited chemostat, while Jung *et al*. (2001) employed a two-stage N-limited chemostat. Configurations used by Preusting *et al*. (1993a) and Hazenberg and Witholt (1997) were essentially identical, apart from reactor size, which were 1 L and 3 L, respectively. Aqueous medium and *n*-octane were fed separately, with the latter comprising 12.5 % (v/v) of the total feed. As described previously, air was pre-saturated with *n*-octane to prevent stripping it from the reactor. At a dilution rate of 0.20 h^{-1} the biomass concentration was 11.6 g/L containing 25.0 wt% PHA (C8 and C6 monomers), translating to a volumetric productivity of 0.58 g $L^{-1}h^{-1}$. Hazenberg and Witholt (1997) made a slight improvement to these results, reporting 12.4 g/L biomass, 29.8 wt% PHA and 0.74 g $L^{-1}h^{-1}$ productivity. In addition, the authors used their system to investigate the effect of other limiting nutrients (P, Mg, Fe and O) on amount of PHA accumulated by *P. putida* GPo1, but none improved on the results obtained through N-limitation. Jung *et al*. (2001) used two 3 L fermentors in series and optimized dilution rates and feeding conditions over a series of experiments. The best results were obtained when R1 and R2 were operated at dilution rates of 0.21 and 0.16 h^{-1}, respectively. The enhancing effect of the second stage was evident by the drastic increases in biomass concentration and PHA content from 10.5 g/L and 38 wt% in R1, to 18.0 g/L and 63.0 wt% in R2. Based on these results, the overall productivity for the system was determined to be 1.06 g $L^{-1}h^{-1}$. These results are the best reported in literature for a continuous MCL-PHA production system and exceed the performance of many fed-batch processes. In addition, the data demonstrate that continuous systems, in particular, two-stage chemostat

systems, are capable of achieving the cell density, polymer content and productivity necessary for economical production of MCL-PHA.

Most recently, Hartmann *et* al. (2010) applied the two-stage chemostat to produce MCL-PHA using *P. putida* GPo1 from OA and $UDA^{=}$. Growth conditions were maintained in the dual nutrient limited growth regime (DNLGR), in which conditions were simultaneously C and N-limited. Two 3.7 L reactors were connected in series; OA was fed in the first stage, while $UDA^{=}$ was fed in the second stage ($D_1 = D_2 = 0.10$ h^{-1}). As expected, MCL-PHA produced in the R1 contained only monomers derived from OA, while the polymer in R2 contained monomers derived from OA and $UDA^{=}$. PHA content increased significantly from R1 to R2 on account of the $UDA^{=}$ fed in the second stage. Cell density, PHA content and overall productivity were 1.53 g/L, 52.4 wt% and 0.040 g $L^{-1}h^{-1}$, respectively.

2.3.2.2 *P. putida* KT2442 as a production strain

Huijberts and Eggink (1996) used an O_2-limited approach for high-cell density MCL-PHA production from oleic acid using *P. putida* KT2442. The 2 L bioreactor was operated at a dilution rate of 0.10 h^{-1}, the C/N ratio was 20 and the DO was maintained below 15% of saturation. Because the conditions were pushed into O-limitation, a cell density of 30 g/L was reached, the highest value reported for a continuous MCL-PHA production system. However, cells contained only 23 wt% PHA, resulting in volumetric productivity of 0.67 g $L^{-1}h^{-1}$. The lower PHA content of this O_2-limited system compared to N-limited fermentations was attributed to the fact that β-oxidation requires oxygen. Hazenberg and Witholt (1997) also observed lower levels of PHA accumulation under O_2-limited versus N-limited conditions in *P. putida* GPo1.

2.3.2.3 Recombinant strains for production

In addition to the fed-batch work using recombinant *E. coli* 193MC1, Prieto and colleagues (1999) completed a chemostat study using recombinant *P. oleovorans* POMC1, which contained an additional copy of the *phaC* gene from its parent strain. The 3 L fermenter was operated at a dilution rate of 0.20 h^{-1},

OA was used as the sole carbon source and the C/N ratio was 15. An inducer was provided for enhanced *phaC* expression. The best results were 1.64 g/L biomass containing 53.2 wt% PHA resulting in a volumetric productivity of 0.17 g $L^{-1}h^{-1}$.

2.3.2.4 *P. putida* KT2440 as a production strain

Jiang (2010) built upon the findings of Sun and coworkers (2009a) by investigating C-limited MCL-PHA production by *P. putida* KT2440 in a single-stage chemostat (1.5 L) incorporating β-oxidation inhibition by AA. Two different configurations were investigated: OA co-fed with glucose and NA co-fed with glucose. The results demonstrated that C-limited conditions were effective in yielding high PHA content in *P. putida* KT2440 in a continuous system. Furthermore, as previously described in Section 2.3.1, AA enhanced PHA yield from OA and NA and the proportion of longer chain monomer units. For OA, a biomass concentration of 5.0 g/L containing 48 wt% PHA resulted in a volumetric productivity of 0.60 g $L^{-1}h^{-1}$. NA feeding produced slightly better results: 5.8 g/L biomass, 50 wt% PHA and 0.73 g $L^{-1}h^{-1}$ productivity.

2.3.2.5 Summary

Over the past 20 years, drastic improvements to MCL-PHA production systems have been made, to the point at which intracellular PHA content exceeding 70 wt% is now attainable. These improvements stem from a more complete understanding of the metabolic pathways associated with MCL-PHA synthesis and the growth conditions that promote polymer accumulation. Reactor configurations, feeding strategies and strain selections are continuously modified to strive for new levels of performance (see page 85 for a complete summary table). Two stage chemostat systems have been studied sparingly in literature, but have produced encouraging results in *P. putida* GPo1 fermentations using *n*-octane (Jung *et al*., 2001) and OA and $UDA^{=}$ (Hartmann *et al*., 2010). Therefore it is an ideal candidate to improve on the impressive results reported by Jiang (2010) for a single stage C-limited fermentation of *P putida* KT2440.

Chapter 3

Materials and Methods

3.1 General fermentation protocols

This section discusses the methods and practices that are common to most of the experimental work discussed in this thesis. Detailed procedures for specific experiments are described in the subsections that follow.

3.1.1 Transfer and maintenance of bacterial cultures

Frequently used bacterial cultures were maintained on agar plates, which were stored in a refrigerator at 4°C. Cultures were transferred to fresh plates at least once per month. All bacterial cultures were preserved on polymer beads and stored at -80°C in a deep freezer. Transfer to polymer beads was accomplished by pipetting a small volume of well-grown liquid culture to a vial of sterile beads. The vial was sealed and shaken to evenly distribute the liquid culture among the beads before freezing. Resuscitation of bacterial cultures from polymer beads was achieved by placing one to two beads in a 500 mL Erlenmeyer shake flask containing rich liquid media (i.e. nutrient broth). A cultivation time of 24 hours at 30°C and 200 rpm was usually sufficient to achieve adequate growth, at which point the liquid culture was used to inoculate agar plates. This resuscitation procedure was used to periodically refresh agar plates of frequently used strains. All culture transfers were completed in a laminar flow hood using proper aseptic technique.

3.1.2 Setup for chemostat fermentations

Single-stage and two-stage chemostat setups were used for all of the fermentations discussed in this thesis. The components of the reactor setup comprise the following:

- 2 L Electrolab Series 351 Fermenter(s) (Electrolab Ltd., UK)
- pH electrode(s), open junction, S8 interface (Cole Parmer Canada Inc.)
- Dissolved oxygen probe(s), Model D100 Series OxyProbe® (Broadley James Corp., USA)

- Masterflex® peristaltic pumps (Cole Parmer Canada Inc.)
- Digital balance(s)
- Guardian+ carbon dioxide monitor(s) (Topac Inc., USA)
- Glass wool air filters, 10 cm depth
- Liquid trap on the air outlet line(s)
- Desktop computer(s) with LabVIEW software (National Instruments, USA)

Detailed schematics of the chemostat setups are shown in Figures 3-1 and 3-2.

3.1.3 Preparation of chemostat for autoclaving

The glass reactor vessel and associated tubing was configured in a specific fashion for safe autoclaving. The pH electrode and dissolved oxygen probe were installed in the reactor prior to autoclaving. Exposed leads were covered with protective caps to prevent damage. Calibration of the pH electrode was done prior to autoclaving, while the dissolved oxygen probe was calibrated afterwards. Probes ends were submerged in reactor media at all times during autoclaving to prevent them from drying out. Reactor ports were connected to flexible peroxide-cured silicon tubing (Tygon® for nonanoic acid) and clamped in suitable locations to prevent 1) contamination and 2) media from escaping. Some tubing was connected to filter-vented flasks that were used to deliver inoculum, base and nonanoic acid (NA) to the reactor. The inlet, outlet and sampling lines had free tubing ends, which were wrapped with cotton and packaged in aluminum foil. Free tubing ends were clamped after covering the opening with cotton and wrapping in aluminum foil. The outlet air line was not clamped because it was used as a vent to prevent pressure build-up during autoclaving. A glass wool air filter on the vent line maintained sterility. The reactor was autoclaved with the appropriate batch media, whose pH was adjusted below 3 using strong acid to prevent precipitation of medium components during autoclaving. After autoclaving and cooling, the pH was re-adjusted using base.

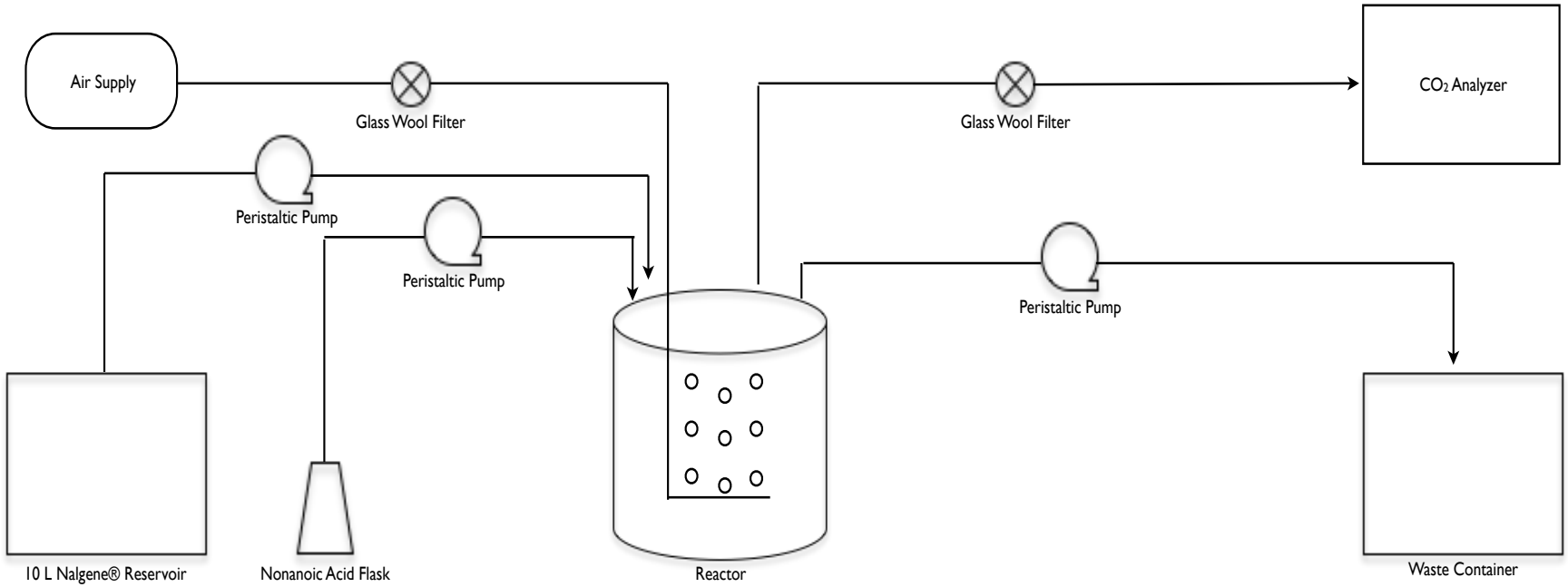

Figure 3-1: Schematic of the singe-stage chemostat setup

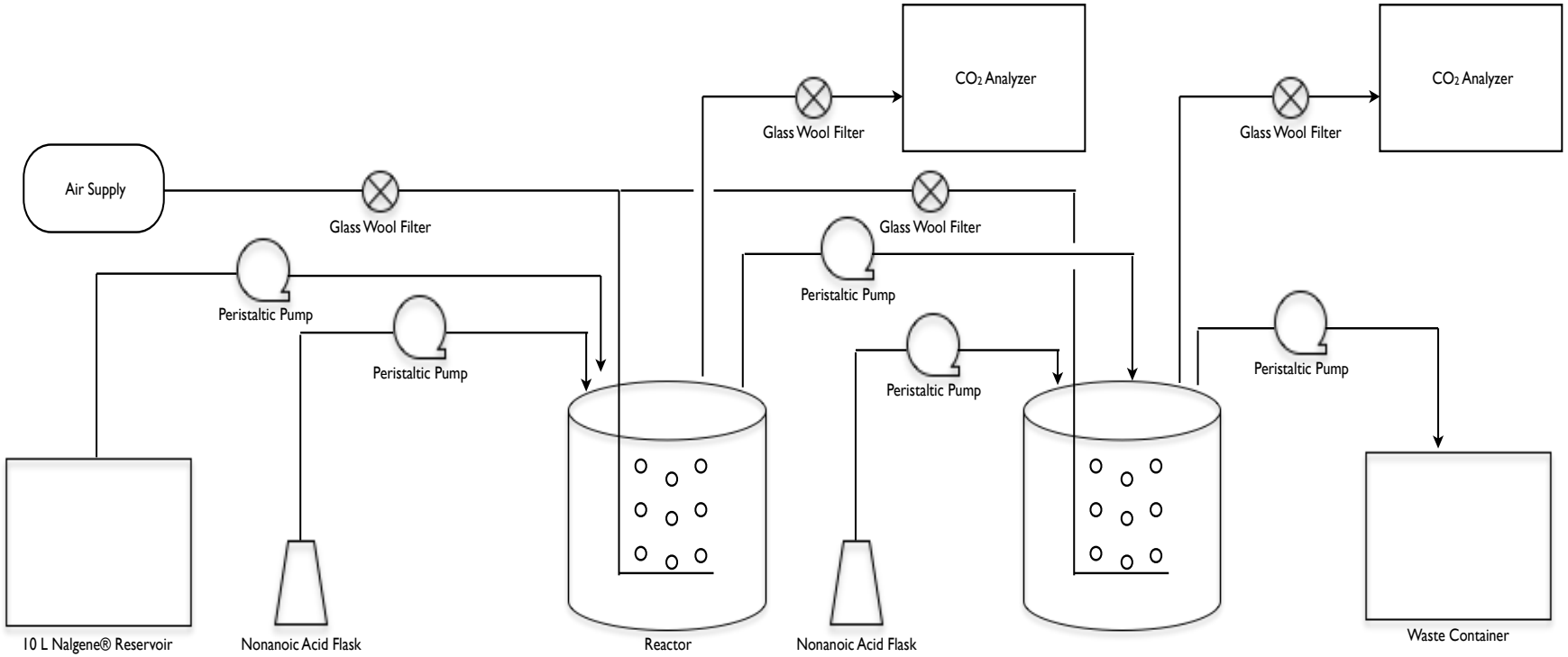

Figure 3-2: Schematic of two-stage chemostat setup

3.1.4 Operation of the chemostat

Peristaltic pumps were used to deliver nutrients, sample, control dilution rate and deliver ammonium hydroxide (NH_4OH) for pH control. A carbon dioxide (CO_2) analyzer was used for on-line monitoring of fermentations. The fraction of CO_2 in the outlet gas was used for CO_2 production rate CPR calculations. Sterile aqueous media was stored in a 10 L Nalgene® reservoir, which was agitated using a magnetic stirrer to maintain well-mixedness during operation. When NA was required, it was fed in its pure form from a separate flask due to its immiscibility with water. The flask was placed on a digital balance to accurately measure the mass flow rate at regular time intervals. *P. citronellolis* DSM 50332 fermentations (section 3.4) used a manually controlled low-speed pump to maintain the desired feeding rate, while *P. putida* KT2440 fermentations (Section 3.5) used a simple feedback control loop in LabVIEW to toggle a pump on or off, based on the balance reading. In both cases, the liquid feeding rate of NA represented a small fraction of the aqueous liquid feeding rate; therefore it was considered to be negligible with respect to overall dilution rate.

3.1.5 Seed culture preparation

Two 500 mL Erlenmeyer flasks were inoculated from a fresh agar plate and grown at 28.0°C and 200 rpm for 12-18 hours. Shake flasks contained 100 mL of mineral salts media containing glucose and nutrient broth (Table 3-1). Media was autoclaved in separate flasks to avoid precipitation, cooled and mixed and distributed in a laminar flow hood before use. One flask, representing a 10% (v/v) inoculum, was used for batch mode start-up.

Table 3-1: Seed culture medium formulation for chemostat fermentations

Compound	Concentration (g/L)	Autoclave Flask
Glucose	9.00	1
Sodium hydrogen phosphate (Na_2HPO_4)	6.36	2
Potassium dihydrogen phosphate (KH_2PO_4)	2.70	2
Ammonium sulfate ($(NH_4)_2SO_4$)	4.70	3
Magnesium sulfate ($MgSO_4$)	0.39	3
Nutrient broth	1.00	3

3.1.6 Preparation of chemostat media

Medium components were autoclaved independently to prevent precipitation. Four separate flasks were used to prepare aqueous solutions of 1) glucose, 2) Na_2HPO_4 and K_2HPO_4, 3) $(NH_4)_2SO_4$ and $MgSO_4$, and 4) trace element solution. Trace element solution contained 10.0 g/L $FeSO_4 \cdot 7H_2O$, 3.0 g/L $CaCl_2 \cdot 2H_2O$,

2.2 g/L $ZnSO_4 \cdot 7H_2O$, 0.5g/L $MnSO_4 \cdot 4H_2O$, 0.3 g/L H_3BO_3, 0.2 g/L $CoCl_2 \cdot 6H_2O$, 0.15 g/L $Na_2MoO_4 \cdot 2H_2O$, 0.02 g/L $NiCl_2 \cdot 6H_2O$ and 1.00 g/L $CuSO_4 \cdot 5H_2O$. Nalgene® reservoirs (10 L) were fitted with rubber stoppers and 0.2 μm disc filters on the vent lines for autoclaving. Reservoirs were autoclaved with enough distilled water to bring the final liquid volume to 10 L, after adding the individual medium components. When AA was required, it was added directly to the reservoir along with the other components. All mixing of media was done in a laminar flow hood after cooling liquids to room temperature.

3.1.7 Sampling

Chemostat sampling was conducted at each steady state point. At each steady state, a minimum of two samples were taken, at least three hours apart, using a peristaltic pump. Each sample was divided into two 10 mL aliquots for processing and analysis. Before collecting each sample, any residual liquid in the tubing from previous samples was discarded in a waste beaker. At the outlet, the silicon tubing was connected to a small piece of metal tubing fitted in a rubber stopper. When not in use, sampling line tubing was clamped and the rubber stopper at the outlet was fitted in a small vial of formaldehyde, which served as an antibacterial agent. The system was judged to be at steady state by observing relatively constant on-line data values for dissolved oxygen and CPR. Additionally, as a rule of thumb, no sampling was conducted until five to six reactor volumes passed through the system to allot adequate time for the system to achieve steady state. For a working volume of 1.1 L and a dilution rate (D) of 0.25 h^{-1}, five to six reactor volumes corresponded to 20-24 hours of fermentation time.

3.2 Analytical methods

This section describes the methods used to process and analyze liquid culture samples from shake flask and chemostat experiments.

3.2.1 Determination of dry cell weight (DCW)

Two 10 mL aliquots were taken from each shake flask or chemostat sample and centrifuged at *8000 g* for 10 minutes. The supernatant was decanted into 10 mL glass screw cap vials and stored in a freezer for subsequent nutrient analysis. Biomass pellets were washed with 10 mL of distilled water and centrifuged at *8000 g* for another 10 minutes. Wash water was discarded into a waste beaker; biomass pellets were

transferred to glass vials of known mass and stored in a freezer for lyophilization. Vials were weighed after lyophilization to determine DCW.

3.2.2 Determination of ammonium (NH_4^+)

Ammonium (NH_4^+) concentrations in supernatant samples were assayed using the phenol-hypochlorite method described by Weatherburn (1967). The two required reagents are described in Table 3-2.

Table 3-2: Reagents used for analysis of NH_4^+ in sample supernatants

	Compound	Concentration in distilled water (g/L)
Reagent 1	Sodium nitroprusside ($Na_2(Fe(CN)_5NO)\cdot 2H_2O$	0.025
	Phenol (C_6H_5OH)	5.0
Reagent 2	Sodium hydroxide (NaOH)	2.5
	Sodium hypochlorite (NaOCl)	4.2 (mL)

A standard concentration curve ranging from 0.00 to 0.40 g/L NH_4^+ was made using a solution of $(NH_4)_2SO_4$. Supernatant samples were diluted with distilled water to bring the NH_4^+ concentration within this range. 40 µL of standard/supernatant sample was mixed vigorously in a test tube with 2500 µL of each reagent 1 and reagent 2. Test tubes were left at room temperature for 30 minutes for colour development and then placed in an ice bath for 5 minutes. Absorbance at 630 nm was recorded for each sample using a spectrophotometer. NH_4^+ concentration for each supernatant sample was calculated based on the standard, taking the dilution factor into account.

3.2.3 Determination of glucose

Glucose concentration was determined using the colorimetric method developed by Lever (1972). Two reagents were required for this reaction (Table 3-3).

Table 3-3: Reagents used for analysis of glucose in sample supernatants

	Compound	Concentration in distilled water (g/L)
Reagent 1	Sodium hydroxide (NaOH)	20.0
Reagent 2	4-Hydroxybenzoic hydrazide (PAHBAH)	50.0
	Hydrochloric acid (HCl)	40.0 (mL)

Supernatant samples were diluted by an appropriate factor to bring the glucose concentration within the range of the standard curve: 0.00 to 5.00 g/L. The analysis reagent was prepared just prior to use by mixing reagent 1 and reagent 2 in a ratio of 9:1. A 15 µL portion of standard/supernatant sample was mixed with

4500 µL of analysis reagent in a test tube and heated in a water bath at 100°C for six minutes. Test tubes were then cooled in cold water for three minutes. Absorbance at 410 nm was measured for each sample. Glucose concentration in supernatant samples was calculated based on the standard curve and the dilution factor.

3.2.4 Determination of Phosphate (PO_4)

Phosphate (PO_4) was determined by measuring the reduction of phosphomolybdate to molybdenum blue (Clesceri *et al*., 1999). The reagents used for this analysis are listed Table 3-4.

Table 3-4: Reagents used for analysis of PO_4 in sample supernatants

	Compound	Concentration (g/L)
Reagent 1	Sodium borate ($Na_2B_4O_7 \cdot 10H_2O$)	19.8
	Sodium metabisulfite ($Na_2S_2O_5$)	18.1
Reagent 2	Sodium molybdate ($NaMoO_4$)	24.2
	Concentrated sulfuric acid (H_2SO_4)	70.0 (mL)
Reagent 3	4-(methylamino) phenol sulfate ($(C_7H_{10}NO)_2SO_4$)	9.99
	Sodium metabisulfite ($Na_2S_2O_5$)	30.4
Reagent 4	Sodium carbonate (Na_2CO_3)	42.4
	Sodium sulfite (Na_2SO_3)	6.9

KH_2PO_4 was used to generate a standard concentration curve ranging from 0.00 to 0.50 g/L PO_4. Supernatant samples were diluted to bring the estimated PO_4 concentration into this range. 100 µL of standard/supernatant sample was mixed vigorously in a test tube with 200 µL of reagent 1, 1000 µL of reagent 2 and 200 µL of reagent 3 and left at room temperature for 15 minutes. 2000 µL of reagent 4 was then added to each test tube, mixed thoroughly and left at room temperature for another 15 minutes. Absorbance at 710 nm was recorded for each sample. PO_4 concentrations in supernatant samples were interpolated from the standard concentration curve, accounting for the dilution factor.

3.2.5 Analysis of PHA using gas chromatography (GC)

PHA content and composition were determined using a modified version of the procedure described by Lagaveen *et. al* (1988), whereby 3-hydroxy-methyl esters of PHA are analyzed by gas chromatography (GC). Lyophilized biomass samples and PHA standards of known mass were distributed into 10 mL glass screw cap vials. Two milliliters (2 mL) of chloroform and 1 mL of methanol containing 15 % (v/v) concentrated sulfuric acid (H_2SO_4) and 0.2% (w/v) benzoic acid (internal standard) were added to each vial, and sealed with rubber coated plastic cap. Vials were vortexed vigorously and incubated at 100°C in a

water bath for four hours. After cooling, 1 mL of distilled water was added to each of the vials and mixed thoroughly to extract 3-hydroxy methyl esters into the chloroform phase. One microliter (1 µL) of the organic phase was injected into a Varian CP3900 gas chromatograph equipped with a flame ionization detector (FID). The GC heating profile is shown in Figure 3-3. FID and injector temperatures were 275°C and 250°C, respectively.

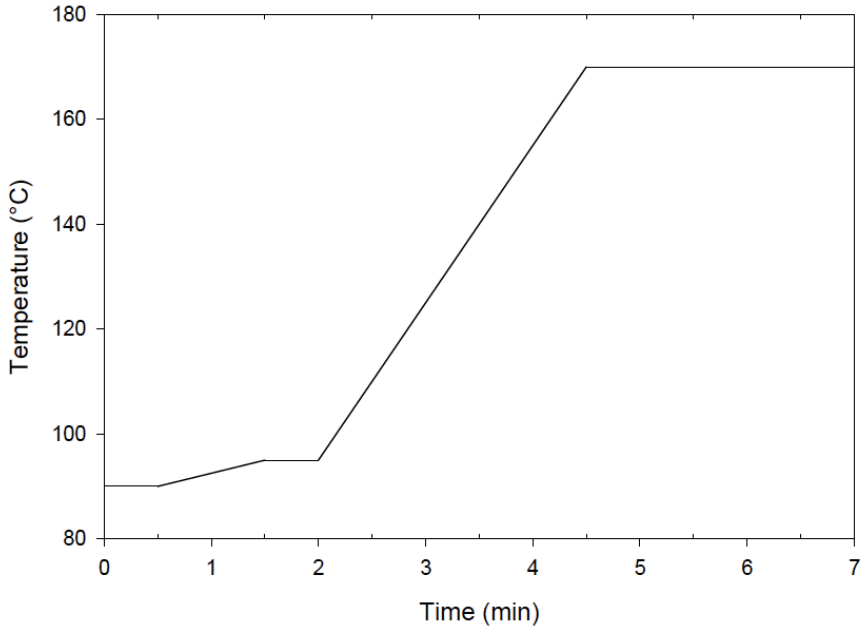

Figure 3-3: GC heating profile for analysis of PHA methyl esters
(90°C hold, 0.5 min; +5°C/min, 1 min; 95°C hold, 0.5 min; +30°C/min, 2 min; 170°C hold 2.5 min)

PHA content and composition of biomass samples was calculated using the chromatogram data from the PHA standards, whose compositions were previously established through proton nuclear magnetic resonance (^{1}H-NMR) analysis.

3.2.6 Analysis of PHA using ^{1}H-NMR and ^{13}C-NMR

^{1}H-NMR and ^{13}C-NMR were used to help quantify a couple of PHA samples believed to have some probability of containing a side chain carboxyl group. PHA was extracted from biomass and purified by dissolution in chloroform, followed by precipitation in cold methanol. Purified samples were dissolved in deuterated chloroform ($CDCl_3$), yielding a final concentration of about 25 mg/mL. Spectra were recorded on a Bruker Avance 400 MHz spectrometer.

3.2.7 Analysis of carboxylic acids using GC

Residual carboxylic acids in supernatant samples were analyzed using a gentler version of the methyl ester derivatization used for PHA analysis. The internal standards used for analyses of nonanoic acid and azelaic acid were decanoic acid and sebacic acid, respectively. 2 mL of methanol containing 2% (v/v) concentrated sulfuric acid and 0.5% (w/v) internal standard were added to each 1 mL of supernatant in 10 mL glass screw cap vials and mixed thoroughly. 1 mL of distilled water was added to vials containing pure nonanoic acid and azelaic acid as external standards. Vials were sealed with rubber-coated caps and incubated in a water bath at 100°C for one hour. After cooling, the methyl esters of carboxylic acids were extracted with 2 mL of chloroform and 2 mL of distilled water. 1 µL of the organic phase was injected into a Varian CP3900 GC using the identical operating conditions and heating profile previously described (Figure 3-3).

3.2.8 Analysis of acrylic acid (AA)

AA was analyzed according to the methodologies of Qi *et al*., (1998). 2 mL of supernatant samples were acidified with 1/10 volume of 2 M HCl containing 0.02% (v/v) isovaleric acid as an internal standard as suggested by Baksanova *et al*., (2002). Several external standards were prepared using a range of AA concentrations in deionized water. 10 µL were injected into a Hewlett Packard 5890 GC equipped with a polyethylene glycol (PEG) column (Carbowax®) and FID. FID and injector temperatures were 275°C and 250°C, respectively. The temperature profile for this analysis is shown in Figure 3-4.

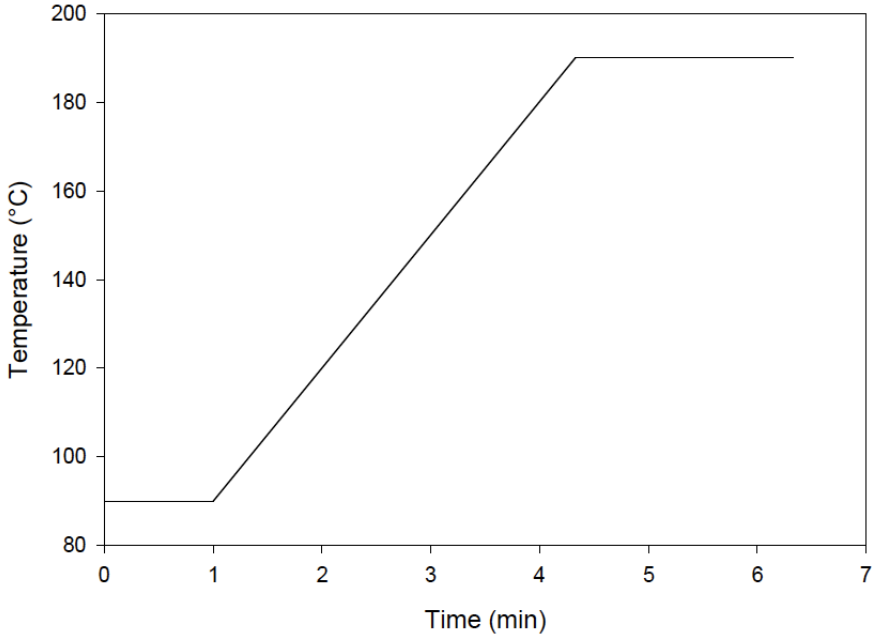

Figure 3-4: GC heating profile for analysis of carboxylic acid methyl esters
(90°C hold, 1 min; +30°C/min, 3.3 min; 190°C hold 2 min)

3.3 Shake flask studies

This section explains the procedures pertinent to shake flask studies conducted as a part of this thesis. Each shake flask experiment is described in separate subsections.

3.3.1 Screening for PHA Accumulation from nonanoic acid (NA) for *P. citronellolis* DSM 50332 and *P. fluorescens* ATCC 17400

Nitrogen (N) limited shake flask studies were conducted for *P. citronellolis* DSM 50332 and *P. fluorescens* ATCC 17400. The medium for the inoculum and experimental flasks contained 0.50 g/L $(NH_4)_2SO_4$, 0.39 g/L $MgSO_4$, 6.35 g/L Na_2HPO_4, 2.70 g/L KH_2PO_4 and 1.00 g/L glucose in addition to NA. The inoculum media contained 1.0 g/L NA, while the six experimental flasks contained 0.0, 0.5, 1.0, 1.5, 2.0 and 3.0 g/L NA. Each 500 mL shake flask was given a 2.5% (v/v) inoculum and was cultivated at 28°C and 200 rpm. Growth was monitored regularly using optical density measurements at 630 nm and phase contrast microscopy. Biomass determination, PHA characterization and analysis of residual NH_4^+ were accomplished according to the previously described methods.

3.3.2 Screening for PHA accumulation from azelaic acid (AzA) for *P. citronellolis* DSM 50332 and *P. fluorescens* ATCC 17400

An identical set of shake flask experiments was completed using azelaic acid (AzA) instead of NA. The inoculum media contained 1.0 g/L AzA, while the six experimental flasks contained 0.0, 1.0, 2.0, 3.0, 4.0 and 6.0 g/L AzA. Optical density (630 nm), biomass concentration, PHA content and composition and residual NH_4^+ were measured.

3.3.3 Acrylic acid (AA) toxicity on *P. citronellolis* DSM 50332

Six 500 mL shake flasks were prepared with the following range of AA concentrations: 0.00, 0.10, 0.20, 0.40, 0.80 and 2.00 g/L. The medium for the inoculum and shake flasks contained, 4.70 g/L $(NH_4)_2SO_4$, 0.39 g/L $MgSO_4$, 6.35 g/L Na_2HPO_4, 2.70 g/L KH_2PO_4, 1.00 g/L nutrient broth and 9.00 g/L glucose. Each shake flask was given a 2.5% (v/v) inoculum and cultivated at 28°C and 200 rpm for 36 hours. Optical density measurements at 630 nm were taken at regular intervals.

A second experiment was completed in order to quantify the AA toxicity threshold, specifically with respect to β-oxidation inhibition. NA was provided as used as the sole carbon source for this purpose. The medium for the inoculum and shake flasks contained: 2.50 g/L NA 4.70 g/L $(NH_4)_2SO_4$, 0.39 g/L $MgSO_4$, 6.35 g/L Na_2HPO_4, 2.70 g/L KH_2PO_4 and 1.4 mL/L trace element solution. AA concentrations of 0.00, 0.005, 0.01, 0.02, 0.04, 0.06, 0.08 and 0.10 g/L were used in shake flasks.

3.4 Chemostat work involving *P. citronellolis* DSM 50332

Three separate chemostat studies were conducted using *P. citronellolis*, the specific experimental details of which are described in the subsections below. Chemostat operating parameters were constant for all experiments (Table 3-5).

Table 3-5: Chemostat operating parameters for work involving *P. citronellolis* DSM 50332

Working volume (L)	1.1
Flow rate of aqueous media (L/h)	0.28
Dilution rate (h^{-1})	0.25
Aeration rate (L/min)	0.75
Volume of air per reactor working volume per minute, VVM (min^{-1})	0.68
pH set point	6.85

3.4.1 Chemostat preparation and start-up

The reactor vessel was prepared for autoclaving according to the protocol described in Section 3.1.3. Biomass was established by operating the reactor in batch mode prior to switching to continuous mode. Batch media had the following composition: 6.36 g/L Na_2HPO_4, 2.70 g/L KH_2PO_4, 4.70 g/L $(NH_4)_2SO_4$, 0.39 g/L $MgSO_4$ and 1.40 mL/L of trace element solution. Concentrations of carbon sources in the batch media were 3.90 g/L glucose and 2.90 g/L NA. The fraction of CO_2 in the outlet gas was monitored throughout the course of the batch until a sufficiently high biomass concentration was established. At this point, typically corresponding to an outlet gas CO_2 content of between 1.0 and 1.2%, the reactor was transitioned to chemostat mode.

3.4.2 Chemostat study: Effect of phosphorus (P) limitation on the accumulation of MCL-PHA from nonanoic acid (NA) by *P. citronellolis* DSM 50332

PO_4 concentrations in the 10 L aqueous media reservoirs were gradually decreased to achieve P-limited growth conditions. Aqueous media contained: 3.90 g/L glucose, 4.00 g/L $(NH_4)_2SO_4$, 0.503 g/L $MgSO_4$ and 1.4 mL/L trace element solution. To maintain pH buffering, the concentrations of Na_2HPO_4 and KH_2PO_4 were always maintained in a ratio of 2.37:1 (Na_2HPO_4:KH_2PO_4) when adjusting the total phosphate concentration (Table 3-6). NA feeding rate was fixed at 0.80 g/h, which corresponded to an equivalent concentration of 2.90 g/L based on the aqueous media flow rate of 0.28 L/h.

Table 3-6: Inlet PO_4 concentrations for P-limited chemostat using *P. citronellolis* DSM 50332

Total PO_4 (g/L)	Na_2HPO_4 concentration (g/L)	KH_2PO_4 concentration (g/L)
1.142	1.185	0.500
1.000	1.027	0.433
0.800	0.821	0.345
0.600	0.616	0.260
0.400	0.411	0.173
0.275	0.285	0.120
0.250	0.256	0.108
0.225	0.234	0.099
0.200	0.207	0.088
0.180	0.187	0.079

3.4.3 Chemostat study: Accumulation of MCL-PHA from nonanoic acid (NA) and azelaic acid (AzA) under phosphorus (P) limitation by *P. citronellolis* DSM 50332

AzA concentration in the aqueous media was increased at each steady state. Medium composition comprised the following components: 3.90 g/L glucose, 4.00 g/L $(NH_4)_2SO_4$, 0.503 g/L $MgSO_4$, 0.234 g/L Na_2HPO_4, 0.099 g/L KH_2PO_4 and 1.4 mL/L trace element solution. Total PO_4 concentration was fixed at 0.225 g/L; the value corresponding to maximum PHA content from the previous experiment. The feeding rate of nonanoic acid was fixed at 0.80 g/h (2.90 g/L). Due to the poor solubility of AzA in water, it was solubilized in aqueous potassium hydroxide (KOH) and adjusted to a pH of 7 prior to autoclaving and adding to the reservoir of chemostat media. A mass ratio of AzA to KOH of approximately 1.6 allowed an AzA concentration of 50 g/L to be achieved with near-neutral pH. AzA concentrations of 0.70, 1.00, 1.50, 2.00 and 2.50 g/L were investigated in this chemostat study.

3.4.4 Chemostat study: Effect of β-oxidation inhibition using acrylic acid (AA) on the accumulation of MCL-PHA from nonanoic acid (NA) and azelaic acid (AzA) under phosphorus (P) limitation by *P. citronellolis* DSM 50332

AA concentrations in the 10 L aqueous media reservoirs were gradually increased at each steady state value to increase the severity of β-oxidation inhibition. Chemostat media had the following composition: 3.90 g/L glucose, 2.50 g/L azelaic acid, 4.00 g/L $(NH_4)_2SO_4$, 0.503 g/L $MgSO_4$, 0.234 g/L Na_2HPO_4, 0.099 g/L KH_2PO_4 and 1.4 mL/L trace element solution. NA feeding rate was fixed at 0.80 g/h (2.90 g/L). AA concentrations of 0.010, 0.020, 0.025, 0.030, 0.035 and 0.040 g/L were used in this study.

3.5 Chemostat work involving *P. putida* KT2440

Two *P. putida* KT2440 chemostat studies were conducted: one using a single-stage setup illustrated in Figure 3-1 and one using a two-stage setup illustrated in Figure 3-2. See Table 3-7 for a list of operating parameters associated with these experiments.

Table 3-7: Chemostat operating parameters for *P. putida* KT2440 fermentations

	Reactor 1 (R1)	Reactor 2 (R2)
Working volume (L)	0.90	1.10
Flow rate of aqueous media (L/h)	0.28	0.28
Dilution rate (h^{-1})	0.30	0.25
Aeration rate (L/min)	0.75	1.00
Volume of air per reactor working volume per minute, VVM (min^{-1})	0.83	0.91
pH set point	6.85	6.85

3.5.1 Chemostat preparation and start-up: Single stage

Preparation and start-up was identical to the protocol detailed in Section 3.4.1, with one exception. The reactor was initially operated in fed-batch mode with respect to NA feeding. NA was delivered based on a target growth rate (μ) of 0.20 h^{-1}, an initial biomass concentration (X_0) of 0.50 g/L and a biomass yield from nonanoic acid ($Y_{X/NA}$) of 0.80 g/g.

3.5.2 Chemostat preparation and start-up: Two stage

Reactor 2 (R2) was autoclaved containing only phosphate salts, 6.36 g/L Na_2HPO_4 and 2.70 g/L KH_2PO_4, to buffer pH. Reactor 1 (R1) start-up was accomplished as described above (Section 3.5.1). When the CO_2% in R1 reached a sufficiently high level the switch to continuous mode was accomplished. This entailed using a peristaltic pump to transfer the contents of R1 into R2, allowing biomass to be established in the second stage. An additional peristaltic pump was used to transfer the contents of R2 into a waste container (Figure 3-2).

3.5.3 Chemostat study: Single-stage high-cell density carbon (C) limited chemostat cultivation of *P. putida* KT2440 producing MCL-PHA from nonanoic acid (NA) in the presence of acrylic acid (AA) as a β-oxidation inhibitor

In the first part of this experiment, glucose and NA were fed into the chemostat in different ratios, while the total amount of carbon fed was fixed at 6.50 g/L. Each steady state point represented a different ratio of these two carbon sources. The dilution rate was held constant; glucose feeding was adjusted by changing the concentration in the reservoir of aqueous media. Chemostat media contained 7.50 g/L $(NH_4)_2SO_4$, 0.503 g/L $MgSO_4$, 1.30 g/L Na_2HPO_4, 0.54 g/L KH_2PO_4, 2.20 mL/L trace element solution and 0.15 g/L AA. NA to glucose (NA:glu) ratios of 0.72, 0.88, 1.00, 1.15 and 1.29 were investigated.

In the second part of this experiment, the NA:glu ratio 1.15 while the concentration of acrylic acid was increased gradually. Inlet acrylic acid concentrations of 0.15, 0.25, 0.40, 0.50, 0.60 and 0.70 g/L were used.

3.5.4 Chemostat study: Production of MCL-PHA in a two-stage carbon limited chemostat from nonanoic acid using *P. putida* KT2440

The conditions in R1 were held constant throughout the duration of the fermentation. NA and glucose were fed at a ratio of 1.29 (6.50 g/L total carbon), while the concentration of acrylic acid in the feed was fixed at

0.40 g/L. The feeding rate of NA into R2 was increased at each steady state, according to following sequence: 0.00, 0.50, 1.00, 2.00, 4.00, 6.00 and 8.00 g/L. Concentrated glucose solution was fed into R2 from a 500 mL Erlenmeyer flask at a rate corresponding to an inlet concentration of 0.50 g/L.

To ensure that growth conditions in R2 remained C-limited at increased NA feeding rates, the concentration of mineral salts in the aqueous media reservoir at the inlet of R1 had to be increased. This was done to facilitate adequate carry-over of key mineral salts from R1 to R2. Chemostat media contained as much as 12.5 g/L $(NH_4)_2SO_4$, 0.60 g/L $MgSO_4$, 1.40 g/L Na_2HPO_4, 0.60 g/L KH_2PO_4 and 2.20 mL/L trace element solution. Concomitant sampling of both reactors was completed at each steady state according to the methodology described earlier (Section 3.1.7).

Chapter 4

Investigations into the *in vivo* production of MCL-PHA containing a side chain carboxyl group by *P. citronellolis* DSM 50332

4.1 Preliminary screening and selection of microorganism

Prior experimental work in our group revealed that *P. putida* KT2440 was incapable of growing on AzA as a sole source of carbon and energy. However, work by Choi and Yoon (1994) and Hoet and Stanier (1970) revealed that *P. citronellolis* DSM 50332 and *P. fluorescens* ATCC 17400, respectively, could grow on AzA as a sole source of carbon and energy, but, the ability of these strains to accumulate MCL-PHA had not been well characterized. To this end, N-limited shake flask experiments were undertaken for both strains (Sections 3.3.1 and 3.3.2). The first used NA as the sole source carbon substrate, because it contains the same number of carbon atoms as the carbon source of interest, AzA, and because it is known to support MCL-PHA production in other *Pseudomonads* such as *P. putida* KT2440 (Sun *et al.,* 2006), *P. putida* GPo1 (formerly *P. oleovorans*, Lageveen *et al.,* 1988) and *P. aeruginosa* PA01 (Noghabi *et al.,* 2008). NA acid concentrations above 3.0 g/L were found to be inhibitory for *P. putida* KT2440 (Sun *et al.*, 2006) so 3.0 g/L was the maximum value used in this initial shake flask study. A second N-limited shake flask study used AzA as the sole carbon source, because it provided the highest probability of yielding MCL-PHA containing a side chain carboxyl group.

4.1.1 Nonanoic acid shake flask study for MCL-PHA accumulation

The optical density time course profiles (Figure 4-1 and 4-2) were representative of the relative biomass concentrations and clearly illustrated the onset of either C or N-limitation during the growth cycle. Plateaus in the growth curves corresponded to the depletion of these nutrients in the medium and consequent limitation of biomass growth. The value of optical density in the plateau region increased with the amount of NA present in the shake flask for NA concentrations up to 1.0 g/L. For the higher NA concentrations (1.5, 2.0 and 3.0 g/L) plateaus occurred at approximately the same optical density.

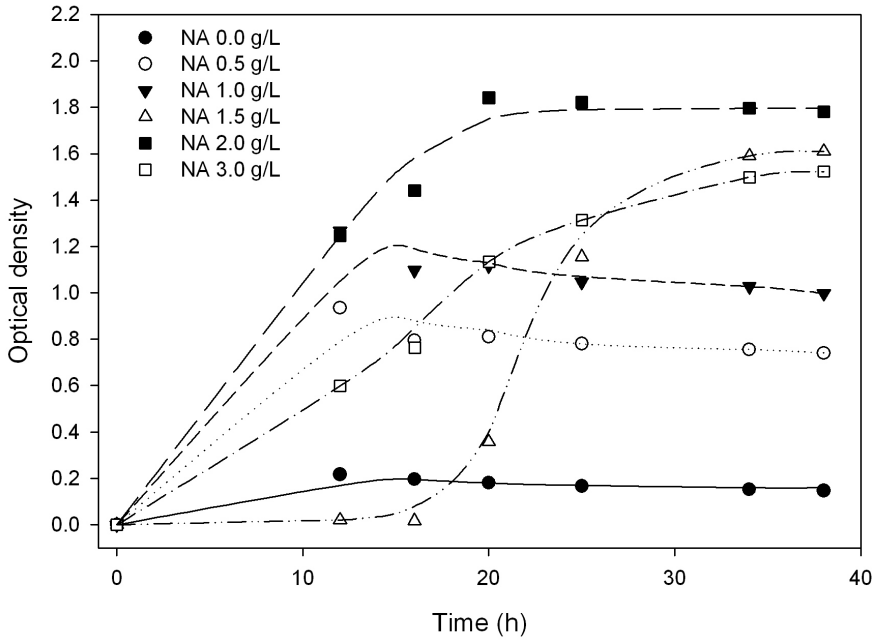

Figure 4-1: Optical density time course: NA shake flask for *P. citronellolis* DSM 50332

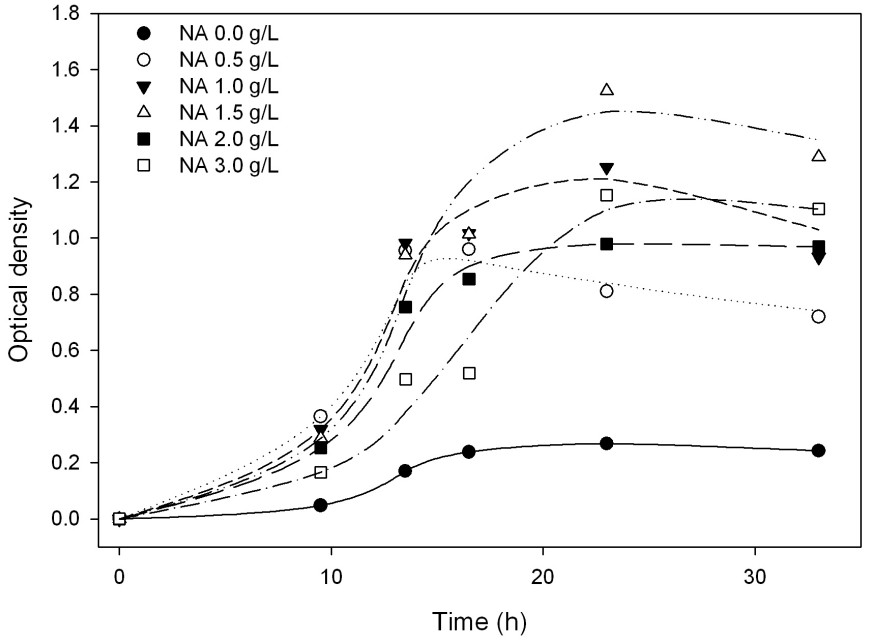

Figure 4-2: Optical density time course: NA shake flask for *P. fluorescens* ATCC 17400

For the *P. citronellolis* DSM 50332 shake flasks, one can reasonably conclude that the onset of N-limitation occurred after roughly 1.0 g/L of NA was consumed. Although no NH_4^+ was detected in the flasks containing 1.0 g/L NA, there was no PHA produced (Table 4-1). Upon examining Figure 4-1, the 1.5, 2.0 and 3.0 g/L flasks plateau at roughly the same optical density, while the flask containing 1.0 g/L plateaued

considerably earlier. This is evidence that the nitrogen and carbon in the medium were depleted almost concurrently under these conditions. Presumably, there was insufficient carbon available to yield MCL-PHA after nitrogen depletion, which would have increased the optical density plateau to a value consistent with high NA concentrations. The same trend appears to have occurred for the *P. fluorescens* ATCC 17400 flasks, but it was not as well illustrated in the optical density time course (Figure 4-2).

Table 4-1: Final biomass, NH_4^+, PHA content and PHA composition for NA shake flask study

		Nonanoic acid in shake flask (g/L)					
		0.0	**0.5**	**1.0**	**1.5**	**2.0**	**3.0**
P. citronellolis DSM 50332	**NH_4 (g/L)**	0.15	0.06	ND	ND	ND	ND
	Biomass (g/L)	0.17	0.73	1.10	1.26	1.21	0.97
	PHA (wt%)	ND*	ND	ND	16.3	18.2	31.7
	C_9 (mol%)	-	-	-	77.6	79.8	75.1
	C_7 (mol%)	-	-	-	22.4	20.2	24.9
P. fluorescens ATCC 17400	**NH_4 (g/L)**	0.06	0.03	0.01	ND	ND	ND
	Biomass (g/L)	0.26	0.68	0.82	1.02	0.66	0.66
	PHA (wt%)	ND	ND	ND	ND	ND	1.9
	C_9 (mol%)	-	-	-	-	-	78.8
	C_7 (mol%)	-	-	-	-	-	21.2

*ND = not detectable

It is apparent that *P. citronellolis* DSM 50332 was a better natural producer of MCL-PHA producer than *P. fluorescens* ATCC 17400 when grown on NA under N-limitation. Like most MCL-PHA producing strains, *P. citronellolis* DSM50332 required nutrient limitation for polymer production. *P. fluorescens* ATCC 17400 produced only a minor amount of MCL-PHA at the highest concentration of NA. Flasks containing residual NH_4^+ did not yield any PHA. This suggests that nutrient limitation was necessary for *P. citronellolis* DSM 50332 to accumulate MCL-PHA, which is common for most MCL-PHA producing strains. PHA content increased according to the amount of carbon present after the onset of N-limitation. PHA composition remained relatively constant at roughly 77 mol% 3-hydroxynonanoate (C9) and 23 mol% 3-hydroxyheptanoate (C7) for all carbon to nitrogen ratios. Choi and Yoon (1994) completed a shake flask study using *P. citronellolis* DSM 50332 grown on 10.0 g/L nonanoate under N- limitation. Despite the significantly higher concentration of carbon source compared to this study, PHA content reached only reached 10.1%. PHA composition was comparable to the values obtained in this study.

4.1.2 AzA shake flask experiment

An identical N-limited shake flask experiment was completed using AzA as the sole carbon source, as producing MCL-PHA with a side chain carboxyl group was the main objective of this work. As with the NA shake flask data, growth profiles showed clear evidence of N-limitation (Figures 4-3 and 4-4).

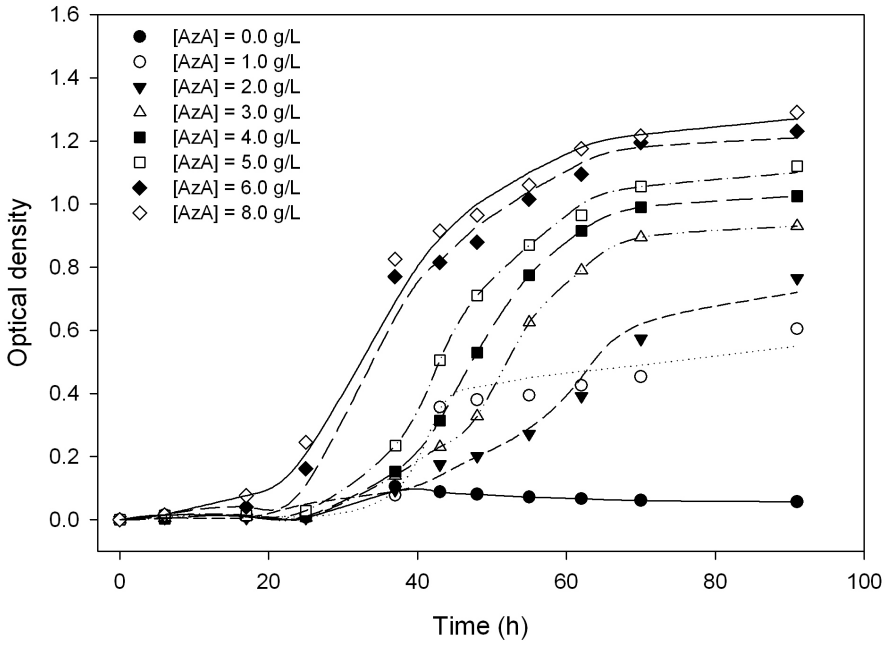

Figure 4-3: Optical density time course: AzA shake flasks for *P. citronellolis* DSM 50332

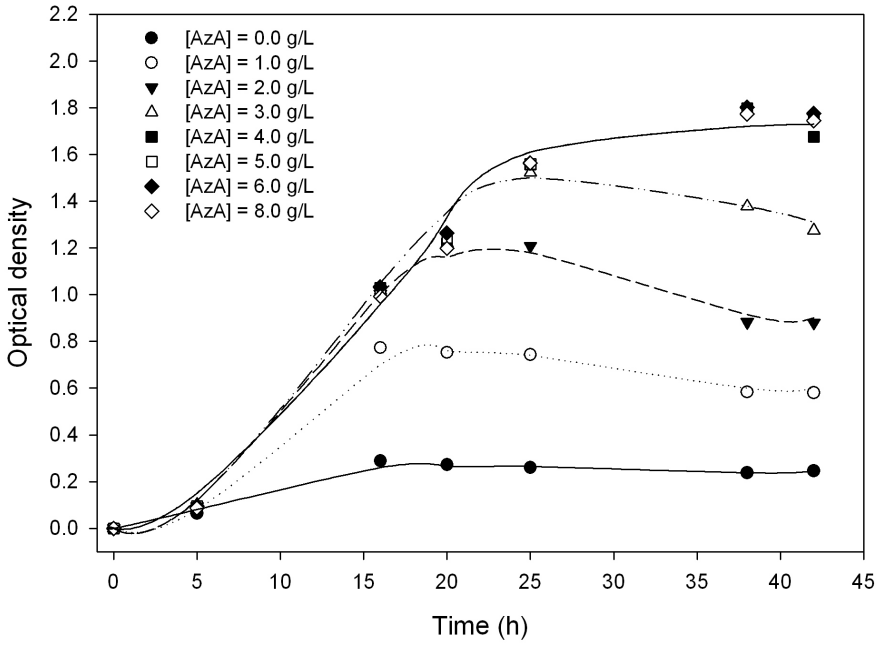

Figure 4-4: Optical density time course: AzA shake flasks for *P. fluorescens* ATCC 17400

Time course plateaus cluster for AzA concentrations of 3.0 g/L and greater, which is in agreement with the residual NH_4^+ data in Table 4-2.

Table 4-2: Final biomass, NH_4^+, PHA content and PHA composition for AzA shake flask study

		Azelaic acid in shake flask (g/L)							
		0.0	**1.0**	**2.0**	**3.0**	**4.0**	**5.0**	**6.0**	**8.0**
P. citronellolis DSM 50332	**NH_4 (g/L)**	0.09	0.02	ND	ND	ND	ND	ND	ND
	Biomass (g/L)	0.07	0.53	0.96	0.98	1.06	1.10	1.27	1.35
	PHA (wt%)	ND	ND	4.5	14.0	17.8	19.1	19.3	20.1
	est. C_{10} (mol%)	-	-	76.9	76.8	76.6	75.4	75.2	74.2
	est. C_8 (mol%)	-	-	23.1	23.2	23.4	24.6	24.8	25.8
P. fluorescens ATCC 17400	**NH_4 (g/L)**	0.05	0.02	ND	ND	ND	ND	ND	ND
	Biomass (g/L)	0.38	0.60	1.06	1.21	1.51	1.62	1.58	1.66
	PHA (wt%)	ND	ND	ND	ND	ND	ND	ND	ND
	est. C_{10} (mol%)	-	-	-	-	-	-	-	-
	est. C_8 (mol%)	-	-	-	-	-	-	-	-

*ND = not detectable

P. citronellolis DSM 50332 produced MCL-PHA, up to a maximum of 20.1 wt% from AzA, in flasks that were N-limited. This MCL-PHA was a copolymer of 3-hydroxyoctanoate (C8) and 3-hydroxydecanoate (C10) monomers, having a composition of about 25 mol% C8 and 75 mol% C10 (estimated). No C10 standard was available for GC analysis, therefore C10 composition was estimated based on the calculated amount of C8 (using C8 standard) and the ratio of C10 peak area to C8 peak area. These results compare favourably to shake flask work done by Choi and Yoon (1994), which yielded 8.2% PHA having a composition of 28 mol% C8 and 63 mol% C10 from *P. citronellolis* grown on 8 g/L azelaic acid under N-limitation. In their case, the balance was attributed to the presence of unsaturated 3-hydroxy-1-dodecenoate (C12:1, 7.3 mol%) and 3-hydroxy-1-tetradecenoate (C14:1, 1.6 mol%) monomers detected by ^{1}H-NMR. *P. fluorescens* ATCC 17400 did not produce any PHA from AzA, despite growing well on it. Due to poor PHA production, *P. fluorescens* ATCC 17400 was eliminated as a potential production strain of MCL-PHA containing side chain carboxyl groups.

Because AzA is a nine-carbon compound, any MCL-PHA precursors derived from the β-oxidation pathway should contain an odd-number of carbon atoms (i.e. nine and seven carbons). The even-numbered carbon monomers comprising the MCL-PHA produced from AzA (C8, C10) suggest that it was derived from *de novo* fatty acid biosynthesis, the route by which MCL-PHA is produced by pseudomonads from unrelated carbon sources (Kim and Lenz, 2001). For this to occur, AzA must have been completely degraded to

acetyl-CoA, which then entered the *de novo* fatty acid biosynthesis pathway to generate fatty acids with an even number of carbon atoms. These fatty acids were then channeled to the MCL-PHA production pathway. This is supported by the similarities in MCL-PHA composition in Table 4-2 compared to MCL-PHA produced from glucose by *Pseudomonas* sp. strain NCIMB 40125 (Haywood *et al.*, 1990), *P. citronellolis* DSM 50332 (Choi and Yoon, 1994) and *P. putida* KT2442 (Eggink *et al*., 1992) and gluconate by various strains of *P. aeruginosa, P. denitrificans* DSM 1650 and *P. mendocina* DSM 50017 (Timm and Steinbüchel, 1990).

4.1.3 Shake flask studies to determine acrylic acid (AA) toxicity

AA was employed in an attempt to force AzA into the MCL-PHA synthesis pathway by inhibiting its degradation via β-oxidation. However, it was necessary to first establish the AA toxicity threshold concentration for *P. citronellolis* DSM 50332. A shake flask experiment was designed to investigate AA concentrations up to 2.00 g/L (Section 3.3.3). Optical density was measured periodically (Figure 4-5).

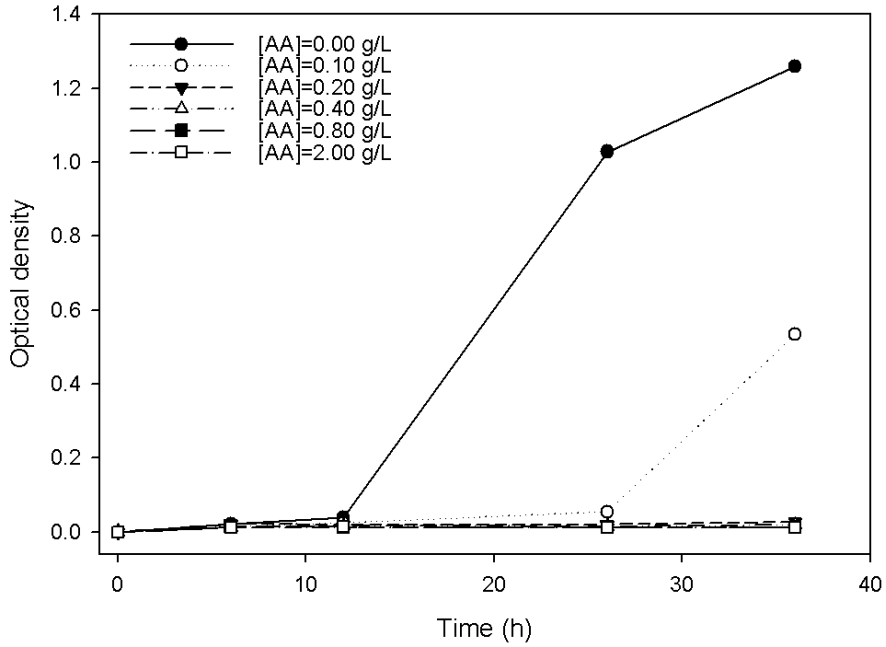

Figure 4-5: AA shake flask optical density profiles for *P. citronellolis* DSM 50332 (part 1)

P. citronellolis DSM 50332 was found to be highly sensitive to AA toxicity. A concentration of only 0.10 g/L severely inhibited growth on glucose and nutrient broth, to the extent that optical density did not increase until the 36-hour mark. Interestingly, *P. putida* KT2440 was determined to be a much more robust strain with respect to AA exposure, having a threshold concentration of about 0.50 g/L (Jiang, 2010).

Based on these results it was apparent that the range of AA concentrations used in this shake flask study was far too broad to establish an accurate toxicity threshold concentration.

Consequently, a second AA shake flask experiment was designed using a narrower range of lower AA concentrations. NA was used as the sole carbon source to target the inhibitory effect of acrylic acid on β-oxidation. Optical density profiles are shown in Figure 4-6.

While concentrations above 0.005 g/L reduced growth rate, the AA toxicity threshold for *P. citronellolis* DSM 50332 was determined to be approximately 0.05 g/L, representing a tenfold increase in AA sensitivity compared to *P. putida* KT2440. This was inferred from the data, which shows that little to no growth occurred at 0.06 g/L, while impaired or delayed growth occurred at 0.04 g/L.

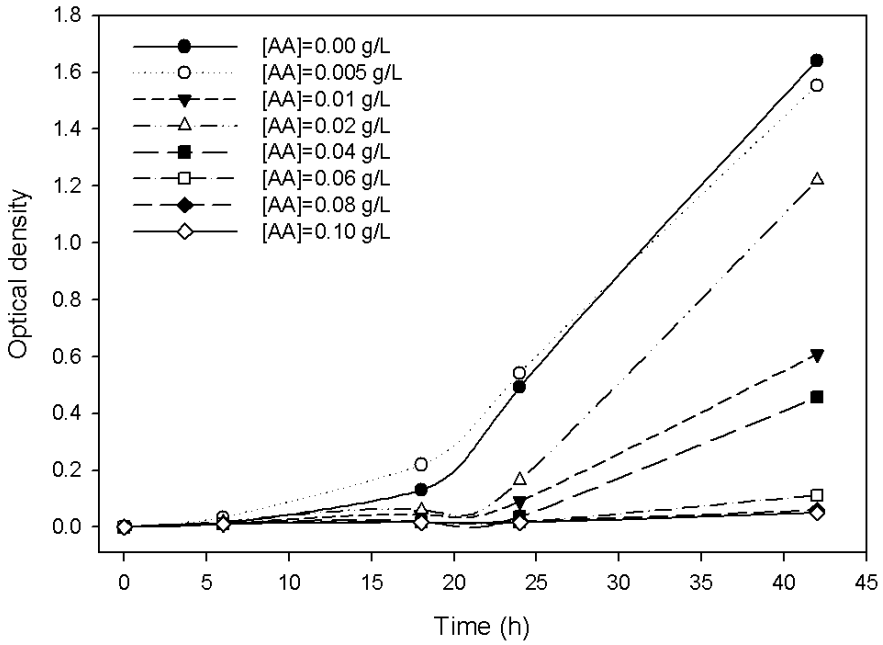

Figure 4-6: AA shake flask optical density profiles for *P. citronellolis* DSM 50332 (part 2)

4.2 Chemostat studies

This section contains the results and discussion for three different chemostat experiments conducted using *P. citronellolis* DSM 50332. Each experiment is discussed in detail in a separate subsection. In all figures, error bars represent one standard deviation of values calculated at each steady state (Section 3.1.7).

4.2.1 Accumulation of MCL-PHA from nonanoic acid (NA) by *P. citronellolis* DSM 50332 under phosphorus (P) limited conditions

The effect of P-limitation on MCL-PHA accumulation from NA was studied (Section 3.4.2).

4.2.1.1 Results and discussion

As expected, PO_4 concentration in the reactor at steady state decreased with the amount of PO_4 at the inlet (Figure 4.7a). The onset of P-limitation occurs at an inlet PO_4 concentration of about 0.300 g/L, at which point, there is no residual PO_4 in the reactor. It is important to note that growth conditions do not become N-limited at any point.

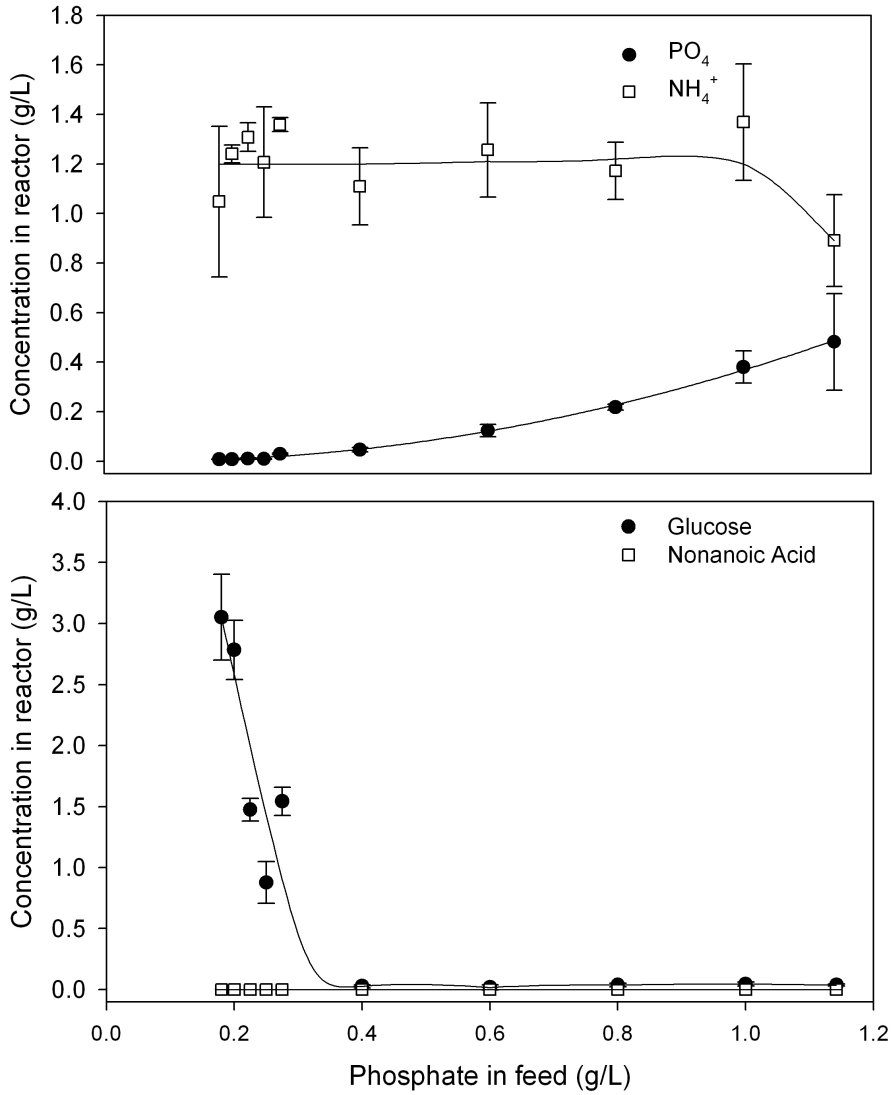

Figure 4-7a: Steady state NH_4^+ and PO_4 concentrations in reactor versus PO_4 in feed and 4-7b: Steady state glucose and NA concentrations in reactor PO_4 in feed (D=0.25 h^{-1})

The onset of P-limitation is reflected in the glucose and NA data (Figure 4-7b), as well as the CPR and biomass data (Figure 4-8a). C-limited growth prevails for PO_4 concentrations of 0.400 g/L and above, which is highlighted by several key features in these figures. Residual PO_4 and NH_4^+ were present in the reactor, biomass and CPR values were relatively constant and both carbon sources were completely consumed. As conditions transition to the P-limited regime, CPR and biomass decreased and glucose began to accumulate in the reactor. P-limitation resulted in more glucose accumulating in the reactor; however, regardless of the extent of P-limitation, NA was completely consumed.

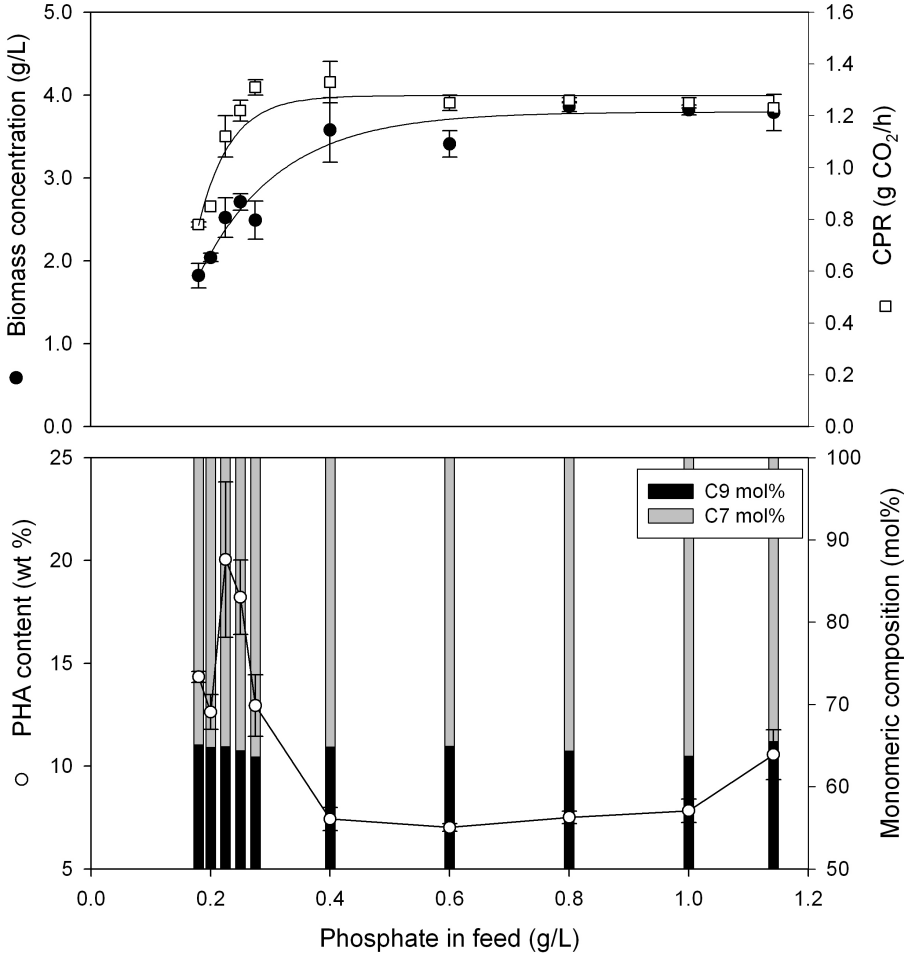

Figure 4-8a: Steady state biomass concentration and CPR versus PO_4 in feed and 4-8b: Steady state PHA content and composition versus PO_4 in feed (D = 0.25 h^{-1})

To a certain degree, P-imitation increased the amount of MCL-PHA produced by *P. citronellolis* DSM 50332. A baseline PHA content of approximately 7-10% was sustained for all C-limited steady states (PO_4 greater than 0.300 g/L). As conditions became increasingly P-limited, there was a corresponding increase

in PHA content up to a maximum value of 20.0 wt% at an inlet PO_4 concentration of 0.225 g/L. Lower PO_4 concentrations had a detrimental effect on PHA content, possibly due to the disruption of normal growth and maintenance of cells at the specific growth rate. Polymer composition was constant at approximately 65 mol% C9 and 35 mol% C7 for all experimental conditions.

Interestingly, *P. citronellolis* DSM 50332 did not produce PHA from NA under C-limited conditions in a shake flask, but did in this chemostat experiment. The cause for this phenomenon is not known, but it may be related to the non-constant and constant specific growth rates associated with batch and chemostat systems, respectively. Another explanation may be the provision of glucose as a second carbon source. In Sun *et al.* (2009a) that the yield of MCL-PHA from NA by *P. putida* KT2440 improved when glucose was provided as a second substrate.

Because the flow rate of NA was held constant for all steady state points, the trend in PHA yield mirrored the trend in PHA content (Figure 4-8b). The maximum PHA yield from NA ($Y_{PHA/NA}$) was 0.18 g/g, which occurred at 0.225 g/L PO_4. This was understandably lower than the values reported by Sun *et al.* (2009a) and Jiang (2010) for *P. putida* KT2440, which is a bona fide production strain capable of accumulating MCL-PHA as high as 75% of the DCW (Sun *et al*., 2007b).

4.2.1.2 Conclusions

A chemostat study investigated the ability of *P. citronellolis* DSM 50332 to produce MCL-PHA from NA under P-limitation. It was clearly demonstrated that: 1) *P. citronellolis* DSM 50332 was able to produce an appreciable amount of MCL-PHA from NA in a chemostat and; 2) P-limitation alone enhanced PHA production and therefore, PHA yield from NA. More than a two-fold increase in PHA content was achieved over the baseline value under C-limited conditions to a maximum value of 20.0 wt%. P-limitation had a significant effect on PHA content. A clear maximum emerged at an inlet PO_4 concentration of 0.225 g/L, deviation from which, in either direction (more or less PO_4), yielded less PHA. Future work should focus on altering the ratio of NA to glucose under PO_4 limitation to determine whether PHA content can be improved further.

4.2.2 Accumulation of MCL-PHA from nonanoic acid (NA) and azelaic acid (AzA) by *P. citronellolis* DSM 50332 under phosphorus (P) limited conditions

AzA was introduced as an additional carbon source in the chemostat study of *P. citronellolis* DSM 50332. The objective was to determine if, in the presence of another carbon source known to promote MCL-PHA production (NA), AzA could be used to produce MCL-PHA containing a side chain carboxyl group. In this experiment, the concentration of PO_4 was fixed at 0.225 g/L based on the recommendations of the initial chemostat study (Section 4.2.1). Feeding rates of glucose and NA fed to the reactor were maintained at the same levels, while AzA was fed as described in Section 3.4.3.

4.2.2.1 Results and discussion

Biomass and CPR were not largely affected by the feeding rate of AzA to the reactor (Figure 4.9a). Apart from the first point (no AzA), which had an elevated CPR and a low biomass concentration, the values were relatively constant. PHA content and composition remained constant as AzA feeding was increased (Figure 4-9b). Consistent with the results of the initial P-limitation study (section 4.1.1), an inlet PO_4 concentration of 0.225 g/L yielded polymer content between 18.2 and 22.1 wt%. The MCL-PHA produced contained only C9 and C7 monomer units (65 mol% and 35 mol%, respectively). $Y_{PHA/NA}$ ranges from 0.17 to 0.26 g/g, according to the fluctuations in PHA content. The compositional data suggest that AzA was not being used for MCL-PHA production. If this were the case, one would expect to observe a copolymer containing carboxylated monomers from β-oxidation, or C8 and C10 monomers from *de novo* fatty acid biosynthesis following complete β-oxidation to acetate (Section 4.1.2).

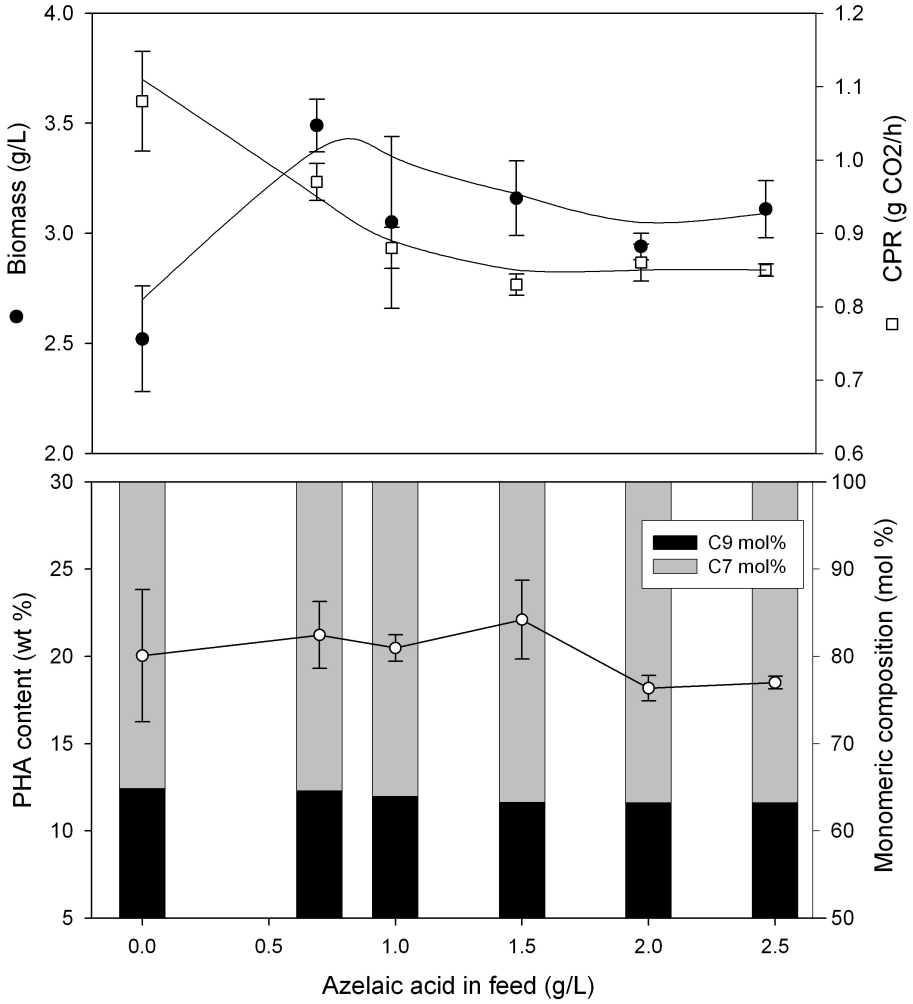

Figure 4-9a: Steady state biomass concentration and CPR versus AzA in feed and 4-9b: Steady state PHA content and composition versus AzA in feed (D = 0.25 h^{-1})

Despite the fact that more carbon was being fed, biomass growth was limited by the amount of PO_4 fed throughout the experiment (Figure 4-10a). AzA appeared to be consumed, since the concentrations detected in reactor samples were significantly less than the inlet concentrations (Figure 4-10b). The steady state concentrations of AzA increased linearly with respect to AzA fed, while glucose appeared to follow a similar trend, excluding the initial point. This trend of glucose accumulation in the reactor indicates that AzA was likely supplementing some of the carbon and energy originally derived entirely from glucose. NA was completely consumed under all conditions.

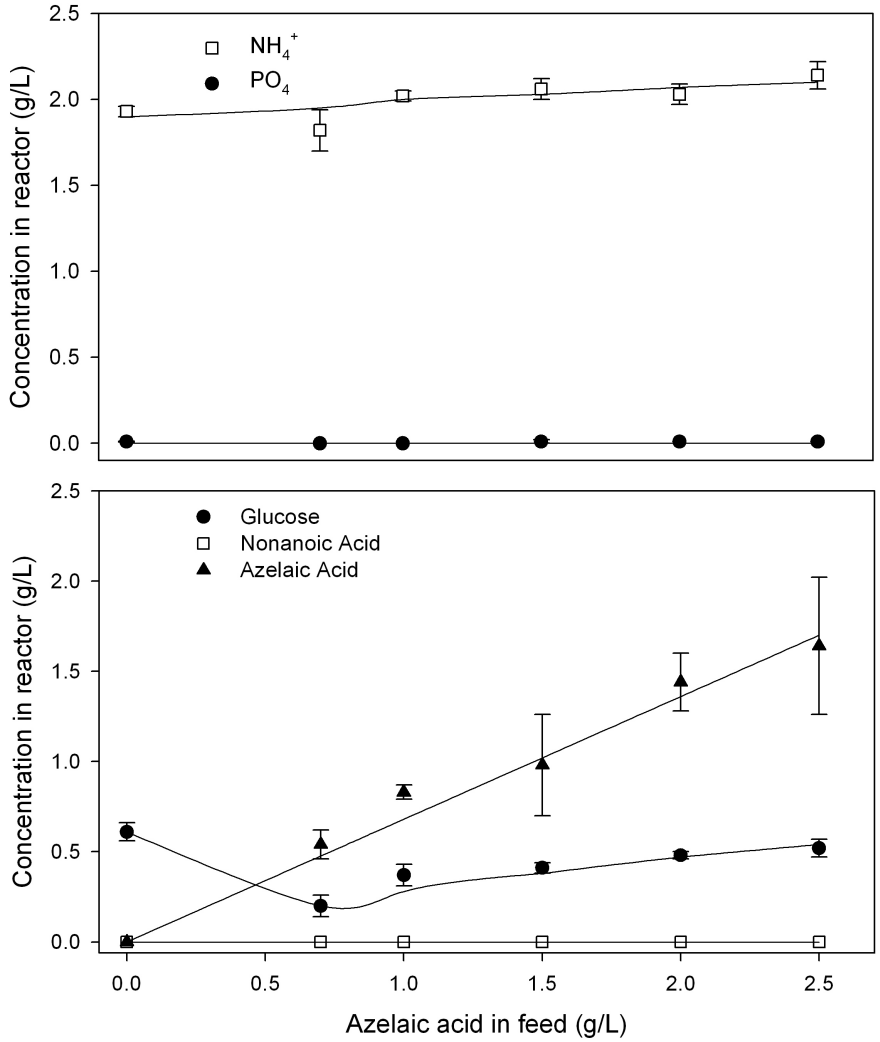

Figure 4-10a: Steady state NH_4^+ and PO_4 in reactor versus AzA in feed and 4-10b: Steady state glucose, NA and AzA concentrations in reactor versus AzA in feed (D = 0.25 h^{-1})

4.2.2.2 Conclusions:

A chemostat experiment was designed to determine whether *P. citronellolis* DSM 50332 was capable of producing carboxylated MCL-PHA from AzA in the presence of NA, an efficient carbon source for MCL-PHA synthesis. While the disappearance of AzA from the chemostat media was detected, the MCL-PHA produced was derived entirely from NA, evident by its monomeric composition (exclusively C7 and C9). Therefore, it was completely degraded to acetate through β-oxidation rather than having intermediates channeled into the MCL-PHA production pathway. Inhibition of β-oxidation was identified as a possible method of producing carboxylated precursors derived from AzA for MCL-PHA production. This was the basis for the work described in the following section.

4.2.3 Accumulation of MCL-PHA from nonanoic acid (NA) and azelaic acid (AzA) by *P. citronellolis* DSM 50332 under phosphorus (P) limited conditions in the presence of acrylic acid as a β–oxidation inhibitor

AA was introduced to the chemostat media to inhibit enzymes in the β-oxidation pathway. In theory, this increases the probability that one of the terminal carboxyl groups on AzA is preserved during β-oxidation. If key enzymes lack the specificity to exclude carboxylated intermediates, then there is a strong possibility of incorporating side chain carboxyl groups into MCL-PHA.

Building on the data collected from the shake flask experiments (Section 4.1.3), a range of AA concentrations ranging from 0.00 to 0.05 g/L was chosen for the chemostat study. All conditions for this study were identical to those described in the previous experiment, with the concentration of AzA fixed at 2.50 g/L.

4.2.3.1 Results and discussion

No steady state was achieved for an inlet AA concentration of 0.05 g/L, due to AA toxicity. CPR decreased steadily above 0.02 g/L AA, indicating a decreased rate of cellular respiration due to increasingly severe inhibition of β-oxidation. However, despite the decreasing CPR, biomass remained constant for all steady states (Figure 4-11a). The probable explanation for constant biomass concentration and decreasing CPR is increased polymer content. Inhibition of β-oxidation restricts the supply of fatty acid derived acetyl-CoA that is available to Krebs cycle, reducing the rates at which its main products, CO_2 (CPR) and reduced nicotinamide adenine dinucleotide (NADH), are generated. The rate of adenosine-5'-triphosphate (ATP) production is also reduced, since it is mainly generated through oxidative phosphorylation, which requires NADH. This leads to a net decrease in the rate of cellular respiration and rest biomass (biomass excluding polymer). In order for overall biomass to remain constant as rest biomass decreases, intracellular polymer content must increase. Figure 4-11b clearly shows that PHA content increased enough to offset decreases in rest biomass. PHA content increased from 18.2% (no AA) to a maximum of 28.1% at an AA concentration of 0.035 g/L. PHA yield from NA ($Y_{PHA/NA}$) also increased from 0.19 g/g (no AA) to a maximum of 0.26 g/g at 0.035 g/L AA.

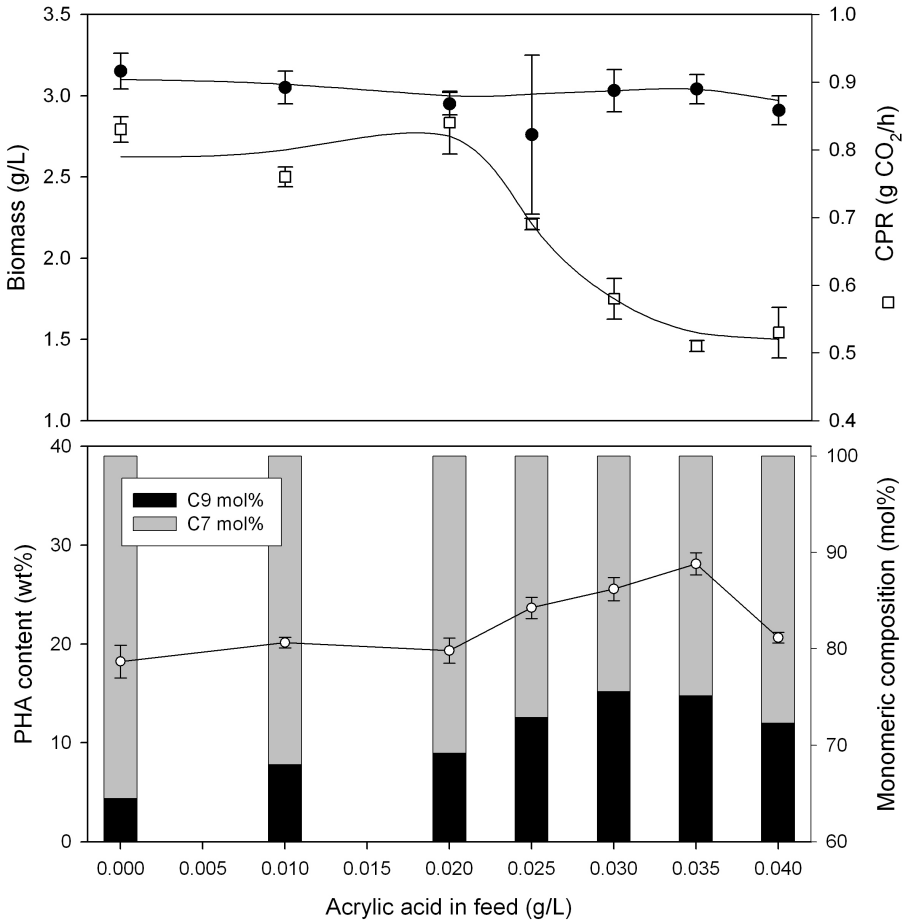

Figure 4-11a: Steady state biomass concentration and CPR versus AA in feed and 4-11b: Steady state PHA content and composition versus AA in feed (D = 0.25 h^{-1})

The composition of the MCL-PHA produced indicated that the polymer was entirely derived from NA (exclusively C9 and C7 monomers). The inhibitory effect of AA on β-oxidation was evident by the compositional shift towards the longer C9 monomer units. A maximum C9 content of 75.6 mol% was achieved at an AA concentration of 0.035 g/L, which was an increase of 11.1 mol% compared to the natural composition of MCL-PHA produced from NA (no AA). The enrichment of longer chain monomers by inhibition of β-oxidation with AA was also reported in *P. putida* KT2440 (Jiang, 2010) and *P. fluorescens* BM07 (Choi *et al*., 2009). Although, *P. putida* KT2440 is capable of producing MCL-PHA from NA with much higher C9 content when AA is used as a β-oxidation inhibitor. At an identical dilution rate and carbon feeding conditions to this chemostat experiment, *P. putida* KT2440 was able to achieve a C9 content of 95 mol% at 0.15 g/L AA (Jiang, 2010). The fact that *P. citronellolis* DSM 50332 has an AA toxicity

threshold that is an order of magnitude less than that of *P. putida* KT2440, suggests that AA may have other inhibitory effects on *P. citronellolis* DSM 50332.

AA did not have any significant effect on the steady state consumption of the three carbon sources: glucose, NA and AzA (Figure 4-12a). NA was completely consumed for all but the highest AA concentration (0.040 g/L), at which point the severity of β-oxidation inhibition caused it to accumulate in the reactor. The consumption of glucose remained fairly constant throughout the experiment varying from 0.31 to 0.49 g/L.

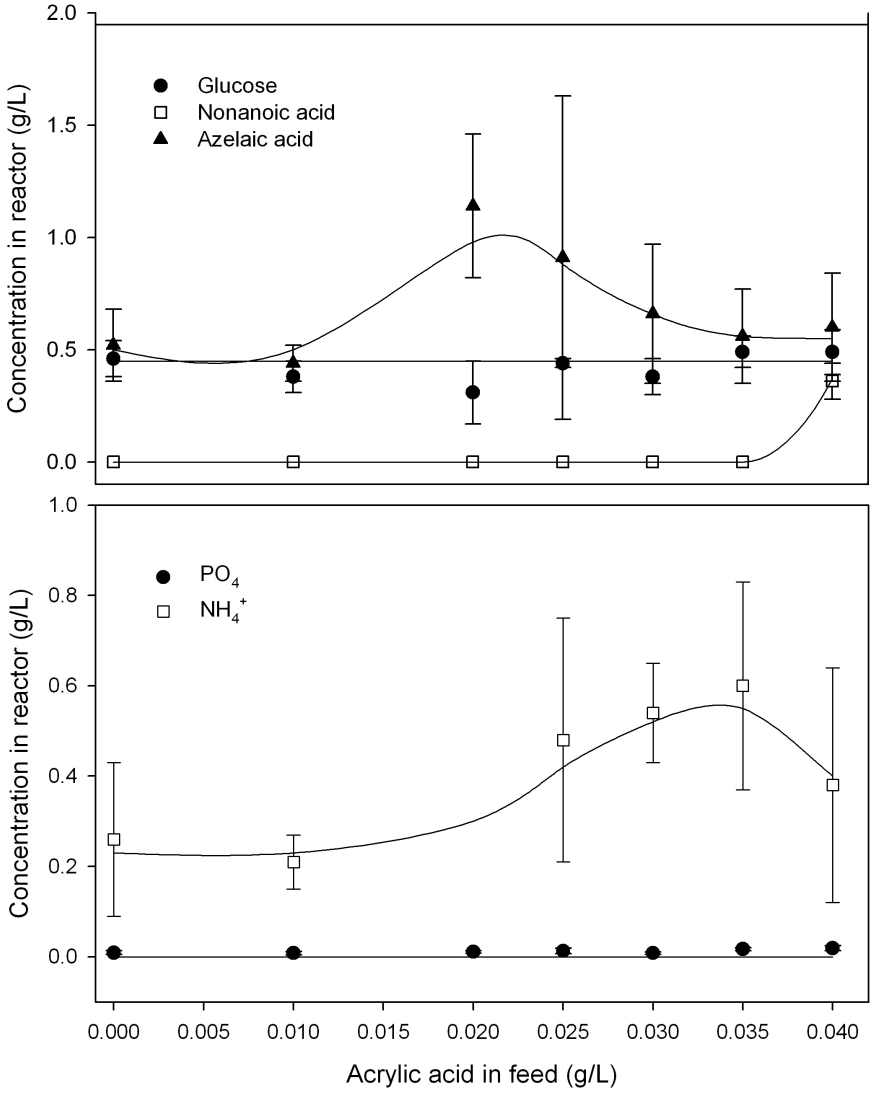

Figure 4-12a: Steady state glucose, NA and AzA concentrations in reactor versus AA in feed and 4-12b: Steady state NH_4 and PO_4 in reactor versus AA in feed (D = 0.25 h^{-1})

AzA concentration in the reactor was also fairly constant, with the exception of an unexplained increase at 0.020 and 0.025 g/L AA. The large error bars for these points, especially 0.025 g/L, indicate that one of the samples may have been poorly mixed, leading to a measurement that was not representative of the true reactor conditions. One would expect the increase in NA concentration at 0.040 g/L to coincide with a proportionate increase in AzA concentration since both substrates are catabolized via the β-oxidation pathway. However, there was no appreciable increase in the measured AzA concentrations between 0.035 and 0.040 g/L AA. Growth conditions were P-limited for the duration of the experiment and there was residual NH_4^+ present in the reactor at all of the steady state points (Figure 4-12b).

In order to ensure that the MCL-PHA did not contain any side chain carboxyl groups originating from AzA, ^{1}H-NMR and ^{13}C-NMR were employed to verify the results of the GC analysis, which detected only C9 and C7 monomers (alkyl side chains). Polymer was extracted and purified from a large biomass sample taken from the 0.025 g/L AA steady state point (Figures 4-11 and 4-12). A known C9/C7 MCL-PHA standard was used as a basis for comparison. ^{13}C-NMR and ^{1}H-NMR spectra were essentially identical, indicating that the sample contained C9 and C7 monomers only. No carboxyl groups were detected. Figure 4-13 shows the ^{13}C-NMR spectrum with assignments (Table 4-3) for the C9/C7 MCL-PHA standard. Figure 4-14 shows stacked ^{13}C-NMR spectra, normalized for comparison, illustrating concurrences in carbon peaks between the MCL-PHA standard and the purified sample produced in the chemostat.

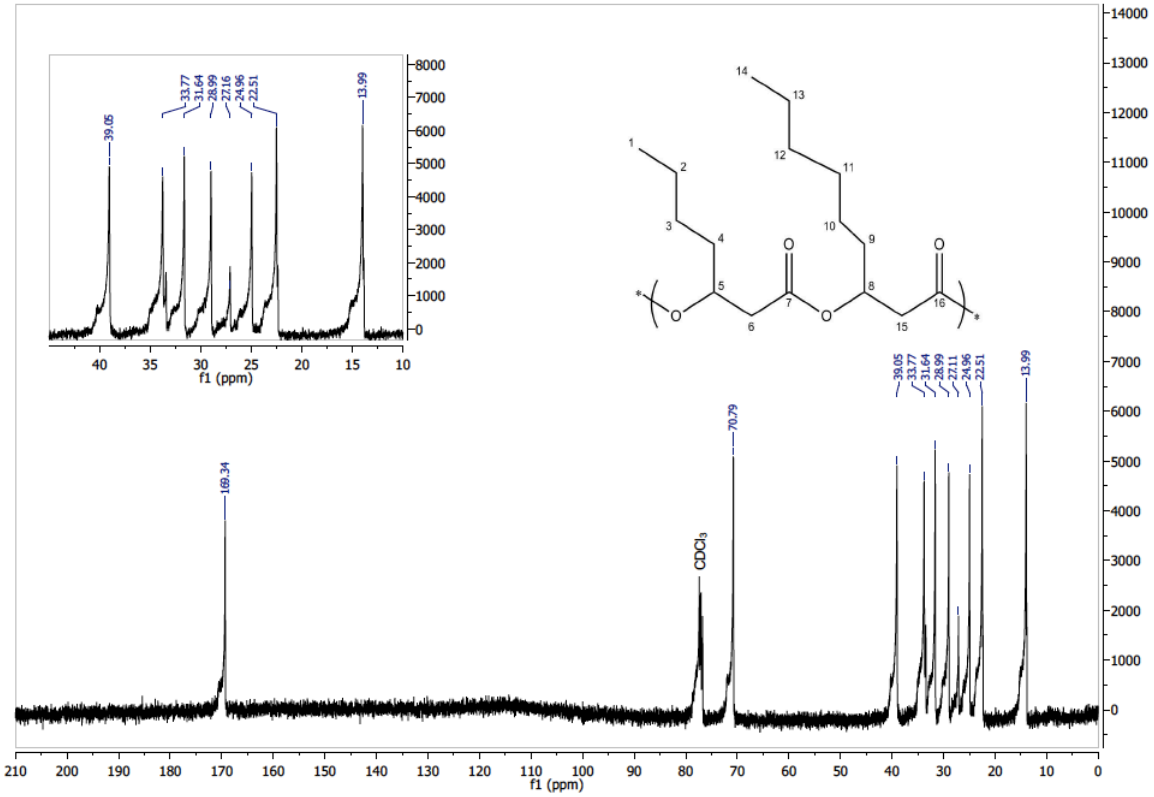

Figure 4-13: ^{13}C-NMR spectrum for C9/C7 MCL-PHA standard

Table 4-3: Assignments for ^{13}C-NMR spectrum in Figure 4-13

Shift (ppm)	Carbon number
13.99	1,14
22.51	2,13
24.96	10
27.11	3
28.99	11
31.64	12
33.77	4,9
39.05	6,15
70.79	5,8
169.34	7.16

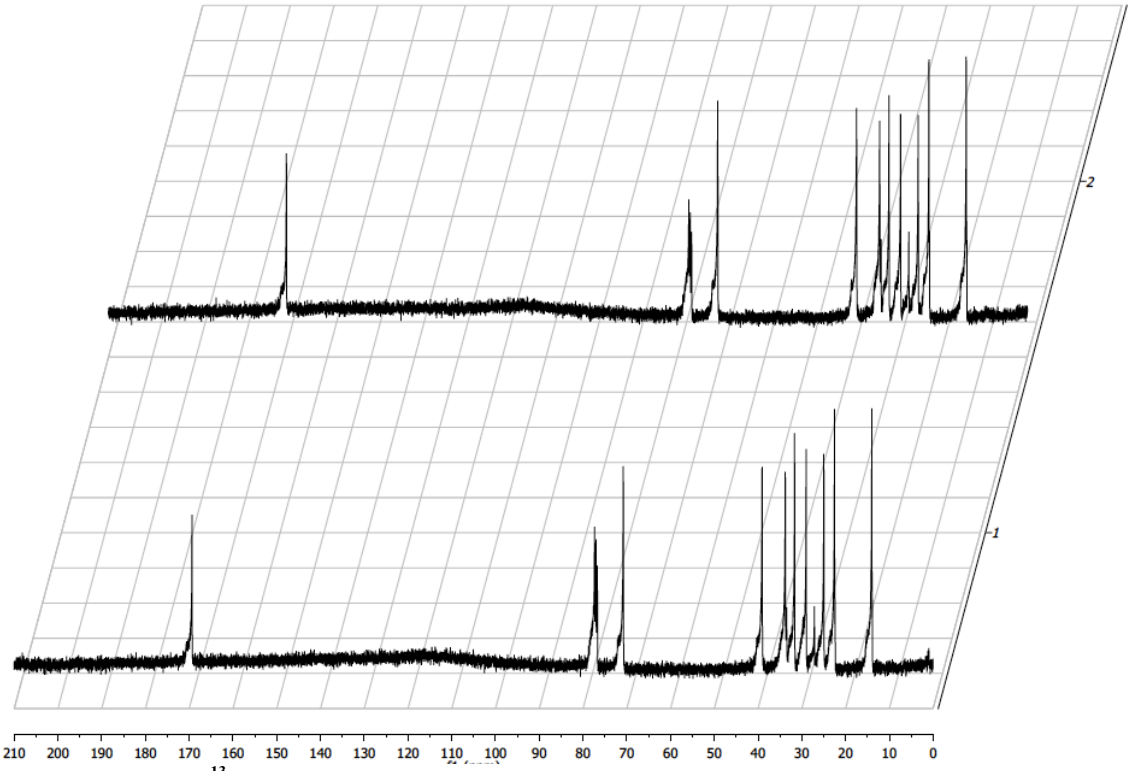

Figure 4-14: Stacked ^{13}C-NMR spectra for chemostat sample (1) and C9/C7 MCL-PHA standard (2)

Likewise, Figure 4-15 shows the ^{1}H-NMR spectrum with assignments (Table 4-4) for the C9/C7 standard and Figure 4-16 shows the stacked spectra.

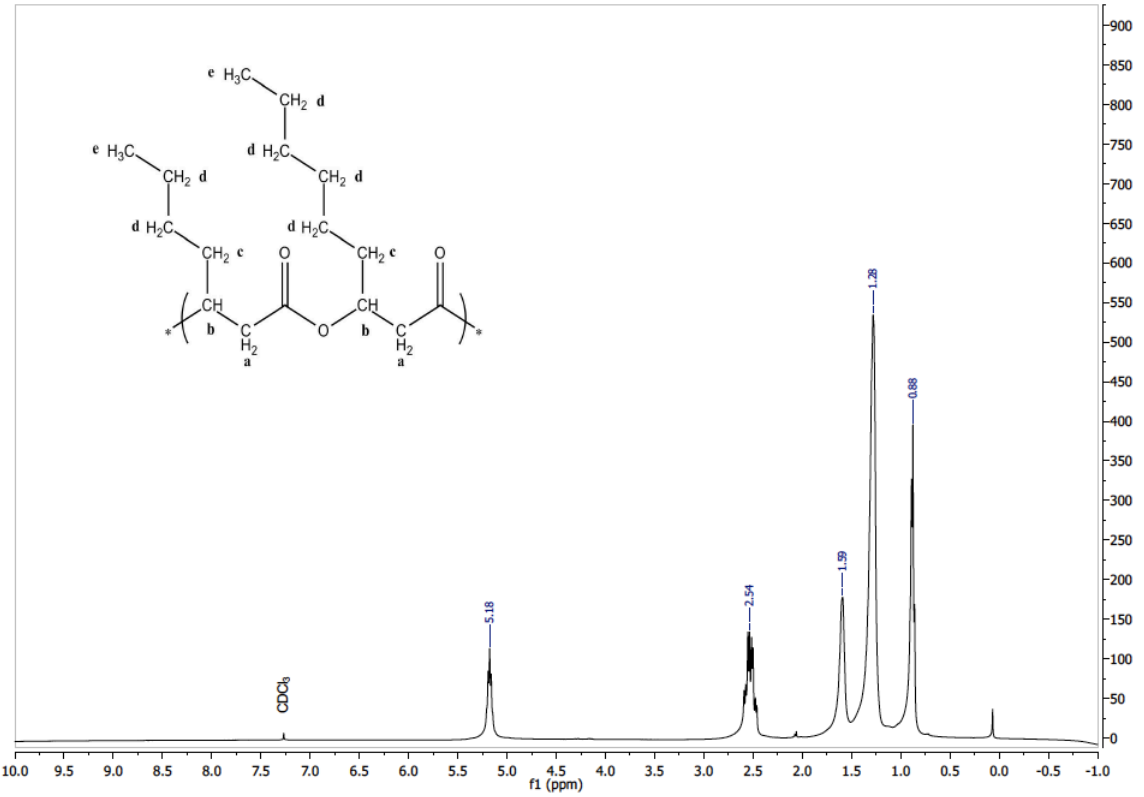

Figure 4-15: ^{1}H-NMR spectrum for C_9/C_7 MCL-PHA standard

Table 4-4: Assignments for ^{1}H-NMR Spectrum in Figure 4-15

Shift (ppm)	Hydrogen designation
0.88	e
1.28	d
1.59	c
2.54	a
5.18	b

The ratio of the peak areas corresponding to the ‘d’ and ‘b’ designated hydrogen atoms is representative of the length of the side chain relative to the backbone. PHA composition can be calculated in this fashion.

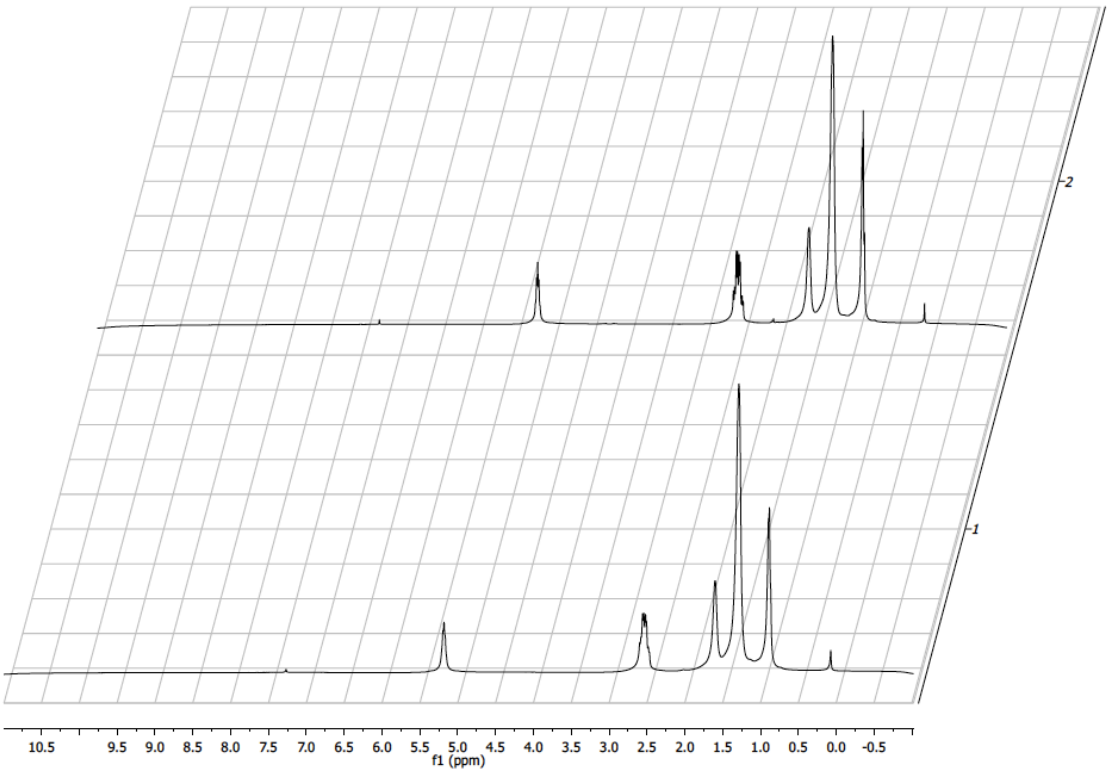

Figure 4-16: Stacked ^{1}H-NMR spectra for chemostat sample (1) and C9/C7 MCL-PHA standard (2)

4.2.3.2 Conclusions

P. citronellolis DSM 50332 was unable to produce MCL-PHA containing a side chain carboxyl group from AzA, even through inhibition of β-oxidation by AA. In fact, there was no evidence to suggest that AzA was being used for MCL-PHA production at all. Despite this, AA was found to have the effect of compositional control in *P. citronellolis* DSM 50332, a feature that is common to a number of other strains. AA was able to achieve 11.1% enrichment in C9 content in the MCL-PHA produced from NA, compared to the natural composition in the absence of inhibitor.

P citronellolis DSM 50332 was able to catabolize AzA via β-oxidation; however, it was not incorporated into the polymer. Rather, it appeared to be consumed completely, yielding acetyl-CoA, which entered Krebs cycle. There are several possible explanations for this phenomenon.

The fact that AzA was being consumed indicates that enzymes in the β-oxidation pathway were capable of utilizing AzA and its intermediates, as substrates. However, the state of the terminal carboxyl groups on

these intermediates was unknown. In order for carboxylated MCL-PHA to be created, one carboxyl terminus must be preserved (unreacted) through β-oxidation, eventually culminating with its incorporation into MCL-PHA by PHA synthase. If the enzymatic reactions in β-oxidation occur simultaneously or sequentially at both ends, then a carboxyl group will not be preserved. Assuming that β-oxidation proceeds exclusively from one end at a time, the capacity for producing carboxylated MCL-PHA becomes contingent on the specificity of the first two enzymes in the β-oxidation pathway (acyl-CoA dehydrogenase and enoyl-CoA hydratase), the enzymes linking β-oxidation to MCL-PHA production (FabG and PhaJ) and the PHA synthase. Carboxylated MCL-PHA cannot be synthesized if certain combinations of these enzymes are unable to catalyze reactions involving a substrate with a carboxyl group (based on location, Figure 2-1). Furthermore, if one of the four enzymes in the β-oxidation cycle cannot utilize a carboxylated substrate, these intermediates will accumulate. Reaction of their free carboxyl terminuses then becomes more probable as a means of restoring full functionality to the cycle.

More experimental work is required to help elucidate the enzymatic treatment of dicarboxylic acids in the β-oxidation pathway. This will help to explain the mechanism of oxidation, specifically how it proceeds in the presence of two terminal carboxyl groups. A particularly intriguing step is the activation of the fatty acid preceding β-oxidation, which is catalyzed by acyl-CoA thiokinase. If both carboxyl ends convert to CoA-thioesters before entering β-oxidation, none of the pathway intermediates will contain a free carboxyl group. In addition, the identification of enzymes that cannot accommodate carboxylated substrates would be beneficial. Future work should involve looking at site-directed mutagenesis or other mutagenic techniques to alter the structure of key enzymes, particularly PHA synthase, to accommodate carboxylated substrates. Finally, the use of other dicarboxylic acids a carbon sources, as well as other bacterial strains should also be investigated thoroughly to determine potential in synthesizing carboxylated MCL-PHA.

Chapter 5

Two-stage high-cell density cultivation of *P. putida* KT2440 producing MCL-PHA from nonanoic acid

5.1 Single-stage high-cell density chemostat studies

Production of MCL-PHA by *P. putida* KT2440 in a high-cell density C-limited two-stage chemostat was the main objective of this chapter. However, in order to determine the appropriate growth conditions for the two-stage setup, a single-stage setup was first investigated. Two separate chemostat were used to determine growth conditions that would ensure good performance in the two-stage setup. Air was used for aeration in all cases (no pure O_2). Reported error is one standard deviation of the values calculated at each steady state (Section 3.1.7).

5.1.1 Effect of nonanoic acid (NA) to glucose ratio on PHA production in a carbon-limited (C-limited) single-stage high-cell density chemostat

Different ratios of NA to glucose (NA:glu) were investigated to determine the conditions yielding the best PHA content and reactor performance. The total carbon fed to the reactor was fixed at 6.50 g/L for all conditions, while AA concentration in the feed was fixed at 0.15 g/L.

5.1.1.1 Results and discussion

As the ratio of NA:glu was increased, biomass values decreased slightly to a minimum of 6.39 g/L at a ratio of 1.00 and rise to a maximum of 8.02 g/L at 1.29 (Figure 5-1a). CPR was constant at about 2.15 g/h until NA:glu of 1.00, followed by a sharp decrease at NA:glu of 1.15 (1.65 g/h CPR) and 1.29 (1.22 g/h CPR). As with the *P. citronellolis* DSM 50332 data in Chapter 4 the trends in biomass and CPR data can be attributed to increased intracellular PHA content (Figure 5-1b). Although AA concentration was constant (0.15 g/L), the proportion of NA comprising total carbon increased, causing a decrease in CPR due to inhibition of β-oxidation as previously described (Section 4.2.3.1).

PHA content was greatly affected by NA:glu. Lower proportions of NA in the feed (NA:glu ≤ 1.00) resulted in a PHA content of about 10 wt%. A considerable increase from 10.5 to 48.5 wt% was observed

when the NA:glu was increased from 1.00 to 1.15, followed by an additional increase to the maximum value of 63.1 wt% at 1.29. C9 content was highest (92.6 mol%) at NA:glu of 0.72, before decreasing slightly and fluctuating about an average value of 89.3 mol% for the remaining four points.

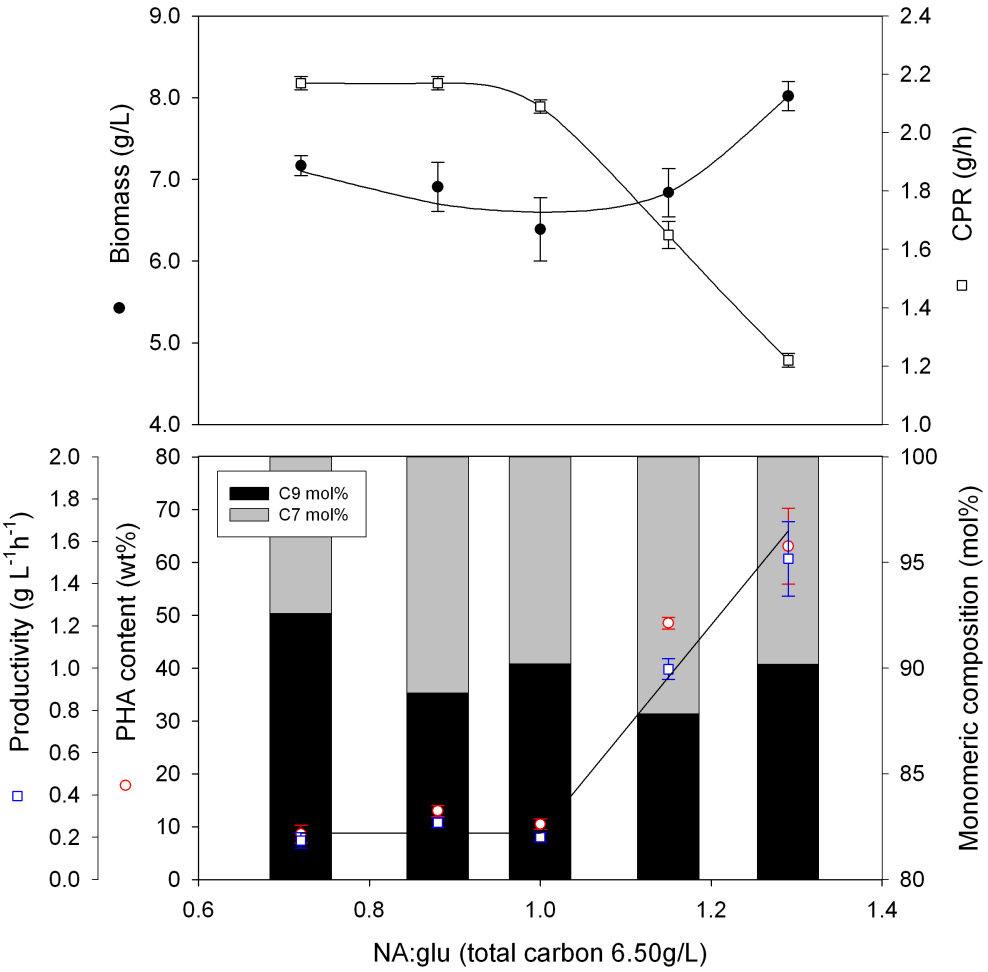

Figure 5-1a: Steady state biomass concentration and CPR versus NA:glu and 5-1b: Steady state PHA content, composition and reactor productivity versus NA:glu (D = 0.30 h^{-1})

Opposite trends were found in similar chemostat work done by Jiang (2010), using the same strain. There were a few minor changes in the operating parameters compared to this study: the glucose feeding rate was fixed as opposed to total carbon, a slightly lower dilution rate was used (0.25 h^{-1} versus 0.30 h^{-1}) and a higher acrylic acid concentration was used (0.20 g/L versus 0.15 g/L). In Jiang (2010) PHA content decreased from about 60% beyond a NA:glu of 1.00, moving towards a minimum of about 33% at NA:glu of 1.70. Interestingly, the C9 monomer content also decreased steadily by about 10% as the NA:glu was increase from 0.50 to 1.70. While the high-cell density chemostat used in this study did not markedly

improve PHA content compared to work by Jiang (2010), there were significant gains in reactor productivity. The maximum productivity of 1.52 g $L^{-1}h^{1}$ represented a vast improvement, owing itself to the to the increased carbon feeding and higher dilution rate. Moreover, productivity of this system compares favourably to literature values for fed-batch MCL-PHA production. This is discussed in detail at the end of the chapter. PHA yield from NA ($Y_{PHA/NA}$) increased from 0.14 to 0.80 g/g as NA:glu was increased from 0.72 to 1.29. This was a significant improvement over the 0.69 g/g achieved by Sun *et al.* (2009a) in a fed-batch system with *P. putida* KT2440, but less than the 0.90 g/g achieved in Jiang's chemostat work (2010).

Steady state NH_4^+ and PO_4 concentrations were fairly constant for all growth conditions, due to the fixed amount of total carbon (Figure 5-2b). Trace amounts of glucose were detected for some of the steady states but, in essence, it was completely consumed. On the other hand, low concentrations of NA were detected in three of the five steady state samples. The large error bars on the first point (0.72 NA:glu) were a result of one of the two steady state samples containing a large amount of NA and the other one containing no NA. This was likely an issue related to the periodic addition of NA to the reactor, resulting in short-lived concentration gradients during sampling. The other two points (1.15 and 1.29 NA:glu) had low concentrations of NA that may have persisted in the reactor at higher feeding rates.

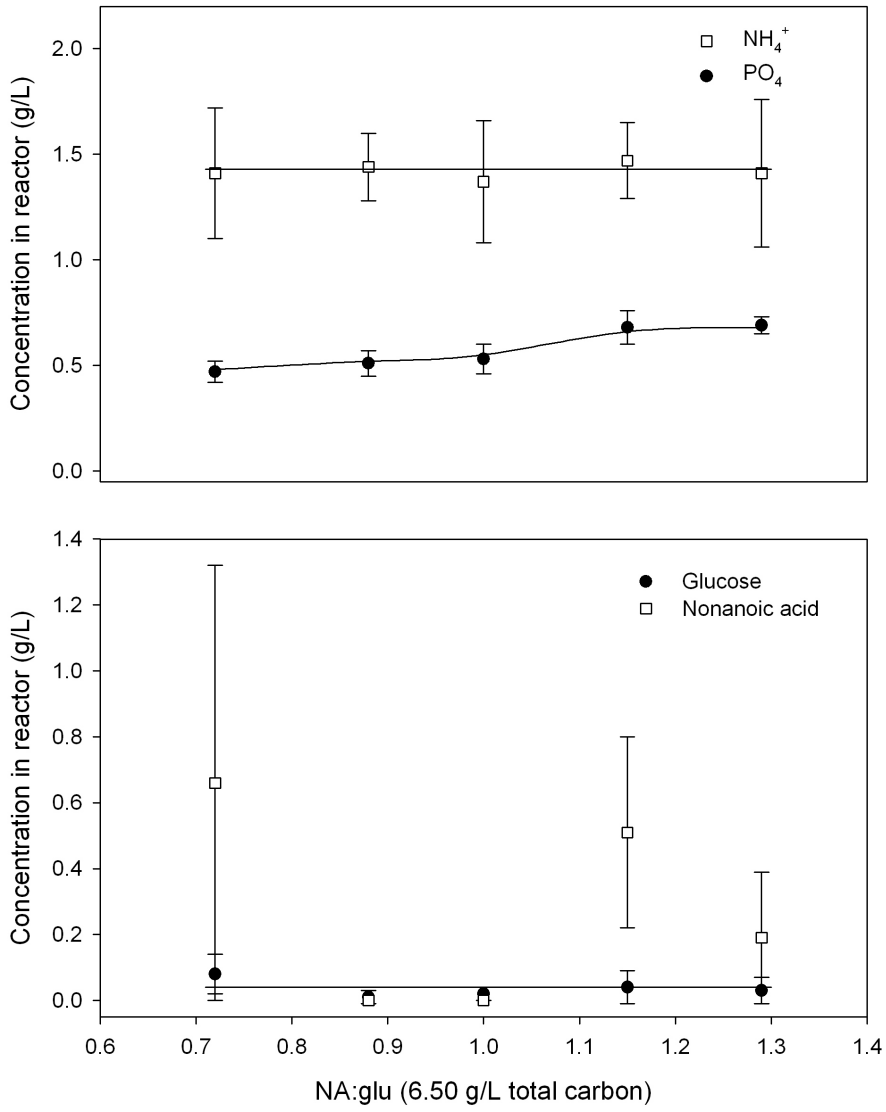

Figure 5-2a: Steady state NH_4^+ and PO_4 concentrations in reactor versus NA:glu and 5-2b: Steady state glucose and NA concentrations in reactor versus NA:glu (D = 0.30 h^{-1})

AA was undetected in the sample supernatants, with the exception of the sample taken at 1.00 NA:glu (Figure 5-3). It is apparent that *P. putida* KT2440 took up AA into the cell, but whether or not AA was metabolized remained unknown. Similar findings were reported in the chemostat work of Jiang (2010), in which AA was fed at a slightly higher concentration (0.20 g/L) than used in this study (0.15 g/L). Regardless of the fate of AA in the cell, its efficacy as a β-oxidation inhibitor was not weakened throughout the course of this study. C9 monomeric composition was sustained at a level, which was significantly higher than normally produced by *P. putida* KT2440 from NA.

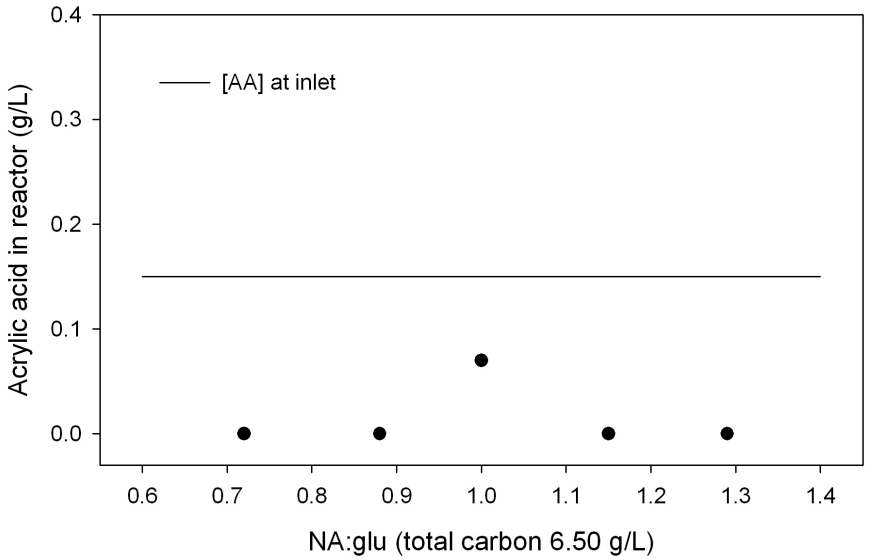

Figure 5-3: Steady state AA in reactor versus NA:glu (D = 0.30 h^{-1})

A carbon balance was completed around the reactor in order to validate the analytical data. All of the carbon-based compounds moving in and out of the reactor were expressed using a basis of grams of atomic carbon per hour (g C/h). The reactor was assumed to be a well-mixed CSTR, therefore the measured quantities for reactor samples were assumed to equal the quantities leaving the reactor. Rest biomass was assumed to be 50% carbon by mass (0.50 g C/g). Carbon comprising MCL-PHA was calculated at each steady state point based on composition and content. The feeding rate of AA was negligible. Figure 5-4 is a block diagram depicting the inlet and outlet streams in the carbon balance.

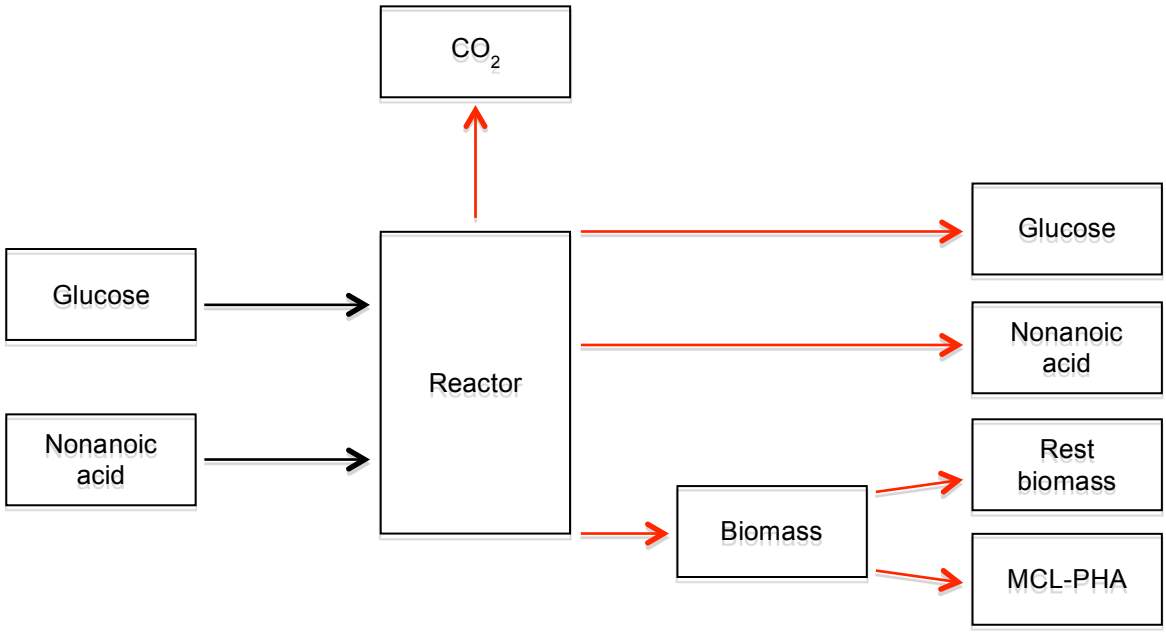

Figure 5-4: Species accounted for in the carbon balance

On the whole, the carbon flow rates in and out of the reactor were in very good agreement with each other (Table 5-1). Some of the outlet carbon flow rates were slightly less than the inlet flow rates, the largest discrepancy occurring at NA:glu of 1.00, at which, the upper limit of the outlet carbon flow rate was 12% lower than the inlet carbon flow rate. Small deteriorations in the inlet flow rate due to tubing wear would have caused to inlet carbon flow rate to drop slightly below 1.79 g C/h.

Table 5-1: Carbon balance for single-stage high-cell density chemostat with varied NA:glu in feed

NA:glu	Carbon IN, g C/h	Carbon OUT, g C/h
0.72	1.79	1.77 ± 0.23
0.88	1.79	1.61 ± 0.08
1.00	1.79	1.50 ± 0.09
1.15	1.79	1.68 ± 0.07
1.29	1.79	1.76 ± 0.13

5.1.2 Effect of acrylic acid (AA) concentration on PHA production in a carbon-limited (C-limited) single-stage high-cell density chemostat

As a continuation of the experimental work from the previous section, the concentration of AA in the feed was increased for a fixed ratio of NA:glu. Initially, this study was designed to use the best-performing NA:glu ratio from the previous work (Section 5.1.1), but both parts were conducted one continuous experiment. Due to the lengthy lead-time required for full sample processing and analysis, the highest PHA content had to be estimated from wet mounts prepared at each steady state. Based on this protocol, the

NA:glu ratio of 1.15 was chosen to investigate different AA concentrations. The best performing NA:glu was actually 1.29, while 1.15 was second best (Figure 5-1b). However, it was reasonable to assume that, for a relatively small change in NA:glu ratio, the trends with respect AA concentration would be the same.

5.1.2.1 Results and discussion

No significant change in biomass or CPR occurred until the AA concentration in the feed reached 0.50 g/L (Figure 5-5a). At 0.50 g/L, biomass dropped from 6.68 g/L to 5.24 g/L, and rapidly decreased to the lowest concentration of 1.72 g/L at 0.70 g/L AA. This trend was mirrored by the CPR data, with one major difference: the onset of the rapid decline was delayed until 0.60 g/L AA, as opposed to 0.50 g/L. At 0.40 g/L AA, PHA content, C9 content and productivity reached their maximum values of 51.5%, 90.5% and 1.03 g $L^{-1}h^{-1}$, respectively.

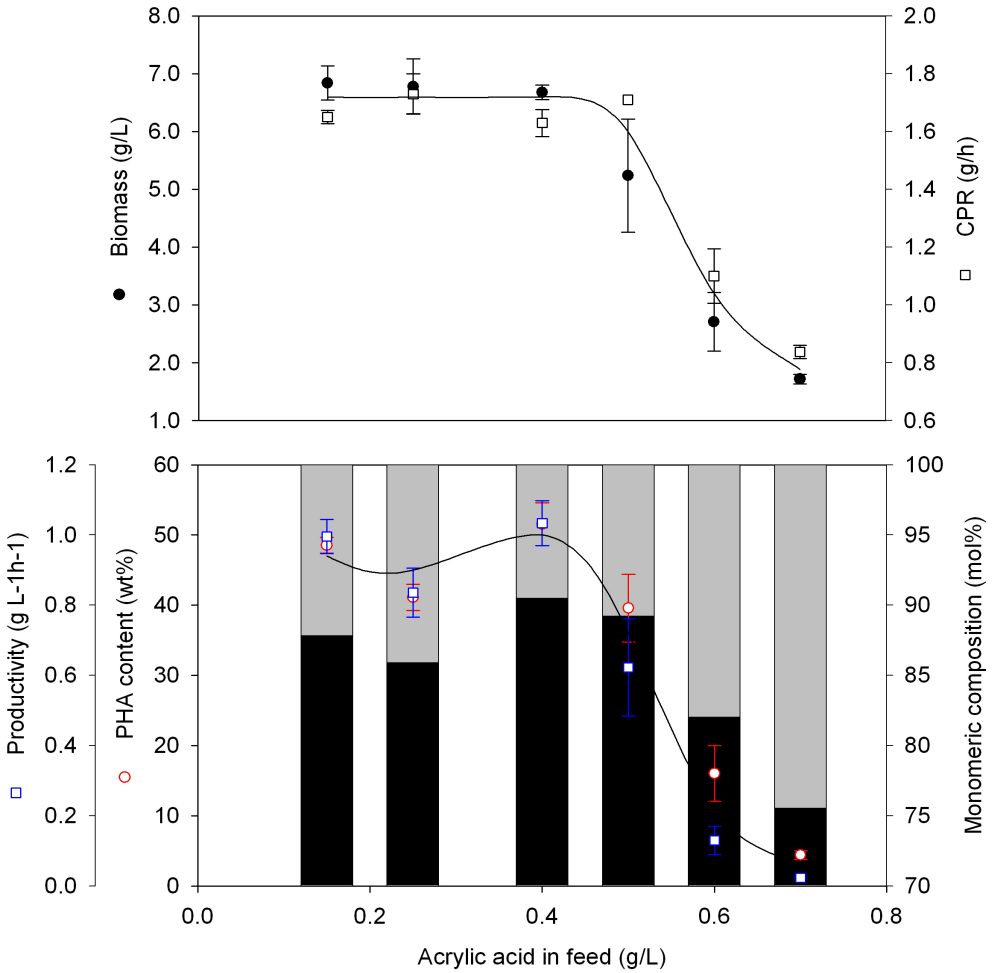

Figure 5-5a: Steady state biomass concentration and CPR versus AA in feed and 5-5b: Steady state PHA content, composition and reactor productivity versus AA (D = 0.30 h^{-1})

Glucose and NA were virtually completely consumed until 0.50 g/L AA, at which point both carbon sources began to accumulate in the reactor due to AA toxicity (Figure 5-6a). NH_4^+ and PO_4 were present in the reactor for all concentrations of AA, indicating that the fermentation was C-limited (Figure 5-6b). Accordingly, NH_4^+ and PO_4 concentrations in the reactor increased above 0.50 g/L AA, due to decreased biomass concentration.

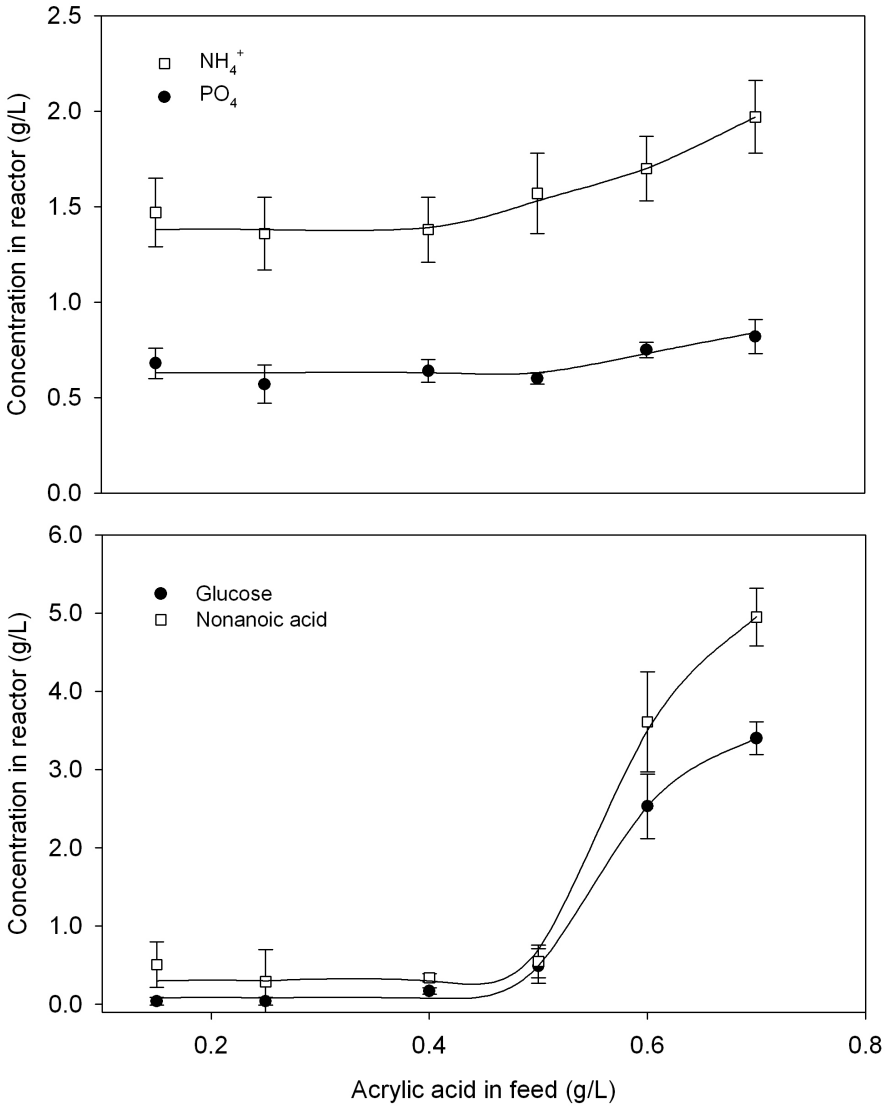

Figure 5-6a: Steady state NH_4^+ and PO_4 concentrations in the reactor versus AA in feed and 5-6b: Steady state glucose and NA concentrations in the reactor versus AA in feed (D = 0.30 h^{-1})

The correlation between AA concentration in the reactor and in the feed was very strong for 0.40 g/L and above, evident by the way in which the points are clustered around the equivalency line (Figure 5-7). For

inlet concentrations of 0.15 and 0.25 g/L, the measured values were significantly lower, 0.00 and 0.11 g/L, respectively. As explained in Section 5.1.1.1, AA may be taken up or consumed by the cell, removing AA from the sample supernatant. However, in light of this data, there may have been an issue with the detection limit for the aqueous phase GC method used to analyze residual AA.

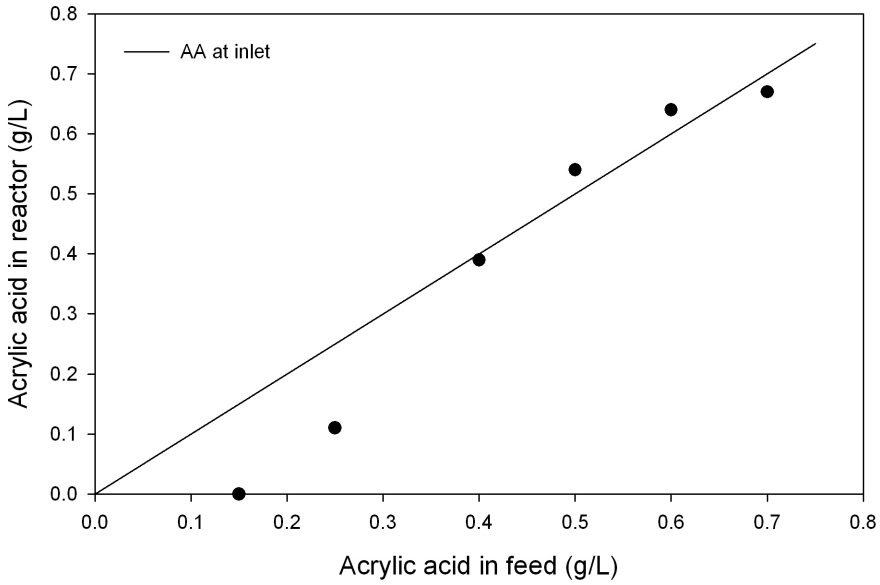

Figure 5-7: Steady state AA in the reactor versus AA in feed (D = 0.30 h^{-1})

A carbon balance for the system is shown in Table 5-2. The carbon flow rates are in reasonably good agreement with one another.

Table 5-2: Carbon balance for the single-stage high-cell density chemostat with varied AA feeding

Acrylic Acid, g/L	Carbon IN, g C/h	Carbon OUT, g C/h
0.15	1.79	1.68 ± 0.07
0.25	1.79	1.63 ± 0.10
0.40	1.79	1.65 ± 0.05
0.50	1.79	1.47 ± 0.14
0.60	1.79	1.68 ± 0.17
0.70	1.79	1.80 ± 0.08

The chemostat performance under these experimental conditions fell short of the best values attained in the previous section, due to the NA:glu ratio used (1.15 instead of 1.29). However, it was reasonable to assume that the same trends in PHA content, composition and productivity with respect to AA concentration would manifest themselves when the NA:glu was increased from 1.15 to 1.29. Therefore, based on the data from both sets of experiments, the best conditions for the high-cell density chemostat were determined to be

NA:glu of 1.29 and an inlet AA concentration of 0.40 g/L. The gain in performance from 0.15 to 0.40 g/L AA was not dramatic, but the deterioration in performance above 0.40 g/L was rapid. Therefore, for future operation it was critical that the AA concentration is tightly controlled around 0.40 g/L to prevent unwanted performance losses.

5.1.2.2 Conclusions

This work discussed herein (Section 5.1) involved the investigation of feeding conditions, specifically the ratio of NA:glu and concentration of AA in the feed, for a high-cell density C-limited single-stage chemostat for MCL-PHA production with *P. putida* KT2440. .The purpose of the work was to establish a set of conditions that could be used to operate a two-stage C-limited chemostat to determine whether further performance gains could be achieved. Based on the criteria of maximum productivity, PHA content and C9 content, the best conditions were determined to be NA:glu of 1.29 and an AA concentration of 0.40 g/L.

5.2 Two-stage high-cell density carbon-limited (C-limited) chemostat

A two-stage high-cell density C-limited chemostat was investigated for improving MCL-PHA content and productivity in *P. putida* KT2440. The purpose of the second stage was used to provide additional cell residence time and more NA to stimulate additional MCL-PHA production. The first stage was operated according to the conditions identified previously (Section 5.1.2.1), while the NA feeding rate in the second stage was increased at each steady state. A small amount of glucose (0.5 g/L) was also fed to the second reactor for the purposes of cell maintenance. Conditions in the first reactor (R1) were constant throughout the entire duration of the experiment. Pure O_2 was not used to aerate either reactor under any conditions. In all figures and tables, reported error is one standard deviation of the values calculated at each steady state (Section 3.1.7).

5.2.1 Results and discussion

Figures 5-8a and 5-8b show the biomass and CPR trends for both reactors for the various NA feeding rates into R2. Simultaneous samples were taken from both reactors at each steady state. Therefore, the data points for R1 correspond to the NA feeding rate in R2 when the samples were taken. While the conditions

in R1 were unchanged for the duration of the experiment, the data reflect the changes that occurred in the R1 over time.

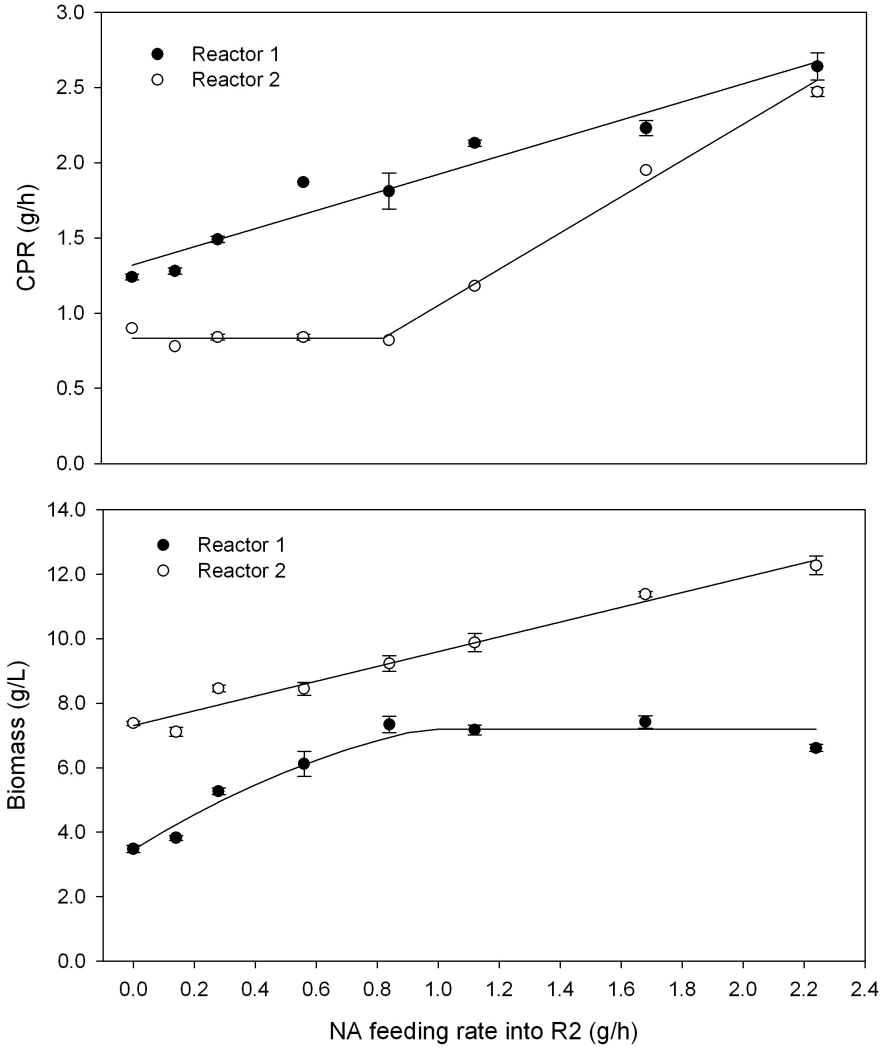

Figure 5-8a: Steady state CPR in R1 and R2 and 5-8b: Steady state biomass concentration in R1 and R2 ($D_1 = 0.30\ h^{-1}$; $D_2 = 0.25\ h^{-1}$)

There was a large linear increase in CPR in R1 from 1.24 to 2.64 g CO_2/h. Unexpectedly, the trend in biomass was slightly different, increasingly linearly from 3.48 to 7.34 g/L for the first four points, before plateauing for the final four points. By contrast, the trends in CPR and biomass for R2 were slightly different. CPR was constant for the first five points before increasing from 1.18 to 2.47 g CO_2/h over the final three points. Biomass increased linearly from 7.38 to 12.27 g/L throughout the entire range of NA feeding rates, because more carbon was fed and growth conditions were not nutrient limited.

The total CPR and biomass were also plotted as a function of the total NA feeding rate into both reactors (Figures 5-9a and 5-9b). Trends were linear for both data sets.

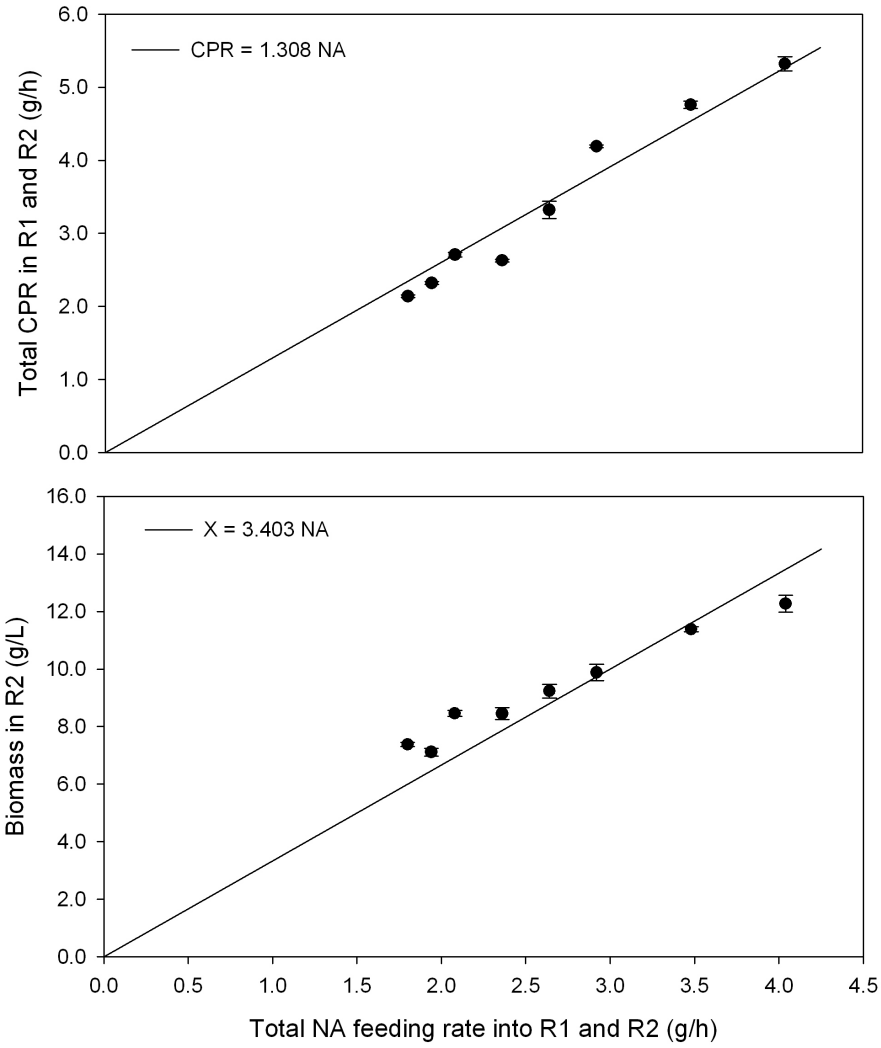

Figure 5-9a: Total steady state CPR versus total NA feeding rate and 5-9b: Total steady state biomass concentration versus total NA feeding rate (D_1 = 0.30 h^{-1}; D_2 = 0.25 h^{-1})

PHA content and composition data for each R1 and R2 are shown in Figures 5-10a and 5-10b, respectively. PHA content in R1 increased to a maximum value of 58.5% at the fifth point (1.00 g/h), before falling to a minimum value of 25.8% at the last point (2.0 g/h). PHA composition in R1 fluctuated more than anticipated, given the relatively high concentration of AA in the feed. Composition was generally between 85 and 90 mol% C9, with the exception of the third and fourth points (0.28 and 0.56 g/h), which decreased to 80 mol% C9. The PHA content data for R2 followed a similar trend to R1, given the fact that the reactors were arranged in series. Compared to R1, gains of 5-10% in PHA content were achieved in R2

through the first five points, achieving a maximum content of 58.5% at 0.84 g/h NA. The decline in PHA content in R1 caused a coincidental decline in R2. Interestingly, cells in R2 actually contained less PHA than those in R1 for the final two data points.

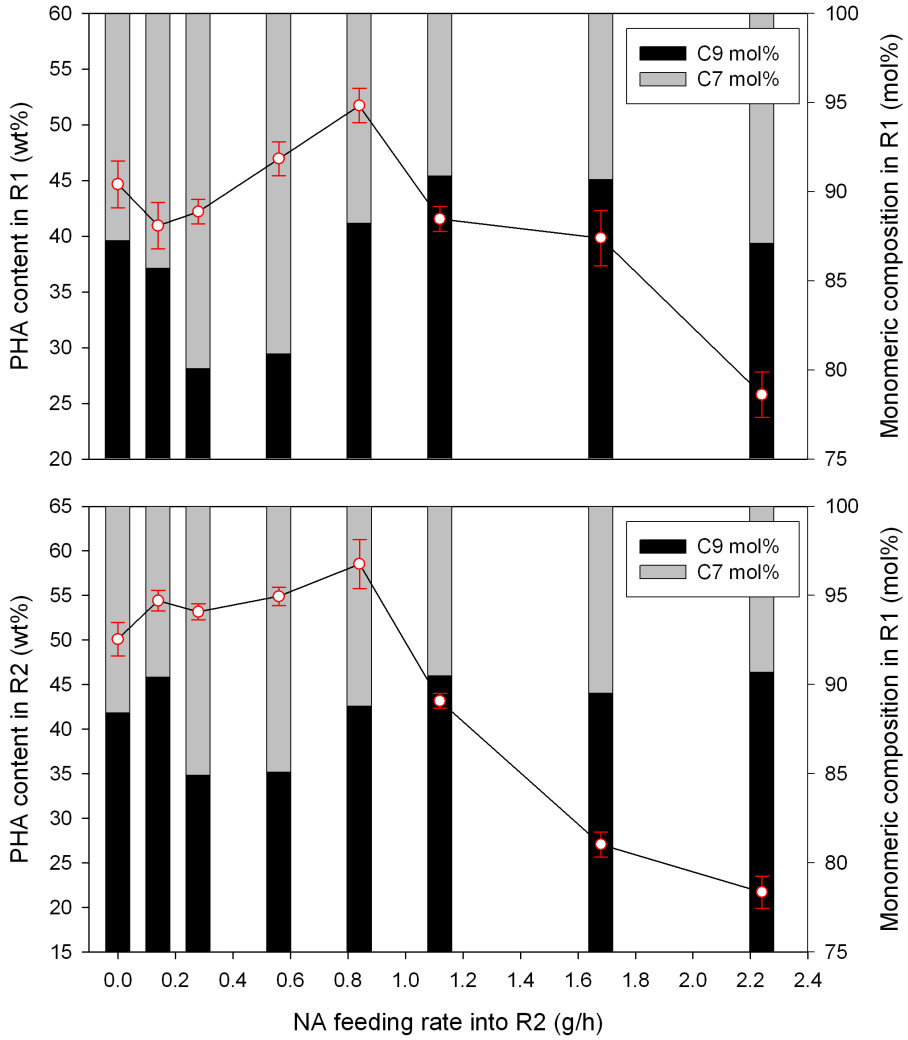

Figure 5-10a: Steady state PHA content and composition in R1 and 5-10b: Steady state PHA content and composition in R2 (D_1 = 0.30 h^{-1}; D_2 = 0.25 h^{-1})

Residual glucose and NA concentrations in both reactors are shown in Figure 5-11a and 5-11b, respectively. High concentrations of NA and low concentrations of glucose were present in R1 initially, gradually decreasing to the point at which they were completely consumed (Figures 5-11a and 5-11b). In R2, both carbon sources were essentially consumed completely for all points.

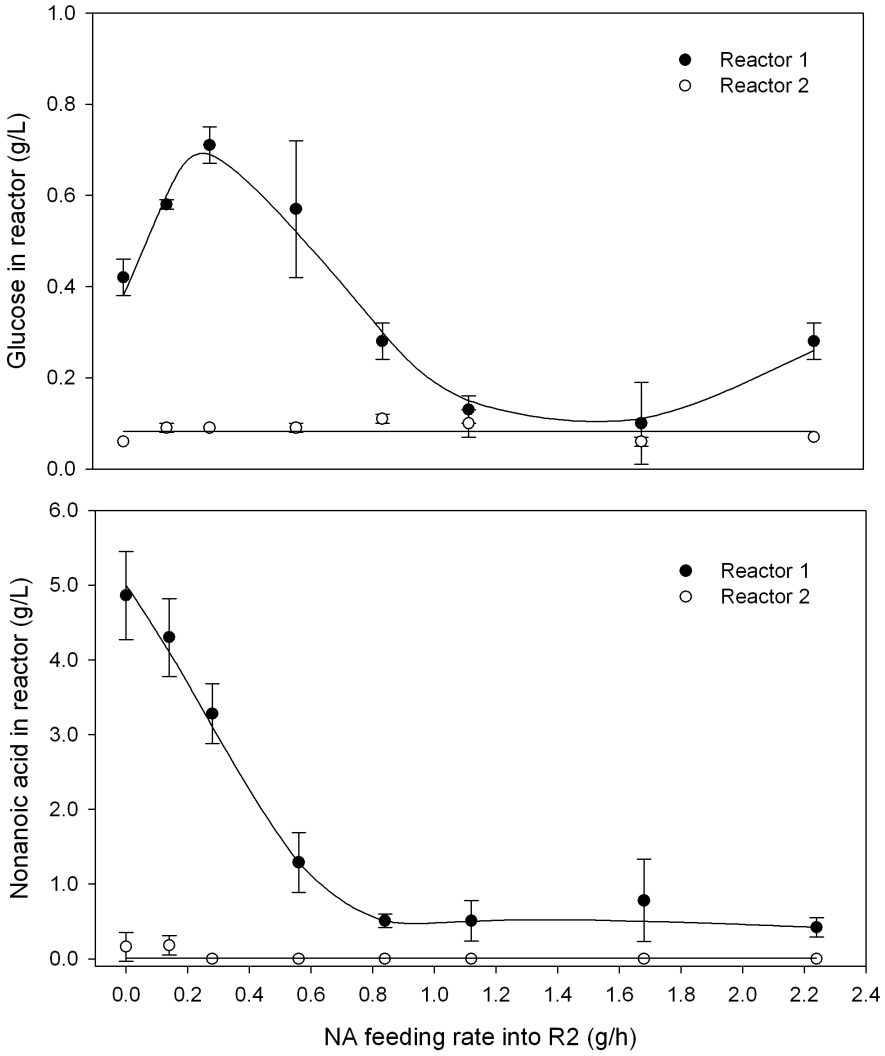

Figure 5-11a: Steady state glucose concentrations in R1 and R2 and 5-11b: Steady state NA concentrations in R1 and R2 (D_1 = 0.30 h^{-1}; D_2 = 0.25 h^{-1})

The fermentation was C-limited for its duration since NH_4^+ and PO_4 were present in both reactors for all feeding conditions (Figures 5-12a and 5-12b).

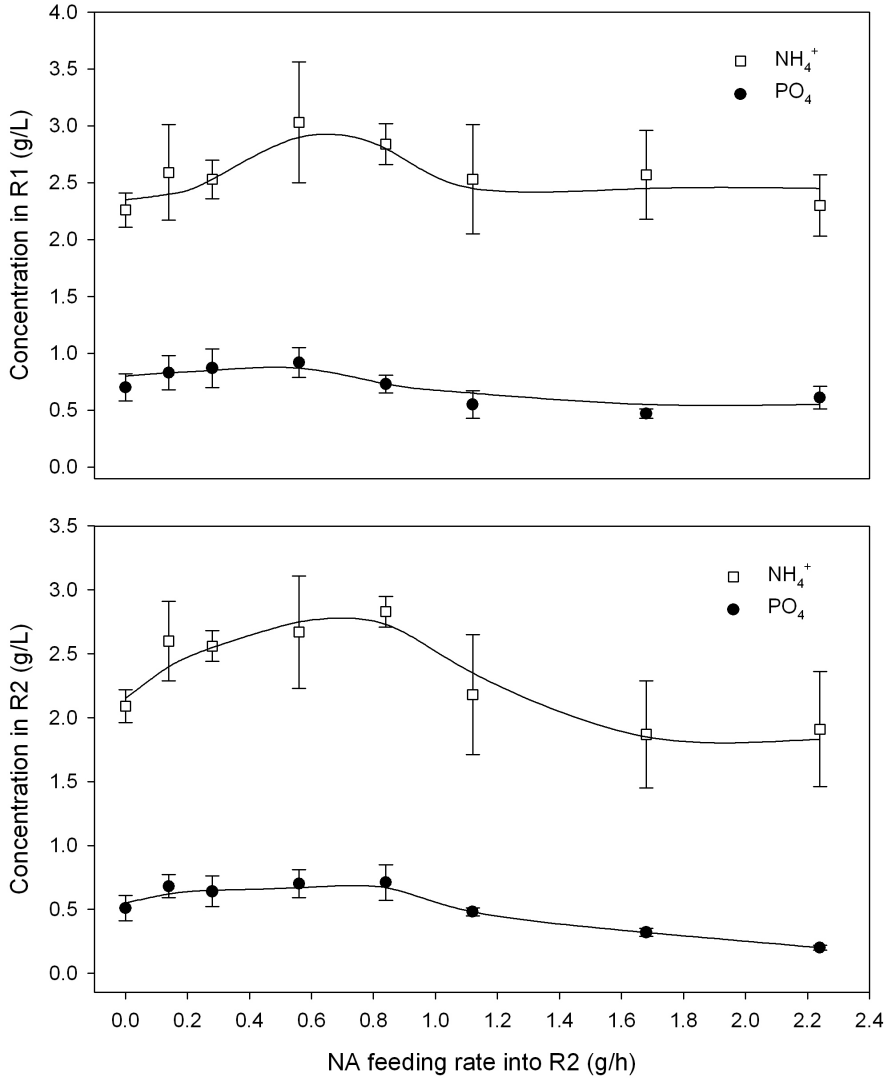

Figure 5-12a: Steady state NH_4^+ and PO_4 concentrations in R1 and 5-12b: Steady state NH_4^+ and PO_4 concentrations in R2 (D_1 = 0.30 h^{-1}; D_2 = 0.25 h^{-1})

Figure 5-13 shows the measured AA concentrations for the samples taken from R1 and R2, respectively. There was a considerable amount of deviation from the line representing the concentration of AA in the feed, especially for R2. The first three R1 samples measurements were 0.30, 0.22 and 0.15 g/L higher than the concentration at the inlet, which was attributed to analytical error. Beyond the third point, the measured values were reasonable as they converged to the feed line. By contrast, AA was hardly detected in R2, with the exception of the points at 0.28, 0.56 and 0.84 g/h NA.

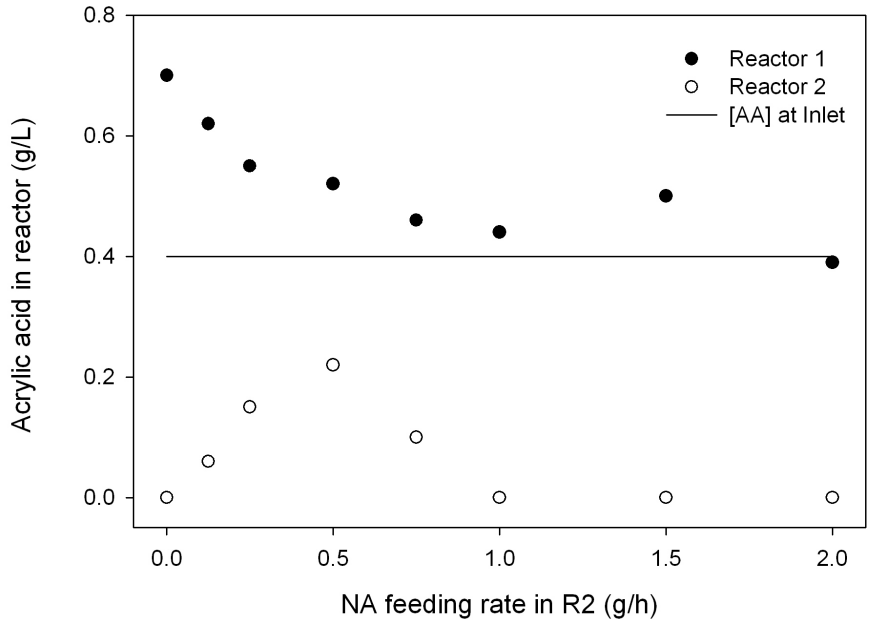

Figure 5-13: Steady state AA concentrations in R1 an R2 (D_1 = 0.30 h^{-1}; D_2 = 0.25 h^{-1})

A carbon balance was performed for the two-stage chemostat system, using the two reactors as the control volume. With respect to Figure 5-4, there were additional species that had to be accounted for in the balance, namely: glucose and NA entering, and CO_2 leaving, R2. On the whole, the calculated outlet and inlet flow rates were in excellent agreement.

Table 5-3: Carbon balance for the two-stage high-cell density chemostat with varied R2 NA feeding

Acrylic acid, g/L	Carbon IN, g C/h	Carbon OUT, g C/h
0.00	1.84	1.85 ± 0.05
0.14	1.94	1.88 ± 0.04
0.28	2.04	2.17 ± 0.02
0.56	2.23	2.16 ± 0.03
0.84	2.24	2.50 ± 0.07
1.12	2.61	2.67 ± 0.04
1.68	2.99	3.06 ± 0.07
2.24	3.38	3.32 ± 0.13

Reactor productivities were calculated at each feeding condition (Table 5-4). Overall system productivity was determined by dividing the total hourly PHA production rate from R2 by the total reactor working volume in the system (R1 and R2).

Table 5-4: Productivities for the two-stage high-cell density chemostat

Acrylic Acid, g/L	R1 productivity, g $L^{-1}h^{-1}$	R2 productivity, g $L^{-1}h^{-1}$	Overall productivity, g $L^{-1}h^{-1}$
0.00	0.47	0.54	0.52
0.14	0.47	0.58	0.54
0.28	0.67	0.57	0.63
0.56	0.86	0.44	0.65
0.84	1.14	0.40	0.76
1.12	0.89	0.32	0.60
1.68	0.89	0.03	0.43
2.24	0.50	0.25	0.37

Productivities in R1 were lower than expected, given the high productivities obtained in the single-stage chemostat study. The highest R1 productivity achieved was 1.14 g $L^{-1}h^{-1}$, which coincided with the peak in PHA content. Despite the high PHA content for the first four points, R1 productivities were generally poor due to low biomass concentrations. Productivity in R2 decreased steadily throughout the course of the fermentation. Initial values were high due to the carry-over of unconsumed NA from R1, causing a large increase in biomass. One would have expected higher NA feeding rates to improve productivity, however, the drastic decline of PHA content at high feeding rates diminished R2 productivity. The best overall productivity for the system was 0.76 g $L^{-1}h^{-1}$. If the PHA in R1 remained high and biomass values were the same as in Figure 5-8b, the overall productivity for the system would have continued to increase with NA feeding rates into R2. For example, if PHA content remained at 55% for the final steady state point, R1, R2 and overall productivities would have been 1.09, 0.78 and 0.94 g $L^{-1}h^{-1}$ respectively.

The overall PHA yield from NA ($Y_{PHA/NA}$) was very consistent over the first five points, averaging 0.59 g/g with its highest value of 0.62 g/g at 0.28 g/h. These values were within the range reported by *Sun et al.* (2009a) for *P. putida* KT2440 in a fed-batch system, but fell short of the chemostat yields from Jiang (2010) and the single-stage chemostat experiment discussed earlier in this chapter.

It is necessary to consider the data from the two-stage study along with the single-stage results to interpret it effectively. From the single stage data, the expected biomass yield in R1 for this experiment was near the plateau value. Therefore, it is apparent that R1 was underperforming for the first four points (Figures 5-8a and 5-8b). While the exact cause is unknown, it was attributed in part to the presence of foam in R1 during

the first four points. When foam was present, the actual working volume of the reactor was considerably lower than it should have been, resulting in a higher dilution rate and, consequently, a lower biomass concentration. The effect of foaming was prevalent in the R2 biomass data. For low NA feeding rates in R2, there should have been little difference between the biomass concentrations in the two reactors. However, for the first point, the biomass concentration effectively doubled from R1 and R2 despite the fact that there was no NA fed into R2. The cause was a large amount of unconsumed carbon source in R1 (Figure 5-11a and 5-11b). Due to foaming, the dilution rate was increased to the point at which bacteria were not capable of utilizing all of the available substrate. As a result, NA carried over to R2, where the dilution rate was sufficiently low to allow the bacteria to consume it completely. As the data illustrate, the gradual subsidence of foaming eventually eliminated this problem.

It appeared as though the second chemostat stage was achieving the desired enrichment in PHA content for the first five steady state points. Gains of 5-10% in PHA content in R2 compared to R1 were observed (Figure 5-10a and 5-10b). However, this observed polishing effect of the second stage was confounded by the carry-over of NA from the R1. Therefore, it was difficult to ascertain what portion of the increase in PHA content was attributed to the carry-over of NA in R1 and what portion was due to increased residence time provided by R2.

The cause of the large and sudden decrease in PHA content at higher NA feeding rates is unknown, but it may have been related to low concentrations of AA in the reactors. At higher NA feeding rates, AA was detected in R1, but not in R2 (Figure 5-13). If AA were metabolized by *P. putida* KT2440, then its positive effect on PHA accumulation as a β-oxidation inhibitor would have diminished. Changes in reactor temperature may have also adversely affected PHA content. The reactor temperatures were difficult to regulate throughout the experiment due to the lack of a temperature controller and widely fluctuating building temperatures. As shown by Jung *et al.* (2001), the rate of MCL-PHA accumulation in *P. putida* GPo1 (formerly *P. oleovorans*) was affected by temperature, which may be true for other *Pseudomonads*, such as *P. putida* KT2440. Despite best efforts, reactor temperatures varied from about 27 to 32°C during

the weeks of running the experiment. This environmental stress may have elicited a response from the cells that led to a reduced PHA content.

Feasibility of the two-stage high-cell density chemostat process for MCL-PHA production is best assessed through comparison to available chemostat and fed-batch data. The most relevant data for comparison come from a series of publications from Sun *et al.*, and work by Jiang (2010), which explore production of the same type of MCL-PHA (from NA) using the same strain (*P. putida* KT2440) as in this work. Broader comparisons to literature involving different bacterial strains and carbon sources for MCL-PHA production are also useful to gauge these results. Table 5-5 compares results for different MCL-PHA production processes reported in literature. Studies that used pure O_2 for aeration are noted.

Table 5-5: Comparison of different MCL-PHA production processes described in literature

Notes	Microorganism	PHA monomer units	Biomass concentration (g/L)	PHA Content (wt%)	Productivity ($g\ L^{-1}h^{-1}$)	Reference
Chemostat – single stage; $D=0.30\ h^{-1}$; nonanoic acid and glucose co-feeding; C-limited; acrylic acid; air only	*P. putida* KT2440	C9 C7	8.0	63.1	1.52	This work
Chemostat – two stage; $D_1=0.30\ h^{-1}$; $D_2=0.25\ h^{-1}$; nonanoic acid and glucose co-feeding; C-limited; acrylic acid; air only	*P. putida* KT2440	C9 C7	7.3 (R1) 9.2 (R2)	51.7 (R1) 58.5 (R2)	1.14 (R1) 0.40 (R2) 0.76 (Overall)	This work
Chemostat – single stage; $D=0.25\ h^{-1}$; octanoic acid and glucose and nonanoic acid and glucose co-feeding; C-limited; acrylic acid; air only	*P. putida* KT2440	C8 C6 (octanoic acid) C9 C7 (nonanoic acid)	5.0 (octanoic acid) 5.8 (nonanoic acid)	48 (octanoic acid) 50 (nonanoic acid)	0.60 (octanoic acid) 0.73 (nonanoic acid)	Jiang (2010)
Chemostat – single stage; $D=0.24\ h^{-1}$; octanoate as sodium salt; N-limited; air only	*P. putida* GPo1 (*P. oleovorans*)	C10 C8 C6 C4 (SCL-MCL)	4.4	13	0.14	Ramsay *et al*., 1991
Chemostat – two stage; $D_1=0.21\ h^{-1}$, $D_2=0.16\ h^{-1}$; *n*-octane; N-limited; air only	*P. putida* GPo1 (*P. oleovorans*)	C8 C6	$R_1=10.5$ $R_2=18.0$	$R_1=38.0$ $R_2=63.0$	$R_1=0.84$ $R_2=1.18$ Overall=1.06	Jung *et al*., 2001
Chemostat – two stage; $D_1=0.10\ h^{-1}$, $D_2=0.10\ h^{-1}$; Octanoic acid in R1; 10-undecenoic acid in R2; dual nutrient limited growth regime (DNLGR); air only	*P. putida* GPo1 (*P. oleovorans*)	C11:1 C9:1 C8 C7:1 C6	$R_1=1.13$ $R_2=1.53$	$R_1=24.2$ $R_2=52.4$	$R_1=0.027$ $R_2=0.053$ Overall=0.040	Hartmann *et al*., 2010
Chemostat – single stage; $D=0.20\ h^{-1}$; *n*-octane; N-limited; air only	*P. putida* GPo1 (*P. oleovorans*)	C8 C6	11.6	25.0	0.58	Preusting *et al*., 1993b
Chemostat – single stage; $D=0.20\ h^{-1}$; *n*-octane; N-limited; air only	*P. putida* GPo1 (*P. oleovorans*)	C8 C6	12.4	29.8	0.74	Hazenberg and Witholt, 1997
Chemostat – single stage; $D=0.25\ h^{-1}$; octanoate as sodium salt; N-limited; air only	*P. resinovorans*	C10 C8 C6 C4 (SCL-MCL)	4.7	8.5	0.10	Ramsay *et al.,* 1992

Chemostat – single stage; D=0.10 h^{-1}; oleic acid; O-limited; air only	*P. putida* KT2442	C14:1 C12:1 C12 C10 C8 C6	30	23	0.67	Huijberts and Eggink, 1996
Chemostat – single stage; D=0.20 h^{-1}; octanoic acid; inducer; air only	*P. oleovorans* POMC1 (recombinant)	C8 C6	1.64	53.2	0.17	Prieto *et al*., 1999
Fed-batch; exponential feeding at μ=0.15 and 0.25 h^{-1}; nonanoic acid; C-limited; pure O_2	*P. putida* KT2440	C9 C7	70.2 (0.15 h^{-1}) 56.0 (0.25 h^{-1})	75.4 (0.15 h^{-1}) 66.9 (0.25 h^{-1})	1.11 (0.15 h^{-1}) 1.44 (0.25 h^{-1})	Sun *et al.*, 2007a
Fed-batch; exponential feeding at μ=0.14, 0.23 and 0.24 h^{-1}; nonanoic acid and 10-undecenoic acid (different molar ratios); C-limited; pure O_2	*P. putida* KT2440	C11:1 C9:1 C7:1 C11 C9 C7	54.1 (0.14 h^{-1}; NA:$UDA^{=}$ = 4.98) 48.1 (0.23 h^{-1}; NA:$UDA^{=}$ = 5.07) 33.6 (0.24 h^{-1}; NA:$UDA^{=}$ = 2.47)	55.6 (0.14 h^{-1}; NA:$UDA^{=}$ = 4.98) 55.8 (0.23 h^{-1}; NA:$UDA^{=}$ = 5.07) 42.6 (0.24 h^{-1}; NA:$UDA^{=}$ = 2.47)	0.71 (0.14 h^{-1}; NA:$UDA^{=}$ = 4.98) 1.09 (0.23 h^{-1}; NA:$UDA^{=}$ = 5.07) 0.63 (0.24 h^{-1}; NA:$UDA^{=}$ = 2.47)	Sun *et al.,* 2009a
Fed-batch; exponential feeding at μ=0.25 h^{-1}, then linear feeding; nonanoic acid and glucose co-feeding; C-limited; pure O_2	*P. putida* KT2440	C9 C7	70.7 (NA:glu=1) 64.2 (NA:glu=1)	56.0 (NA:glu=1) 48.0 (NA:glu=1.5)	1.44 (NA:glu=1) 1.16 (NA:glu=1.5)	Sun *et al.,* 2009b
Fed-batch; exponential feeding at μ=0.15 h^{-1}; nonanoic acid and glucose co-feeding; C-limited; acrylic acid; pure O_2	*P. putida* KT2440	C9 C7	71.4	75.5	1.8	Jiang (2010)
Fed-batch; DO-stat feeding; oleic acid; O_2-limited; air only	*P. putida* KT2442	C14:1 C12 C10 C8 C6	92	45	1.6	Weusthuis *et al*., 1996
Fed-batch; exponential feeding (μ=0.10 h^{-1}); octanoate as sodium salt; N-limited; pure O_2	*P. putida* KT2442	C8 C6	51.5	34	0.40	Kellerhals *et al.,* 1999b
Fed-batch; octanoate as sodium salt; oleic acid; vegetable oil; animal oil; N-limited; pure O_2	*P. putida* KT2442	C8 C6 (octanoate) C14:1 C12 C10 C8 C6 (oleic acid) C14:2 C14:1 C14 C12:1 C12 C10 C8 C6 (vegetable fatty acids and animal fatty acids)	51.2 (octanoate) 89.8 (oleic acid) 73.0 (vegetable fatty acids) 28.5 (animal fatty acids)	35.8 (octanoate) 20.0 (oleic acid) 34.2 (vegetable fatty acids) 54.0 (animal fatty acids)	0.41 (octanoate) 0.57 (oleic acid) 0.56 (vegetable fatty acids) 0.33 (animal fatty acids)	Kellerhals *et al*., 2000

Fed-batch; DO-stat and pH-stat feeding; oleic acid; P-limited; pure O_2	*P. putida* KT2442	C14:1 C12 C10 C8 C6	141	51.4	1.91	Lee *et al*., 2000
Fed-batch; staged feeding; glucose and octanoate as sodium salt; N-limited, O-limited; air only	*P. putida* BM01	C8 C6	55	65	0.92	Kim *et al*., 1997
Fed-batch; batch mode followed by constant rate feeding; *n*-octane; N-limited; air only	*P. putida* GPo1 (*P. oleovorans*)	C8 C6	37.1	33	0.25	Preusting *et al*., 1993a
Fed-batch; exponential feeding (μ=0.19 h^{-1}) followed by constant rate feeding; octanoic acid and ammonium octanoate; N-limited; air only	*P. putida* GPo1 (*P. oleovorans*)	C8 C6	47	55	0.53	Dufresne *et al.*, 1998
Fed-batch; exponential feeding (μ=0.05 h^{-1}); *n*-octane; N-limited; pure O_2	*P. putida* GPo1 (*P. oleovorans*)	C8 C6	112	4	0.07	Kellerhals *et al*., 1999a
Fed-batch; pH-stat feeding; octanoic acid; N-limited; air only	*P. putida* GPo1 (*P. oleovorans*)	C8 C6	63	62	1	Kim *et al*., 2002
Fed-batch; constant feed rate; palmitic acid; inducer; air only	*E. coil* 193MC1 (recombinant)	C10 C8 C6	3.55	12	0.011	Prieto *et al*., 1999
Fed-batch; constant rate feeding; glucose and fructose; P-limited; air only	*P. putida* IPT 046	C10 C8	50	63	0.75	Diniz *et al*., 2004

PHA content and productivity values for the high-cell density chemostat setup used in this work compare favourably to continuous culture and fed-batch data reported in literature. The single-stage high-cell density chemostat yielded the highest productivity to date, 1.52 g $L^{-1}h^{-1}$, for MCL-PHA produced by *P. putida* KT2440. Furthermore, this was the highest value reported for any strain in continuous MCL-PHA production processes and did not require pure O_2. In general, the productivity of this chemostat was significantly higher than most of the fed-batch process reported in literature. It was on par with the best fed-batch values reported by Sun *et al*. (2007a; 2009b, pure O_2), which is both impressive and encouraging for future developments. The PHA content of 63.1 wt% that was attained was among the highest reported values in literature for any MCL-PHA production process. Only two processes achieved higher reactor productivity: Weusthuis *et al*., 1996 and Lee *et al*., 2000, which used oleic acid to produce MCL-PHA from *P. putida* KT2442 in fed-batch setups, yielding productivities of 1.6 (O-limited, air only) and 1.91 (P-limited, pure O_2), respectively.

The two-stage high-cell density chemostat did not perform as impressively as expected, but nonetheless, its results stack up well against literature values. Overall productivity (0.76 g $L^{-1}h^{-1}$) was higher than all other reported values for MCL-PHA production in continuous systems, with the exception of two-stage chemostat work by Jung and coworkers (2001). In comparison to fed-batch systems, the performance of the two-stage chemostat was near the middle of the range of values reported. Productivity of R1 was relatively high (1.14 g $L^{-1}h^{-1}$), but fell considerably short of the precedent set in the single stage portion of this work (1.52 g L^{-1} h^{-1}). In combination with the poor productivity in R2, these factors contribute to the underwhelming overall productivity of the two-stage system.

5.2.2 Conclusions

In light of the results discussed in this section, it is apparent that the two-stage carbon limited chemostat with *P. putida* KT2440 has a considerable amount of untapped potential as a MCL-PHA production process. There is significant room for improvement over the productivity and PHA content values reported herein, especially at higher NA feeding rates in to R2 (Figures 5-10a and 5-10b). The growth conditions

for R1 were identical to those used in the single stage chemostat study; therefore, productivities and PHA contents in the neighbourhood of 1.5 g $L^{-1}h^{-1}$ and 60 wt% respectively, are attainable for R1. Based on the existing data, R2 PHA content approaching 70 wt% is a realistic expectation. Sun *et al*., (2007a) have already shown that *P. putida* KT2440 is capable of producing MCL-PHA from NA in excess of 75% of the dry cell weight. Considering the final biomass concentration (12.27 g/L) at the highest R2 NA feeding rate (2.24 g/h), a PHA content of 70% would correspond to an overall productivity of 1.21 g $L^{-1}h^{-1}$.

Aside from the demonstrated potential for significant performance gains, there are several unique advantages offered by the high-cell density two-stage continuous system that make it an attractive alternative to typical fed-batch processes for MCL-PHA production. As with all continuous systems, the ease of operation and reduced downtime are significantly improved compared to fed-batch systems. Carbon feeding does not require predictive algorithms and the specific growth rates in both reactors are controlled by their respective dilution rates. Though it is unable to match the biomass concentrations of fed-batch processes, high-cell densities help to alleviate the typically elevated downstream separation requirements for continuous production systems. Moreover, the fact that no pure O_2 is required for aeration provides offers a considerable economic advantage over the conventional fed-batch process.

Ultimately, more investigation is required to develop this process. Future work should focus on changing conditions in the R2, particularly looking in to higher NA feeding rates. Changes to the dilution rates in R1 and especially R2 may also lead to increases in PHA content or gains in overall productivity. A dilution rate lower than 0.25 h^{-1} in R2 would further increase residence time and may allow cells accumulate more polymer in the second stage. An important area of interest is the NA:glu in R1, which can be increased beyond 1.29 to determine whether more MCL-PHA can be produced in the first stage. It may also be possible to increase total carbon feeding without aerating with pure O_2 by altering the reactor design help improve oxygen transfer properties.

After the process is fine-tuned, a detailed economic analysis would be a very valuable tool in determining the value of this process. A specific point of interest is the cost savings as compared to fed-batch processes. A large amount of accurate data would allow cost functions to be described in terms of the operating parameters and feeding conditions of the process. These include raw materials costs (substrates, mineral salts, consumables, etc.), operating costs (agitation, aeration, cooling, labour etc.) and downstream processing costs (separation, extraction and purification). Based on these functions, the best operating points could be identified. If the results are promising, this process could be extended to other fatty acids besides NA, that are known to lead to MCL-PHA accumulation in *P. putida* KT2440.

Chapter 6

Conclusions and Recommendations

6.1 *In vivo* production of MCL-PHA containing a side-chain carboxyl group

6.1.1 Summary and conclusions

Chapter 4 of this thesis involved the investigation of *in vivo* production of MCL-PHA containing a side-chain carboxyl group. Through preliminary shake flask experiments, *P. citronellolis* DSM 50332 was identified as a promising strain for production based on its ability to use azelaic acid (AzA), a α,ω-dicarboxylic acid, as a sole source of carbon and energy and more importantly, for MCL-PHA synthesis. Shake flask experiments revealed that the MCL-PHA derived from AzA, a compound having nine carbon atoms, contained 3-hydroxydecanoate (C10) and 3-hydroxyoctanoate (C8) units. Since carboxylic acids are catabolized via β-oxidation, 3-hydroxynonanoate (C9) and 3-hydroxyheptanoate (C7) was the expected composition from a nine-carbon carboxylic acid. The only plausible explanation for this observation is that AzA was degraded completely though β-oxidation, yielding acetyl-CoA which entered *de novo* fatty acid biosynthesis to yield even-numbered carbon fatty acids that served as precursors for MCL-PHA. This is the method by which MCL-PHA is produced from unrelated carbon sources, such as glucose.

Three chemostat experiments were conducted to gain an understanding of the growth conditions required for MCL-PHA accumulation by *P. citronellolis* DSM 50332, and then to investigate the conditions with the highest probability of producing MCL-PHA with a side-chain carboxyl group. In all experiments, dilution rate (D), reactor working volume, NA feeding and glucose feeding were 0.25 h^{-1}, 1.1 L, 2.9 g/L and 3.9 g/L, respectively. The first study explored the effect of P-limitation on the dynamics of PHA accumulation from NA, a well-studied carbon source known to yield MCL-PHA from other pseudomonads. P-limitation was shown to stimulate and improve intracellular PHA content. A maximum PHA content of 20.0 wt% was reached at a specific degree of P-limitation (inlet PO_4 of 0.225 g/L), above and below which there were

significant decreases in PHA content. The second P-limited chemostat study introduced AzA up to 2.5 g/L, to determine whether it could be incorporated into the MCL-PHA produced. Concentration of PO_4 in the feed was fixed at 0.225 g/L, based on the results of the first experiment. The resultant MCL-PHA contained C9 and C7 units exclusively, indicating that the polymer was derived entirely from NA. AzA appeared to be consumed, however, there was no evidence to suggest that it was being used for anything besides a source of carbon and energy. In the final chemostat study, AA was used to inhibit β-oxidation in an attempt to produce carboxylated precursors for MCL-PHA synthesis. Concentrations of AzA and PO_4 at the inlet were fixed at 2.5 g/L and 0.225 g/L, respectively, while the amount of AA was gradually increased. The presence of AA markedly increased PHA content and C9 monomer composition, reaching maximum values of 28.1 wt% and 75.6 mol%, at 0.035 g/L AA, representing improvements of 9.9 wt% and 11.1 mol% over uninhibited values (no AA). However, GC, ^{1}H-NMR and ^{13}C-NMR analyses did not reveal the presence of any carboxyl groups in the polymer. AzA appeared to be consumed, but the composition of the polymer was comprised entirely of C9 and C7 monomers.

Since *P. citronellolis* DSM 50332 is capable of metabolizing AzA, the enzymes in the β-oxidation pathway must be able to use AzA and its derivatives as substrates. However, there may not be a terminal carboxyl group preserved on the molecule, which is a necessity for producing MCL-PHA with a side chain carboxyl group. This occurs if both carboxyl ends of the molecule undergo β-oxidation in a simultaneous or sequential fashion. Enzyme specificity also plays a critical role in determining whether carboxylated MCL-PHA production is possible. If carboxylated intermediates are available, then combinations of key enzymes (based on location) must be able to utilize them as substrates. These key enzymes include acyl-CoA dehydrogenase, enoyl-CoA hydratase, (*R*)-specific enoyl-CoA hydratase (PhaJ), 3-ketoacyl-CoA reductase (FabG) and PHA synthase (PhaC) (Figure 2-1).

6.1.2 Future Work

Further investigation is required to help elucidate the mechanism of β-degradation for dicarboxylic acids in *P. citronellolis* DSM 50332, specifically how the two terminal carboxyl groups are treated. In the same vein, information about the specificities of the enzymes in the β-oxidation and MCL-PHA production pathways is essential to understanding how to produce MCL-PHA containing a side chain carboxyl group *in vivo*. Future work should address the following areas: clarifying the mechanism of β-oxidation for dicarboxylic acids, identifying enzymes that are incapable of using substrates containing a carboxyl group, using point mutations to decrease the specificity of these enzymes and screening for other strains potentially capable of producing carboxylated MCL-PHA.

6.2 High-cell density two-stage carbon-limited chemostat for MCL-PHA production

6.2.1 Summary and conclusions

In Chapter 5, C-limited high-cell density cultivation of *P. putida* KT2440 in a two-stage chemostat for MCL-PHA production from NA, was investigated. Initially, a single-stage configuration was studied to establish an appropriate set of conditions for the two-stage setup. For all single-stage experiments, the dilution rate (D) and working volume of were 0.30 h^{-1} and 0.9 L, respectively. The ratio of NA to glucose (NA:glu) was varied based on a fixed total carbon feeding rate of 6.50 g/L, while 0.15 g/L AA was provided as a β-oxidation inhibitor to improve PHA yield and C9 composition. On the whole, performance improved as NA:glu was increased, with the highest NA:glu (1.29) achieving exceptional performance. PHA content (63.1 wt%) was in the upper range of values reported for MCL-PHA production processes and productivity (1.52 g $L^{-1}h^{-1}$) was higher than any values reported for continuous MCL-PHA production and comparable to the best performing fed-batch systems. Different AA concentrations were also investigated in the single-stage study to determine the best level of β-oxidation inhibition with respect to PHA content and composition. An AA concentration of 0.40 g/L provided the best performance.

Therefore, the best feeding conditions for the two-stage system were determined to be NA:glu of 1.29 (total carbon 6.50 g/L) and AA concentration of 0.40 g/L.

In the C-limited high-cell density two-stage chemostat, the second reactor (R2) was operated at a slightly lower dilution rate ($D_2 = 0.25\ h^{-1}$) than the first reactor (R1, $D_1 = 0.30\ h^{-1}$) to provide increased residence time. The feeding rate of NA into R2 was gradually increased over the course of the experiment, while conditions in R1 were held constant. Overall, the performance of the system did not meet expectations, but the results demonstrated potential for improvement. Best overall productivity was 0.76 g $L^{-1}h^{-1}$, which is in the middle of the range of productivities reported for MCL-PHA production in literature. This coincided with a PHA content of 58.5 wt%, which, despite being a good result was still less than the 63.1 wt% achieved in the C-limited single-stage high-cell density chemostat study. Similarly, the highest productivity in R1 (1.14 g $L^{-1}h^{-1}$) fell short of the maximum value obtained previously (1.52 g $L^{-1}h^{-1}$). PHA content, and therefore productivity, deteriorated rapidly during the later stages of the experiment for reasons that may have been caused by metabolism of AA or temperature-induced stresses. In addition, there were also issues with foaming associated with R1 during the first half of the experiment, which complicated effective interpretation of the data.

6.2.2 Future work

Additional work is required to further develop the C-limited two-stage high-cell density to assess whether it is a viable alternative to fed-batch systems for the production of MCL-PHA. The operational advantages coupled with the potential for enhanced performance over the fed-batch process warrants its further investigation. Better characterization of the feeding conditions into R1 and higher NA feeding rates into R2 should be the main areas of focus in future studies. Proposed work includes investigating NA:glu ratios greater than 1.29 in R1, to determine whether PHA content and productivity can be increased further. With modifications to the bioreactor design, higher total carbon feeding rates (above 6.50 g/L) may also be possible without using pure O_2 for aeration. Varying the dilution rates of R1 and R2 may be able to

improve PHA content and productivity, along with higher NA feeding rates into R2. After more data is collected, an economic model can be developed determine operating costs under different conditions, which can be compared to fed-batch systems.

References

Baksanova LE, Val'tsifer VA, Budnikov VI, Kondrashova NB (2002) Gas chromatographic determination of acrylic acid from aqueous solutions. Russ J Appl Chem 75:1427-1429

Brandl H, Gross RA, Lenz RW, Fuller RC (1988) *Pseudomonas oleovorans* as a source of poly(β-hydroxyalkanoates) for potential applications as biodegradable plastics. Appl Environ Microbiol 54:1977-1982

Chapman PJ, Duggleby RG (1967) Dicarboxylic acid catabolism by bacteria. Biochem J 103:7c-9c

Choi NH, Xu J, Rho JK, Shim JH, Yoon SC (2009) Shifting of the distribution of aromatic monomer-units in polyhydroxyalkanoic acid to longer units by salicylic acid in *Pseudomonas fluorescens* BM07 grown with mixtures of fructose and 11-phenoxyundecanoic acid. Biotechnol Bioeng 102:1209-1221

Choi MH, Yoon SC (1994) Polyester biosynthesis characteristics of *Pseudomonas citronellolis* grown on various carbon sources, including 3-methyl-branched substrates. Appl Environ Microbiol 60:3245-3254

Clesceri LS, Greenberg AE, Eaton, A.D, 1999. Standard methods for the examination of water and wastewater (20th Edn.). American Public Health Association, Washington, DC.

Diniz SC, Taciro MK, Gomez JG, da Cruz Pradella JG (2004) High cell density cultivation of *Pseudomonas putida* IPT 046 and medium-chain-length polyhydroxyalkanoate production from sugarcane carbohydrates. Appl Biochem Biotechnol 119:51–70

Dufresne A, Samain E (1998) Preparation and characterization of a poly(beta-hydroxyoctanoate) latex produced by *Pseudomonas oleovorans*. Macromolecules 31:6426–6433

Eggink G, Dewaard P, Huijberts GNM (1992) The role of fatty-acid biosynthesis and degradation in the supply of substrates for poly(3-hydroxyalkanoate) formation in *Pseudomonas putida*. FEMS Microbiol Rev 103:159–163

Fall RR, Brown JL, Schaeffer TL (1979) Enzyme recruitment allows the biodegradation of recalcitrant branched hydrocarbons by *Pseudomonas fluorescens*. Appl Environ Microbiol 38:715-722

Fiedler S, Steinbüchel A, Rehm BHA (2000) PhaG-mediated synthesis of poly(3-hydroxyalkanoates) consisting of medium-chain-length constituents from non-related carbon sources in recombinant *Pseudomonas fragi*. Appl Environ Microbiol 66:2117-2124

Fiedler S, Steinbüchel A, Rehm, BHA (2002) The role of the fatty acid β-oxidation multienzyme complex from *Pseudomonas oleovorans* in polyhydroxyalkanoate biosynthesis: molecular characterization of the *fadBA* operon from *P. oleovorans* and of the enoyl-CoA hydratase genes *phaJ* from *P. oleovorans and Pseudomonas putida*. Arch Microbiol 178:149-160

Förster-Fromme K, Jendrossek D (2010) Catabolism of citronellol and related acyclic terpenoids in pseudomonads. Appl Microbiol Biotechnol 87:859-869

Franklin FCH, Bagdasarian M, Bagdasarian MM, Timmis KN (1981) Molecular and functional analysis of the TOL plasmid pWWO from *Pseudomonas putida* and cloning of genes for the entire regulated aromatic ring *meta* cleavage pathway. Proc Natl Acad Sci USA 78:7458-7362

Fritzsche K, Lenz RW, Fuller RC (1990) Production of unsaturated polyesters by *Pseudomonas oleovorans*. Int J Biol Macromol 12:85–91

Gross RA, Demello C, Lenz RW, Brandl H, Fuller RC (1989) Biosynthesis and characterization of poly (β-hydroxyalkanoates) produced by *Pseudomonas oleovorans*. Macromolecules 22:1106–1115

Grund A, Shapiro J, Fennewald M, Bacha P, Leahy J, Markbreiter K, Neider M, Toepfer M (1975) Regulation of alkane oxidation in *Pseudomonas putida*. J Bacteriol 123: 546-556

Hartmann R, Hany R, Witholt B, Zinn M (2010) Simultaneous biosynthesis of two copolymers in *Pseudomonas putida* GPo1 using a two-stage continuous culture system. Biomacromolecules 11:1488-1493

Haywood GW, Anderson AJ, Ewing DF, Dawes EA (1990) Accumulation of a polyhydroxyalkanoate containing primarily 3-hydroxydecanoate from simple carbohydrate substrates by *Pseudomonas sp*. strain NCIMB 40135. Appl Environ Microbiol 56:3354-3359

Hazenberg W, Witholt B (1997) Efficient production of medium-chain-length poly(3-hydroxyalkanoates) from octane by *Pseudomonas oleovorans*: economic considerations. Appl Microbiol Biotechnol 48:588–596

Hoet PP, Stanier RY (1970) The dissimilation of higher dicarboxylic acids by *Pseudomonas fluorescens*. Eur J Biochem 13:65-70

Huijberts GNM, Eggink G, Dewaard P, Huisman GW, Witholt B (1992) *Pseudomonas putida* KT2442 cultivated on glucose accumulates poly(3-hydroxyalkanoates) consisting of saturated and unsaturated monomers. Appl Environ Microbiol 58:536–544

Huijberts GNM, Eggink G (1996) Production of poly(3-hydroxyalkanoates) by *Pseudomonas putida* KT2442 in continuous cultures. Appl Microbiol Biotechnol 46:233–239

Huisman GW, de Leeuw O, Eggink G, Witholt B (1989) Synthesis of poly-3-hydroxyalkanoates is a common feature of fluorescent pseudomonads. Appl Environ Microbiol 55:1949–1954

Janota-Bassalik L, Wright LD (1964) Azelaic acid utilization by a pseudomonas. J Gen Microbiol 36:405-414

Jiang, X. Ph.D. Thesis, Queen's University at Kingston, Aug. 2010.

Jung K, Hazenberg W, Prieto M, Witholt B (2001) Two-stage continuous process development for the production of medium-chain-length poly(3-hydroxyalkanoates). Biotechnol Bioeng 72:19–24

Kellerhals MB, Hazenberg W, Witholt B (1999a) High cell density fermentations of *Pseudomonas oleovorans* for the production of mcl-PHAs in two-liquid phase media. Enzyme Microb Technol 24:111–116

Kellerhals MB, Kessler B, Witholt B (1999b) Closed-loop control of bacterial high-cell-density fed-batch cultures: production of mcl-PHAs by *Pseudomonas putida* KT2442 under single-substrate and cofeeding conditions. Biotechnol Bioeng 65:306–315

Kellerhals MB, Kessler B, Witholt B, Tchouboukov A, Brandl H (2000) Renewable long-chain fatty acids for production of biodegradable medium-chain-length polyhydroxyalkanoates (mcl-PHAs) at laboratory and pilot plant scales. Macromolecules 33:4690–4698

Kim BS (2002) Production of medium chain length polyhydroxyalkanoates by fed-batch culture of *Pseudomonas oleovorans*. Biotechnol Lett 24:125–130

Kim GJ, Lee IY, Yoon SC, Shin YC, Park YH (1997) Enhanced yield and a high production of medium-chain-length poly(3-hydroxyalkanoates) in a two-step fed-batch cultivation of *Pseudomonas putida* by combined use of glucose and octanoate. Enzyme Microb Technol 20:500–505

Kim O, Gross RA, Hammar WJ, Newark RA (1996) Microbial synthesis of poly(β-hydroxyalkanoates) containing fluorinated side-chain substituents. Macromolecules 29: 4572-4581

Kim YB, Lenz RW (2001) Polyesters from microorganisms. Adv Biochem Eng Biotechnol 71:51-79

Kurth N, Renard E, Brachet F, Robic D, Guerin P, Bourbouze R (2002) Poly(3-hydroxyoctanoate) containing pendant carboxylic groups for the preparation of nanoparticles aimed at drug transport and release. Polymer 43:1095-1101

Lageveen RG, Huisman GW, Preusting H, Ketelaar P, Eggink G, Witholt B (1988) Formation of polyesters by *Pseudomonas oleovorans*—effect of substrates on formation and composition of poly-(R)-3-hydroxyalkanoates and poly-(R)-3-hydroxyalkenoates. Appl Environ Microbiol 54:2924–2932

Lee MY, Park WH (2000) Preparation of bacterial copolyesters with improved hydrophilicity by carboxylation. Macrmol Chem Phys 201:2771-2774

Lee SY, Wong HH, Choi JI, Lee SH, Lee SC, Han CS (2000) Production of medium-chain-length polyhydroxyalkanoates by high-cell-density cultivation of *Pseudomonas putida* under phosphorus limitation. Biotechnol Bioeng 68:466–470

Lenz RW, Kim YB, Fuller RC (1992) Production of unusual bacterial polyesters by *Pseudomonas oleovorans* through cometabolism. FEMS Microbiol Rev 103:207-214

Lever, M (1972) New reaction for colorimetric determination of carbohydrates Anal Biochem 47:273-279.

Lu J, Tappel RC, Nomura CT (2009) Mini-review: biosynthesis of poly(hydroxyalkanoates). J Macromol Sci Polym Rev 49:226-248

Madison LL, Huisman GW (1999) Metabolic engineering of poly(3-hydroxyalkanoates): from DNA to plastic. Microbiol Mol Biol Rev 63:21–53

Marchessault RH, Morin FG, Wong S, Saracovan E (1995) Artificial granule suspensions of long side chain poly(3-hydroxyalkanoate). Can J Microbiol 41(Suppl. 1):138-142

Meyer T; Keurentjes TF, Polymer Reaction Engineering, an Integrated Approach, In *Handbook of Polymer Reaction Engineering*, 1st Ed.; Meyer T, Keurentjes TF, Eds.; Wiley: Weinheim, 2005; pp. 1-15

Noghaby KA, Zahiri HS, Lotfi AS, Shourian M, Karbalei G, Rad I, Ahadi S, Arabnezhad M (2008) Effect of various carboxylic acids on the biosynthesis of polyhydroxyalkanoate in *Pseudomonas aeruginosa* PA01. Iran J Pharm Sci 4:269-274

Nomura CT, Tanaka T, Eguen TE, Appah AS, Matsumoto Ken'ichiro, Taguchi S, Ortiz CL, Doi Y (2008) FabG mediates polyhydroxyalkanoate production from both related and unrelated carbon sources in recombinant *Escherichia coli* LS5218. Biotechnol Prog 24:342-351

Park SJ, Park JP, Lee SY (2002) Metabolic engineering of *Escherichia coli* for the production of medium-chain-length polyhydroxyalkanoates rich in specific monomers. FEMS Microbiol Lett 214:217-222

Prescott LM; Harley JP; Klein DA; *Microbiology*, 5th Ed.; McGraw Hill: New York, 2002; Chapter 9

Preusting H, Hazenberg W, Witholt B (1993a) Continuous production of poly(3-hydroxyalkanoates) by *Pseudomonas oleovorans* in a high-cell-density, 2-liquid-phase chemostat. Enzyme Microb Technol 15:311–316

Preusting H, Vanhouten R, Hoefs A, Vanlangenberghe EK, Favrebulle O, Witholt B (1993b) High-cell-density cultivation of *Pseudomonas oleovorans*—growth and production of poly (3-hydroxyalkanoates) in 2-liquid phase batch and fed-batch systems. Biotechnol Bioeng 41:550–556

Prieto MA, Kellerhals MB, Bozzato GB, Radnovic D, Witholt B, Kessler B (1999) Engineering of stable recombinant bacteria for production of chiral medium-chain-length poly-3-hydroxyalkanoates. Appl Environ Microbiol 65:3265–3271

Qi Q, Steinbüchel A, Rehm BH (1998) Metabolic routing towards polyhydroxyalkanoic acid synthesis in recombinant *Escherichia coli* (fadR): inhibition of fatty acid beta-oxidation by acrylic acid. FEMS Microbiol Lett 167:89–94

Ramsay BA, Saracovan I, Ramsay JA, Marchessault RH (1991) Continuous production of long-side-chain poly-beta hydroxyalkanoates by *Pseudomonas oleovorans*. Appl Environ Microbiol 57:625–629

Ramsay BA, Saracovan I, Ramsay JA, Marchessault RH (1992) Effect of nitrogen limitation on long-side-chain poly-beta-hydroxyalkanoate synthesis by *Pseudomonas resinovorans*. Appl Environ Microbiol 58:744–746

Ren Q, Sierro N, Witholt B, Kessler B (2000) FabG, an NADPH dependent 3-ketoacyl reductase of *Pseudomonas aeruginosa*, provides precursors for medium-chain-length poly-3-hydroxyalkanoate biosynthesis in *Escherichia coli*. J Bacteriol 182:2978–2981

Rehm BHA, Kruger N, Steinbüchel A (1998) A new metabolic link between fatty acid *de novo* synthesis and polyhydroxyalkanoate synthesis. J Biol Chem 273: 24044-24051

Rehm BHA (2003) Polyester synthases: natural catalysts for plastics. Curr Issues Mol Biol 9: 41-62

Sanchez RJ, Schripsema J, da Silva LF, Taciro MK, Pradella JGC, Gomez JGC (2003) Medium-chain-length polyhydroxyalkanoic acids (PHA(mcl)) produced by *Pseudomonas putida* IPT 046 from renewable sources. Eur Polym J 39:1385–1394

Sato S, Kanazawa H, Tsuge T (2011) Expression and characterization of (*R*)-specific enoyl-CoA hydratases making a channeling route to polyhydroxyalkanoate biosynthesis in *Pseudomonas putida*. Appl Microbiol Biotechnol 90:951-959

Seubert W (1960) Degradation of isoprenoid compounds by microorganisms. I. Isolation and characterization of an isoprenoid-degrading bacterium *Pseudomonas citronellolis*. J Bacteriol 79:426-434

Stanier RY, Palleroni NJ, Doudoroff M (1966) The aerobic pseudomonads: a taxonomic study. J Gen Microbiol 43:159-271

Steinbüchel A, Hustede E, Liebergesell M, Pieper U, Timm A, Valentin HE (1992) Molecular basis for biosynthesis and accumulation of polyhydroxyalkanoic acids in bacteria. FEMS Microbiol Rev 103:217-230

Steinbüchel A, Valentin HE (1995) Diversity of polyhydroxyalkanoic acids. FEMS Microbiol Lett 128:219-228

Stigers DJ, Tew GN (2003) Poly(3-hydroxyalkanoate)s functionalized with carboxylic acid groups in the side chain. Biomacromolecules 4:193-195

Sun Z, Ramsay J, Guay M, Ramsay B (2006) Automated feeding strategies for high-cell density fed-batch cultivation of *Pseudomonas putida* KT2440. Appl Microbiol Biotechnol 71:423-431

Sun Z, Ramsay J, Guay M, Ramsay B (2007a) Carbon-limited fed-batch production of medium-chain-length polyhydroxyalkanoates from nonanoic acid by *Pseudomonas putida* KT2440. Appl Microbiol Biotechnol 74:69–77

Sun Z, Ramsay J, Guay M, Ramsay B (2007b) Fermentation process development for the production of medium-chain-length poly-3-hydroxyalkanoates. Appl Microbiol Biotechnol 75:475-485

Sun Z, Ramsay J, Guay M, Ramsay B (2009a) Fed-batch production of unsaturated medium-chain-length polyhydroxyalkanoates with controlled composition by *Pseudomonas putida* KT2440. Appl Microbiol Biotechnol 82:657-662

Sun Z, Ramsay J, Guay M, Ramsay B (2009b) Enhanced yield of medium-chain-length polyhydroxyalkanoates from nonanoic acid by co-feeding glucose in carbon-limited, fed-batch culture. J Biotechnol 143:262-267

Thijse GJE (1964) Fatty-acid accumulation by acrylate inhibition of L-oxidation in an alkane-oxidizing pseudomonas. Biochim Biophys Acta 84:195-197

Timm A, Steinbüchel A (1990) Formation of polyesters consisting of medium-chain-length 3-hydroxyalkanoic acids from gluconate by *Pseudomonas aeruginosa* and other fluorescent pseudomonads. Appl Environ Microbiol 56:3360–3367

Tsuge T, Fukui T, Matsusaki H, Taguchi S, Kobayashi G, Ishizaki A, Doi Y (2000) Molecular cloning of two (*R*)-specific enoyl-CoA hydratase genes from *Pseudomonas aeruginosa* and their use for polyhydroxyalkanoate synthesis. FEMS Microbiol Lett 184:193-198

Tsuge T, Taguchi K, Taguchi S, Doi, Y (2003) Molecular characterization and properties of (*R*)-specific enoyl-CoA hydratases from *Pseudomonas aeruginosa*: metabolic tools for synthesis of polyhydroxyalkanoates via fatty acid β-oxidation. Int J Biol Macromol 31:195-205

Weatherburn, MW (1967) Phenol-hypochlorite reaction for determination of ammonia. Anal Chem 39:971-974

Weusthuis RA, Huijberts GNM, Eggink G (1996) Production of mclpoly(hydroxyalkanoates) (review). In: Eggink G, Steinbüchel A, Poirer Y, Witholt B (eds) 1996 International symposium on bacterial polyhydroxyalkanoates. NRC Research Press, Ottawa

Witholt B, Kessler B (1999) Perspectives of medium chain length poly(hydroxyalkanoates), a versatile set of bacterial bioplastics. Curr Opin Biotechnol 10:279-285

Wu Q, Wang Y, Chen GQ (2009) Medical application of microbial biopolyesters polyhydroxyalkanoates. Artif Cell Blood Sub 37:1-12